The Circulation and Thermal Structure of False Bay: A Process-Oriented Numerical Modelling and Observational Study.

5th March 2012

Sarah-Anne Nicholson

Thesis presented for the degree of Master of Science
in the Department of Physical Oceanography

UNIVERSITY OF CAPE TOWN
IYUNIVESITHI YASEKAPA • UNIVERSITEIT VAN KAAPSTAD

Abstract

A process-oriented approach has been applied to the circulation and thermal structure of False Bay with a newer generation ocean model, the Regional Oceanic Modelling System (ROMS). The Bay's circulation and thermal structure have been investigated through a hierarchy of experiments, which have been designed to increase in the complexity of the applied physical forcing. By taking this approach the study not only addresses key processes driving the Bay's circulation, but also the relative importance of each process. The study has included observations with five acoustic Doppler current profilers (ADCPs) positioned at selected areas of the Bay, in hopes of gaining a better understanding of the key processes driving the currents.

False Bay is the largest Bay in South Africa and is found in a unique location: on the Western Agulhas Bank positioned between two major oceanic current systems, the warm Agulhas current to the east and the cold Benguela upwelling system to the west. Despite previous studies, there is still uncertainty associated with the circulation and the processes that drive it. Recent water quality concerns, extreme events of rough seas and storm surges have led to a renewed interest in the Bay's physical processes. These concerns and the uncertainty of the exact nature of the circulation are the motivation for this process study.

The first modelling experiment was designed with the objective of determining the importance of the Bay's bathymetry on its circulation and thermal structure. Experiment two focused on the influence of offshore conditions and was investigated by varying the boundary conditions applied through "offline nesting". Experiment three investigated the influence of various sea surface temperatures (SST) restoring terms. The results of these experiments have shown that: (i) the bathymetry adds complexity to the flow structure in the Bay and restricts a proportion of the remotely forced circulation from entering the Bay, thereby effecting the thermal structure, (ii) by adopting more spatially diverse boundary conditions and SST restoring terms, the results of the simulated thermal structure revealed a closer agreement to previous observations, (iii) during winter when the Bay was well mixed, the circulation was mainly cyclonic, while in stratified conditions in summer, the surface flow reacted strongly to the wind forcing, and can be anticyclonic, even though the deeper flow was cyclonic.

The observational results have shown that the Bay's boundary flow was rectilinear, polarised to the coastlines bathymetry and mainly driven by wind and tidal forcing. Inertial flow was singularly absent. The circulation at the Bay centre was complex and highly variable, with weak correlation to wind forcing indicating that other forcing mechanisms are responsible.

PLAGIARISM DECLARATION

I know the meaning of plagiarism and declare that all of the work in the dissertation (or thesis), save for that which is properly acknowledged, is my own. Aside from guidance from my supervisors, I have received no assistance, except as acknowledged.

Supervisors:

1. Professor Frank Shillington: *Department of Oceanography, University of Cape Town, South Africa*
2. Dr Howard Waldron: *Department of Oceanography, University of Cape Town, South Africa*
3. Dr Jennifer Vietch: *Department of Oceanography, University of Cape Town, South Africa*

SIGNATURE: Signed by candidate

DATE: 05/03/2012

Contents

List of Acronyms:

ADCP: Acoustic Doppler Current Profiler

AMJ: April-May-June

AVHRR: Advanced Very High Resolution Radiometer

BC: Boundary Conditions

BVF: Brunt-Väisälä Frequency

CCAM: Conformal-Cubic Atmospheric Model

CFL: Courant–Friedrichs–Lewy

CGS: Council of Geoscience

COADS: Comprehensive Ocean/Atmosphere Data Set

CSIR: Council for Scientific Industrial Research

GSHHS: Global, Self-consistent, Hierarchical, High-resolution Shoreline

IMT: Institute for Maritime Technology

IRD: Institut de Recherche pour le Développement

JAS: July-August-September

JFM: January-February-March

KE: Kinetic Energy

KPP: K-Profile Planetary

MODIS: Moderate Resolution Imaging Spectroradiometer

NE: North East

NW: North West

OND: October-November-December

POM: Princeton Ocean Model

RDU: Research Dive Unit

ROMS: Regional Oceanic Modelling System

RR: Roman Rock

SAfE: Southern African Experiment

SAH: South Atlantic High

SANHO: South African Navy Hydrography Office

SAWS: South African Weather Service

SCRUM: S-Coordinate Rutgers University Model

SE: South East

SPEM: S-coordinate Primitive Equation Model

SSH: Sea Surface Height

SST: Sea Surface Temperatures

SW: South West

UCT: University of Cape Town

WOA: World Ocean Atlas

List of Figures

List of Tables

1 Introduction

False Bay, the largest bay in South Africa, lies between two of the world's most influential current systems: the Agulhas and Benguela Current Systems. False Bay is situated at a biogeographic break (Pitcher et al., 2010), belonging to both the Southern Benguela upwelling system and the Western Agulhas Bank. The oceanography of Southern Africa, particularly this region, is some of the most complex and highly variable in the world (Roberts, 2005). Owing to the surrounding steep orography and its position, the meteorology of the False Bay region is also complex, having wind conditions that are unique when compared to other regions of South Africa (Jury, 1991). It is under these special conditions that the circulation of False Bay is regarded as highly complex.

False Bay is of great human relevance as it is one of the most productive bays of the Southern Benguela upwelling system (Pitcher et al., 2008), providing a sheltered home to various marine species. The Bay supports many livelihoods, being important to the local fishing industry and ecotourism as well as recreational activities. Several towns situated around False Bay, the South African Navy dock yard in Simons Bay, the Coastal Park landfill site on the northern shore and run off from rivers, make the Bay particularly susceptible to negative environmental impacts such as water contamination. During the late summer months, the Bay has been prone to harmful algae bloom events, which also have a negative impact on marine life (Pitcher et al., 2008). The recent water quality concerns, erosion on the northern shore, extreme events of rough seas and storm surges have led to a renewed interest in understanding the Bay's physical processes. Despite previous studies, there remains major uncertainty associated with the detailed circulation and the processes that drive it.

The different forcing mechanisms that need to be understood to accurately determine the circulation of the Bay are complicated; these take place on various spatial and temporal scales (van Ballegooyen, 1991). The observational data collected over the past decades has not provided enough information alone to accurately portray the circulation and long-term residence or transport in the Bay. An appropriate numerical model that could incorporate all relevant dynamics at various spatial and temporal scales could be a tool for understanding the circulation (van Ballegooyen, 1991). Numerical

modelling is ideal for examining the various forcing mechanisms, as different processes can be isolated from each other and investigated separately in a step-by-step increase in complexity. The recent improvements to the numerical algorithms and the advances in computing power now allow high-resolution three dimensional hydrodynamic models to resolve mesoscale coastal circulation features robustly and proficiently (Penven et al., 2001). However, these numerical models have their limitations and constraints. While large-scale basin modelling and mesoscale circulation models have developed considerably, the modelling of the smaller scale features still remains much of a challenge (Rasmussen et al., 2009). To overcome these challenges, a process-oriented approach has been designed to investigate the physical forcing mechanisms responsible for the circulation and thermal structure of False Bay. This approach is used rather than one that attempts to simulate actual conditions. The Regional Oceanic Modelling System (ROMS) was chosen as a suitable tool for this thesis.

The investigation has been carried out systematically through three experiments that increase in the complexity of the physical forcing applied. Experiment One addresses the importance of the Bay's bathymetric effect on the hydrodynamics, utilising climatological and uniform surface forcing and boundary conditions. Two configurations were setup and the results were compared. The first configuration was run with a flat bottom at a depth of 50m and the second with realistic bathymetry obtained from measurements by the Council for Geosciences (CGS). Once the need to include the high-resolution bathymetry when modelling False Bay has been illustrated, the next experiments in the hierarchy adopt the realistic bathymetry as "topographic" forcing.

Experiment Two proceeds to investigate the influence of remote forcing by varying the resolution of the open ocean boundary conditions through an "offline nesting approach". In this experiment uniform World Ocean Atlas (WOA 1°) boundary conditions, consisting of monthly climatological hydrography and geostrophic velocities, are compared with high-resolution offline nested boundary conditions at a 9km spatial resolution provided from the Veitch et al. (2009) ROMS domain.

Experiment Three uses the high-resolution boundary conditions. This experiment investigates the influence of different surface restoring terms on the simulated sea surface temperatures (SST) by comparing the coarser Pathfinder (9km spatial resolution and monthly time resolution) SST data with MODIS SST data at 1km spatial resolu-

tion from combined Terra and Aqua products.

The numerical modelling approach was run in parallel with acoustic based current observations. The data were obtained with the use of five Acoustic Doppler Current Profilers (ADCPs) positioned in selected regions of the Bay. The advantage of applying these two different approaches simultaneously was that commonalities and differences could be integrated together for a more complete understanding. In this study, results of the observations obtained, together with past observational studies have helped towards the setup and design of the modelling experiments. While, the results of the process-based modelling have provided additional insight into some of the observational results.The main objective of this thesis was to determine the important physical forcing controlling the circulation and thermal structure of False Bay, with a view to establishing the relevant contributions of each. The study aims to add to the knowledge of the circulation and to stimulate interest for more refined and detailed future numerical modelling studies in the Bay. The key research questions are:

- What is the role of bottom topography on the Bay's circulation and thermal structure?
- Is remote forcing an important physical forcing factor on the Bay, and if so, how does it influence the circulation and thermal structure?
- Is wind forcing a dominant forcing factor in the Bay?
- How important is tidal forcing?

A comprehensive literature review is presented in the next chapter. Here, an in depth description of the plausible physical driving mechanisms influencing the Bay's dynamics is given. This is followed by a review of the historical observations and past numerical modelling work conducted on the circulation of the Bay. In Chapter 3, the methodology of the observations and numerical modelling approach are discussed separately and in detail. In Chapter 4, the results of the *in situ* observations and the numerical modelling are presented separately. These are later integrated together into the Discussion and Conclusion chapter. Finally, Chapter 5 puts forward recommendations for future numerical modelling work and suggests a framework for the design of future experiments.

2 Literature Review

2.1 Locality and geomorphology

False Bay, situated at the southernmost tip of South Africa, lying directly south of Cape Town, has been described by Spargo (1991) as a perfect example of the dictionary definition of a bay. Very few geological features occurring naturally can be described as perfect in their dimensions, however, the description given by Spargo (1991) is believable when looking at the Google imagery of False Bay, Figure (1). In this image a well defined horseshoe shaped bay of equal proportions can be found. Ironically, the name 'False Bay', would make one believe otherwise. The name, however, has little to do with its authenticity as a Bay. The name originates from the early pioneering navigators who mistook the Bay for Table Bay when seeking to replenish stocks.

False Bay is the largest bay in South Africa having an area of approximately $900km^2$, outranking other eminent bays such as Walvis Bay ($99km^2$) and Saldanha Bay ($92km^2$) by virtually an order of magnitude (Gründlingh et al., 1989).

Figure 1: False Bay and the surrounding geomorphology, adapted from Google Earth.

The Bay is flanked on the western and eastern boundaries by two prominent mountain ranges. On the western boundary lies the Cape Peninsula Mountain chain and on the eastern boundary the Hottentots-Holland Mountains. The shorelines of these two lateral boundaries are dominated by rough terrain with steep rocky outcrops. In contrast, the northern boundary of the Bay is characterised by a low-lying sandy region, known as the Cape Flats. The northern shoreline comprises almost entirely of sandy beaches extending from one corner to another (Muizenberg to Gordon's Bay, Figure (1)). The southern boundary is open, exposing the Bay to the oceanic forcing taking place in the adjacent ocean (Wainman et al., 1987). The existence of this remarkable topography surrounding False Bay is important in that it can result in complex wind fields occurring over the Bay (Jury, 1991) leading to an even more multifaceted hydrodynamic regime (Taljaard et al., 2000).

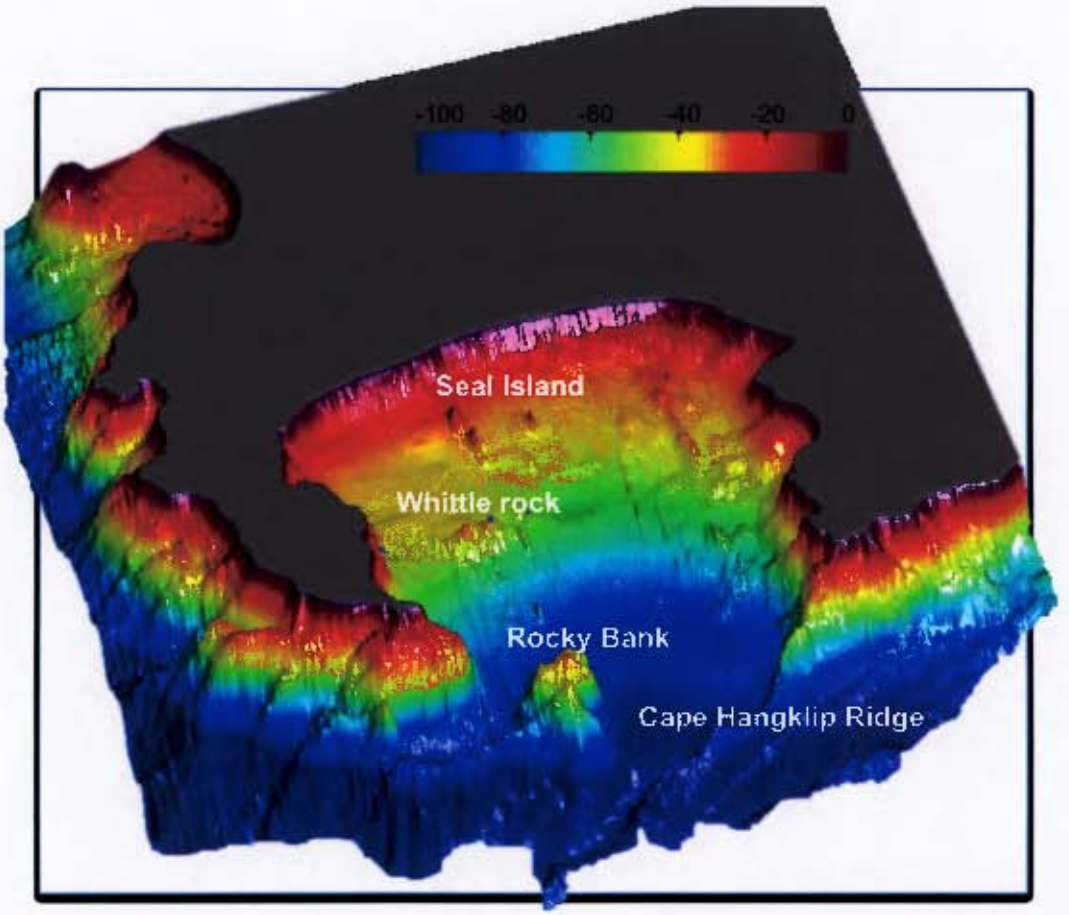

Figure 2: The bathymetry of False Bay. Bathymetric data was provided from the Council of Geoscience (CGS).

The bathymetry of False Bay, Figure (2), is relatively shallow having a mean depth of ~50m. The bathymetry declines gently from the sandy northern border southwards, reaching a maximum depth of ~90m at the mouth of the Bay between Cape Point and Cape Hangklip. At the Bay's lateral boundaries, particularly near the entrance of the bay, the shorelines slope steeply onto the ocean floor. The major bathymetric features found within the Bay include: the extensions of both Cape Point and Cape Hangklip; Rocky Bank (-22m), a sea mount found at the mouth of the Bay; Seal Island and York Shoal (-2m) located near the northern margin and Whittle Rock found (-2m) in the western half of the bay. These features are important in that they have an important influence on both wave climate and circulation within the Bay (Taljaard et al., 2000).

2.2 Oceanographic setting

Oceanographically, False Bay is in an unique location: positioned between two major current systems, the warm western boundary Agulhas Current and cold eastern boundary Benguela Current. The Bay is situated on the Western Agulhas Bank and falls into the southern domain of the Benguela upwelling system (Nelson and Hutchings, 1983). In this sense, False Bay is in the middle of a biogeographic break, with a cold-temperate upwelling region west of the Cape Peninsula and a warm-temperate region to the east (Pitcher et al., 2010). In the larger context, the marine environment of Southern Africa is known as some of the most complex and highly variable in the world, this is partly due to the latitudinal position and related weather (Roberts, 2005). The oceanographic features surrounding False Bay and in the larger setting of Southern Africa are depicted in Figure (3). In his study, Roberts (2005) describes the complex oceanography of Southern Africa which is summarised here with particular focus on the region around False Bay. The Agulhas, a western boundary current, strongly influences the oceanography on eastern coast of Southern Africa including part of the Agulhas Bank (Roberts, 2005). The fast flowing Agulhas current undergoes several fates once it reaches the tip of the Agulhas Bank, the current retroflects back towards the Southern Indian Ocean, anti-cyclonic warm core eddies may spiral off transporting warm water into the Southern Atlantic, and part of the flow continues along the shelf edge of the Western Agulhas Bank. The latter brings Agulhas waters

in close proximity to the region surrounding False Bay, however, whether or not it influences the oceanography inside False Bay is yet to be investigated. The Benguela, one of the four major eastern boundary currents in the world, is largely responsible for the oceanography on the western coast of Southern Africa. The outer coastal shelf is influenced by the slower and less defined Benguela Current. While the inner shelf is influenced by the Benguela Jet, a narrow frontal jet flowing northward between the Cape Peninsula and Cape Columbine (Roberts, 2005). Other features of the inner shelf include a poleward bottom current, upwelling cells, and shelf waves. The inner shelf dynamics are important as they are more likely to influence the oceanography of False Bay.

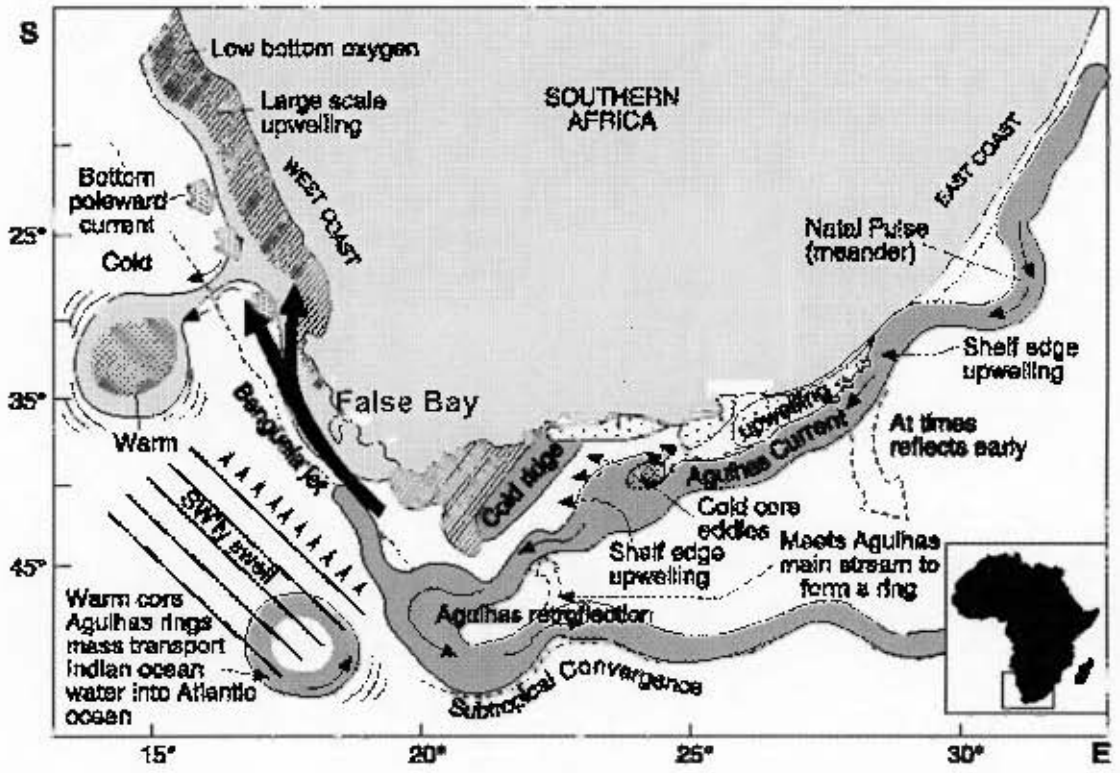

Figure 3: Schematic of large-scale oceanographic features influencing False Bay adapted from Roberts (2005).

The Bay itself encompasses an array of oceanographic phenomenon such as colour fronts (Waldron, H. N and C.K Wainman and M.E Waldron and C.Whittle and G.B Brundrit, 2008), wind induced upwelling (Jury, 1985) and red tides (Horstman et al., 1991). This further makes False Bay of interest to oceanographers with recent studies being focused on internal waves, colour fronts and circulation in False Bay.

2.3 Key physical processes driving False Bay circulation

In order to develop a consistent and comprehensive description of the circulation within the Bay, it is necessary to understand the physical forcing. According to Taljaard et al. (2000) the circulation in the Bay is believed to be as a result of forcing from wind, wave and tidally driven flows as well as remote forcing from currents on the adjacent shelf, bathymetric steering and seasonal fluctuations in thermal structure. The following is a review on the processes that drive the circulation and thermal characteristics of False Bay.

2.3.1 Atmospheric forcing

False Bay is a shallow bay having a mean depth of only ~50m. The orientation and the location of mountains surrounding the Bay expose it to strong bi-directional, seasonal winds blowing from the southeast and northwest during summer and winter respectively. Furthermore, the horseshoe shaped enclosure of the Bay lends itself to enhanced alterations in sea level, a consequence of these strong winds (Wainman et al., 1987). It is under these circumstances that atmospheric forcing has been singled out to be the primary driving force of circulation within the Bay (Atkins, 1970b; Van Foreest and Jury, 1985; Wainman et al., 1987; Gründlingh et al., 1989; Jury, 1991; Taljaard et al., 2000). The atmospheric forcing of this region is governed by the character and time scales of synoptic systems that typify the area (Jury, 1991). Four dominant synoptic patterns and their associated wind regimes have been identified by Jury (1991) and are given in Figure (4). The research by Jury (1991) is summarised below.

The southwesterly (SW) wind regime (Figure 4a) blowing uniformly over the Bay, typically occurs after the passing of a cold front and is associated with the leading edge of the South Atlantic High (SAH). Figure (4b, c) represent the deep and shallow southeasterly (SE) wind regimes respectively. These winds generally occur after the SW wind regime and are distinctive of summer month conditions. The deep SE typically takes place first when the SAH ridges eastwards and is extended over most of the west coast of Africa. During this time, strong wind fields with little directional shear characterise the atmospheric forcing. Due to vertical compression over the Cape Hangklip mountain ridge, the wind accelerates over the mountains into False Bay. The shallow SE has a

subsidence inversion layer that is lowered during this period resulting in the SE being constrained to a height beneath the surrounding mountains, $\leq$1500m. The outcome is a more complex wind field as it is topographically steered into False Bay around the mountains, resulting in a wind shadow over the eastern side of the Bay (Wainman et al., 1987). Lastly, Figure (4 d) shows the north westerly (NW) wind regime, typical of the winter month conditions. NW winds normally occur during the passing of coastal lows and can precede the onset of an approaching cold front, extra tropical cyclone. As a result of topographic steering, the wind field bends around Table Mountain resulting in a more northerly flow over the Bay. Near the mouth of the Bay, the winds are steered into a more westerly direction.

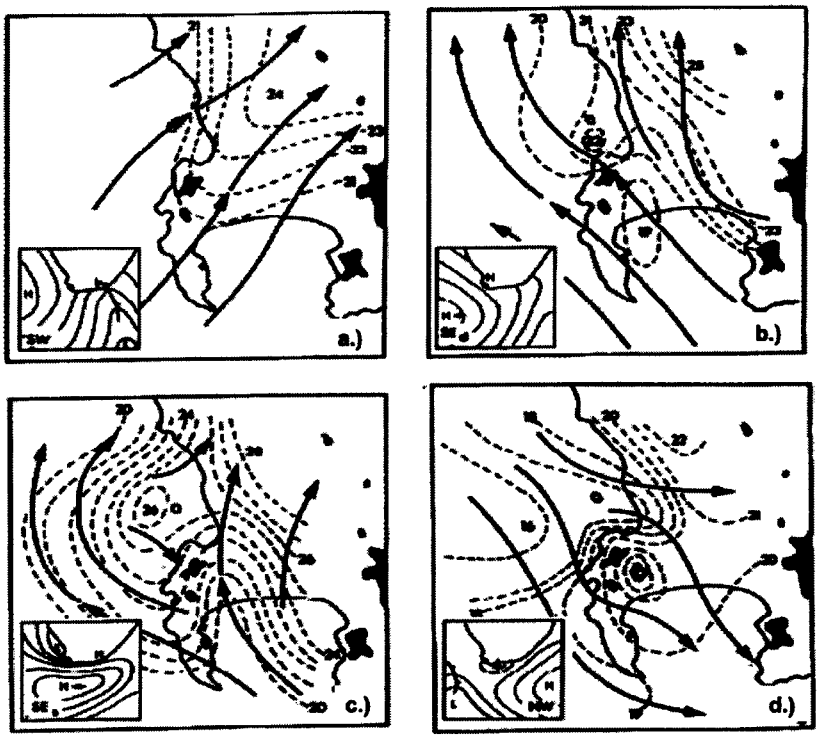

Figure 4: The four main synoptic patterns representing each typical wind patterns over False Bay: a.) SW regime, b.) deep southeast, c.) shallow southeast, and d.) northwest. Heavy lines are aircraft-derived mesoscale wind streamline patterns and the dotted lines are air temperatures at 150m. Land elevations over 600m are dark shaded. The inset shows schematic of synoptic weather patterns with air pressure isobars. (Taljaard et al. (2000) adapted from Jury (1991))

2.3.2 Thermal structure

Numerous studies investigating the vertical thermal structure of False Bay have observed seasonal fluctuations from a stratified water column during summer to a well mixed column during winter (Atkins, 1970a; Gründlingh, 1993; and Wainman et al., 1987). The seasonal fluctuation of sea surface temperatures (SST's) occurring in the Bay is well illustrated in Figure (5). The SST measurements were made daily by sampling surf zone temperatures at Muizenberg and Gordon's Bay. A mooring was positioned between Muizenberg and Gordon's Bay on the 30m isobaths, which recorded bottom temperatures at a depth of 28m. The period of deployment was from July 1989 to July 1991 capturing both the winter and summer seasons. During the winter months the SST's were low (~14°C) with virtually no difference in temperature between the surface and the bottom waters (maximum difference ~2°C). The similarity between bottom and surface temperatures provides evidence of a well mixed water column in winter (Gründlingh, 1993). In contrast, throughout the summer months the SST's were much warmer (~17-19°C) in response to increased solar insolation. The vertical temperature difference was much larger between the surface and bottom waters (maximum difference ~8-9°C). This large difference in surface and bottom temperatures clearly illustrates a stratified water column for this period (Gründlingh, 1993).

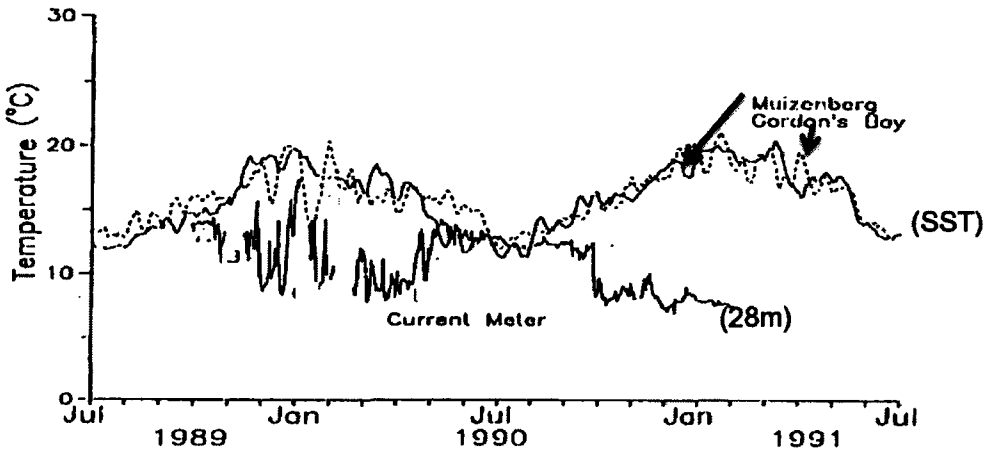

Figure 5: Time series of daily surf zone temperatures (°C) at Gordon's Bay (dashes) and Muizenberg (line) including a near bottom (28m) temperature reading from a current meter positioned between the two moorings, adapted from Gründlingh (1993).

Similar results have been found in other studies such as Atkins (1970a) and Wain-

man et al. (1987). In Atkins (1970a) study, 28 hydrographic stations were distributed across the bay. Temperatures were measured almost entirely from bathythermographs and on occasion a thermistor reading which would record surface, 10, 20, 30 and 50m. A total of 26 cruises were undertaken over three years, the results were therefore relatively synoptic. Data from other cruises were included if in close vicinity to the specified stations. The data was averaged into seasons: January, February, March (JFM); April, May June (AMJ); July, August, September (JAS); and October, November, December (OND). From these measurements, the seasonal mean vertical temperature profile from Cape Point to Cape Hangklip across the mouth of the Bay is provided, Figure (6). Agreeing with results from (Gründlingh, 1993), for the summer mean (JFM), the water column is stratified (10-18°C) and in contrast for the winter mean the water column is well mixed (13-14.9 C).

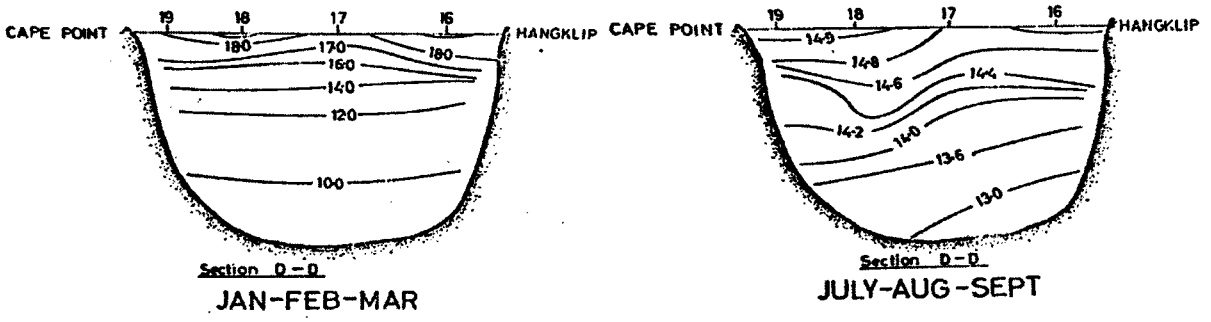

Figure 6: Seasonally averaged vertical temperatures (°C) in False Bay for summer (JFM) and winter (JAS), between Cape Point and Cape Hangklip

This characteristic of the seasonal cycle in the thermal vertical structure is important, as it has been noted to influence processes regarding the circulation in the Bay (Taljaard et al., 2000). During the summer months, the occurrence of highly stratified water may result in the decoupling of surface and deep flows in the Bay (Taljaard et al., 2000), suggesting that the Bay may represent a two-layered system during this time (Gründlingh, 1993). This decoupling effect is believed to have influences on the flow speeds of the bottom circulation, Gründlingh (1992) found that the bottom waters move slower during summer months. As a consequence of this two-layered system, the surface flow is more directly influenced by wind forcing, whereas the bottom flow is weaker, tending to flow in a different direction (Taljaard et al., 2000).

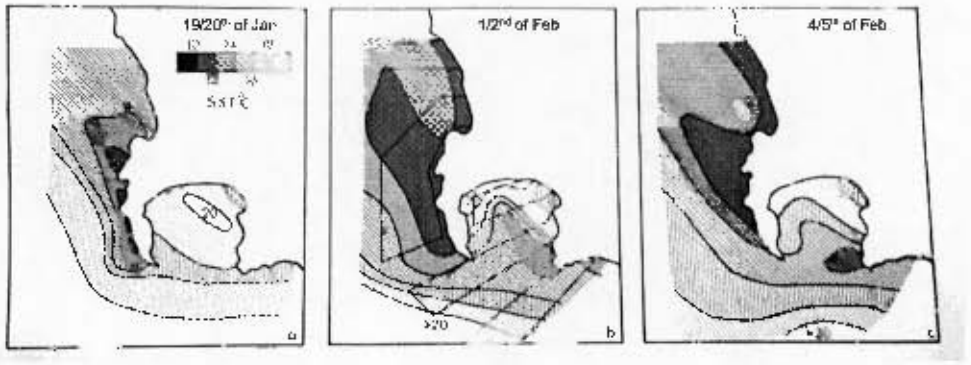

Figure 7: A composite SST distribution sequence for the period 19 January to 5 February 1981 (Jury, 1985)

Like the vertical structure, the horizontal thermal structure undergoes a seasonal change within the Bay. During summer months, in response to the dominant alongshore equator ward winds (SE), the surface waters are driven away from the coast resulting in the upwelling of colder bottom waters in certain regions of the Bay (Jury, 1985). Figure (7) provides as an example of an upwelling event: during the 19-20 of Jan the SSTs were fairly homogeneous in the Bay with a small upwelling cell off the Cape Peninsula (Jury, 1985). After a period of strong SE winds, 1-2 of Feb, the SSTs across the Bay were much more spatially diverse with an upwelling cell stretching from Cape Hangklip into the middle of the Bay and a separate upwelling cell off Gordon's Bay. Upwelling cells have been typically found to occur in these regions off Cape Hangklip and Gordon's Bay (Cram, 1970; Grindley and Taylor, 1970; Jury, 1985; Wainman et al., 1987; Taljaard et al., 2000). There were other areas in the Bay where the warm surface water is pushed towards the shore by these strong SE winds, for example Muizenberg corner where warmer SSTs of up to 20°C occurred. By the 4-5 of Feb, the upwelling cell off Cape Hangklip has reduced in size and extended in an east-west orientation across the mouth of the Bay. As demonstrated by this sequence of SSTs, the summer horizontal structure is variable and can be heterogeneously distributed in the bay. The distribution of SSTs during winter is far more uniform by comparison. This was seen in work by Atkins (1970a) who mapped surface isotherms from 28 hydrographic stations around False Bay. During the winter season (JAS), the SSTs ranged between 14.2-14.8°C whereas the summer months (JFM) had a larger temperature range from 17.8-20.6°C.

2.3.3 Wave forcing

Waves and the focusing of swell into the Bay have been found to have influences on the inshore circulation of the Bay (Wainman et al., 1987). The longshore currents found around the coastal boundary of the Bay are largely wave driven (Taljaard et al., 2000). Typical swell direction is usually from the south, southwest or southeast direction, see Figure (8) by Terhorst (1988) cited in Taljaard et al., 2000

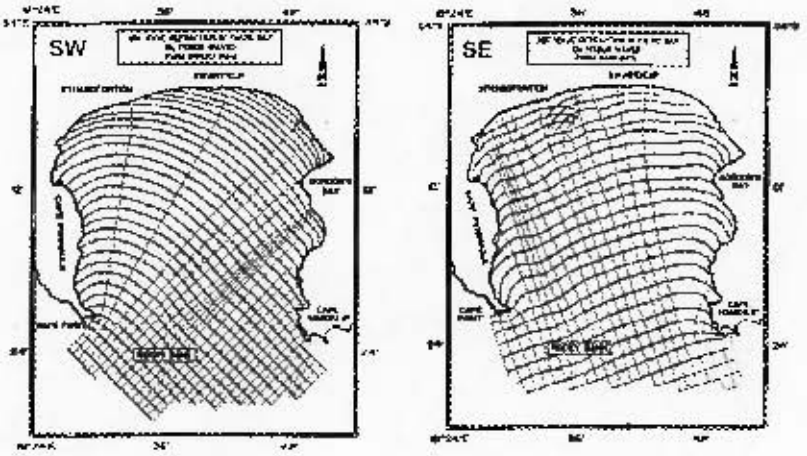

Figure 8: Typical wave refraction patterns for False Bay for both the southwesterly (SW) and southeasterly (SE) swell directions (Taljaard et al., 2000 from Terhorst, 1988)

Refraction of surface waves by bottom topography focuses on either the northwest or northeast sides of the Bay, Figure (8). The concentration of wave energy into these areas may cause a buildup of the surface water level which is released by the development of a flow along the coast directed away from the higher surface levels. This results in the formation of longshore currents as a result of angled incident waves (Taljaard et al., 2000).

2.3.4 Tidal forcing

Tidal forcing has been found to have a contribution to the currents within False Bay, especially during calm and windless conditions, during which the circulation is characterised by oscillatory in and out tidal flows (Atkins, 1970b). The tidal range is approximately 1.6m during spring and 0.8m during neap phase with a maximum tidal prism of 1.4×109 m^3 resulting in an average flow of 4 cms^{-1} in the Bay (Gründlingh

et al., 1989). Generally the tides are believed to be of most significance within the more topographical complex features and shallower regions within the Bay (Taljaard et al., 2000).

2.3.5 Remote forcing

Remote forcing, typically taking the form of sea level changes and currents occurring over the adjacent continental shelf, have been deemed by van Ballegooyen (1991) to be a relevant dynamic influencing the circulation of False Bay. It is expected that remotely forced influences will be the most pronounced near the mouth and deep regions of the Bay (Taljaard et al., 2000). Remotely forced processes such as shelf waves have been identified as potential dominant processes in the sub-tidal circulation of False Bay (Gründlingh and Largier, 1991). Shelf waves, or coastally trapped waves, are generated from the passing of weather systems, which induce changes in sea level and currents, a result of the variations in both the atmospheric pressure and wind stress (Gill and Schumann, 1974). Coastally trapped waves typically have periods that range from a few days to weeks and have been studied to propagate in an anti-clockwise fashion around the sub-continent of South Africa with amplitudes on the order of 0.5m (Schumann and Brink, 1990). The complexity of flow in the Bay is suggested to be a result of the non-linear interaction between these shelf waves, wind-driven flow and tides (Gründlingh and Largier, 1991). It will be shown later, that both tidal and sub-tidal surface variations occur in water depths of 30m within the Bay.

2.4 Past research on the circulation of False Bay

The knowledge pertaining to the circulation of the Bay has typically been based on scarce data sets that are either spatially inadequate or lacking in the temporal resolution required to investigate the seasonal variability (van Ballegooyen, 1991). This has resulted in disparity amongst previous studies and findings. The following section summarises the previous literature contributions concerned with the circulation of False Bay with regards to both observational and modelling studies conducted.

2.4.1 Numerical modelling

To date there has only been one other numerical modelling study attempting to resolve False Bay's circulation. The study was carried out by Van Foreest and Jury (1985) and is summarised below.

A vertically integrated hydrodynamic model was used to investigate the wind-driven circulation. The model, damped by quadratic bottom stress utilised the equations of motion to reproduce the flow in the Bay for a set of steady state, spatially varying wind field scenarios. The solutions to the equations were found using a method of finite difference and solved on a staggered grid (Arakawa C-grid). The main results for the study have been given in Figure (9).

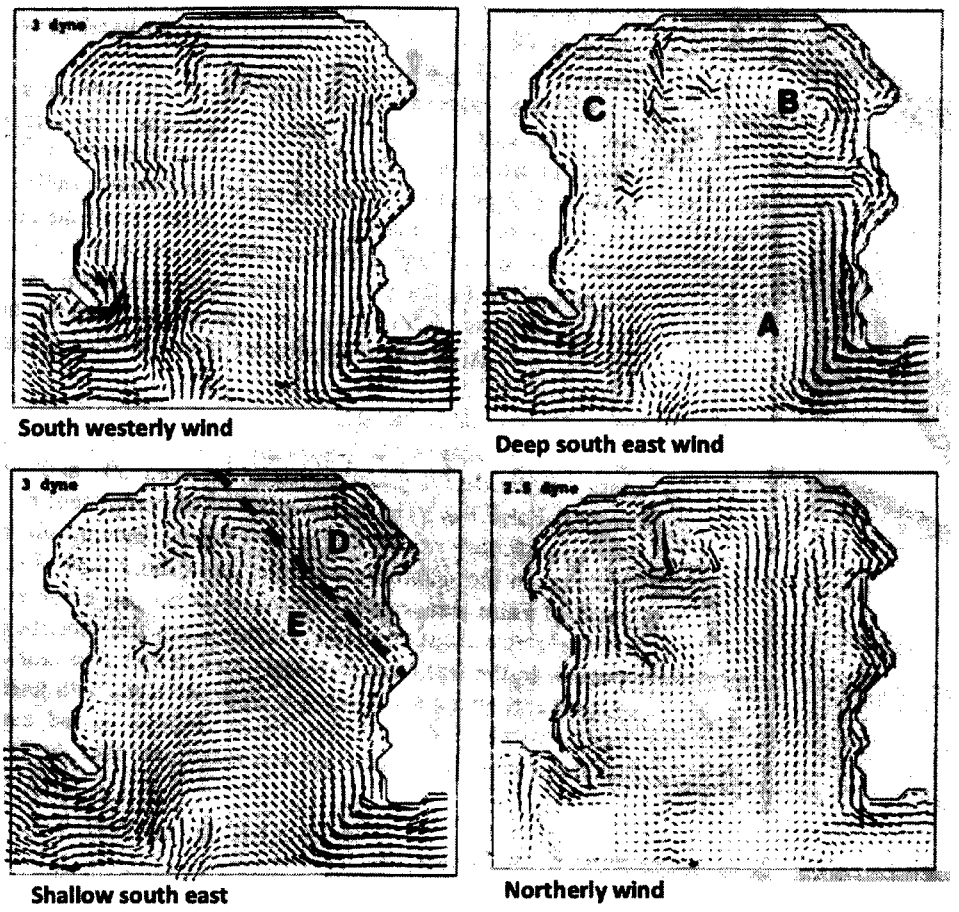

Figure 9: Simulated circulation patterns in False Bay for four main weather scenarios, adapted from Van Foreest and Jury (1985)

The wind conditions studied were northerly, southwesterly, shallow southeasterly and deep southeasterly winds (as discussed in § 2.3.1). During northerly wind direc-

tions the circulation of the Bay was generally found to be in an anticlockwise rotation except for the southward flowing jet along the eastern boundary. During the south-westerly conditions the circulation was generally in a clockwise rotation, with the flow strongest entering the Bay at Cape Point and exiting the Bay flowing eastward at Cape Hangklip. The deep southeasterly wind conditions were characterised by an anticlockwise circulation in the southern half of the Bay at (A), a narrow eastward flow at the northern boundary and two clockwise eddy features at (B and C). Lastly, during the shallow southeasterly winds with a shadow in the north-east of the bay, the resulting circulation features were characterised by two opposing eddies in the north east of the Bay, flowing clockwise at (E) and anti-clockwise at (D). The southern half of the Bay was very similar to that of the deep southeaster, flowing anti-clockwise. Additionally, not depicted in Figure (9), the circulation under a constant southeasterly was found to result in an anti-clockwise flow in the Bay.

The limitations of the study have been highlighted in Gründlingh et al. (1989), Gründlingh and Largier (1991), and Taljaard et al. (2000) and are discussed here. Firstly, by vertically integrating the flow field, the model essentially neglects both stratification and the baroclinicity of the water column (Gründlingh et al., 1989). As mentioned previously (§ 2.3.2), it is believed that during summer months, as a result of stratification, the Bay might have a two-layered flow structure (Taljaard et al., 2000). Secondly, by choosing isolated and fixed wind conditions any critical difference in the flow due to horizontal wind shear would be missed (Gründlingh et al., 1989). Steady state situations are rarely encountered in nature, wind variation time scales are from hours to days, consequently the model precludes the finer temporal resolutions needed for resolving transport and pollutant dispersion (Taljaard et al., 2000). Thirdly, the model domain is such that it excludes important remote forcing affects such as the influences of the circulation on the adjacent shelf (Taljaard et al., 2000). The exclusion of remote forcing may result in uncertainties in the model simulation output (Taljaard et al., 2000). Lastly, Taljaard et al. (2000) suggests that the principle limitation of the study was the exclusion of wave-driven currents and the surf zone exchange at the northern boundary of the Bay. While there were many limitations within the model, the results highlighted the importance of the wind direction and spatial detail of the circulation of the Bay (Van Foreest and Jury, 1985)

2.4.2 Historical observations

Previous observational work relevant to the circulation of False Bay, as summarised and listed in Taljaard et al. (2000) includes: "dye bombs" (Atkins, 1970b), current meter moorings (Wainman et al., 1987; Nelson and Polito, 1987; Gründlingh et al., 1989), drogue-tracking (Van Niekerk, 1983; Botes, 1988; CSIR, 1990, 1991b), and derived circulation flow from water properties and sediment transport (Cram, 1970; Atkins, 1970a; Gründlingh, 1992). The most complete and comprehensive observational studies are those of Atkins (1970b), Wainman et al. (1987) and Gründlingh et al. (1989). The following section is a review of this previous work with focus on the three main studies.

In his study, Atkins (1970b) used "dye bombs"- dye dropped from aeroplanes to obtain a nearly synoptic scaled current measurement giving a short-term visual sign of surface flow under different conditions. The study was initiated in 1964 and consisted of 13 operations for 11 different stations within the Bay. The investigation showed conclusively that the circulation in the Bay has no constant pattern. Atkins (1970b) postulated that the circulation within the Bay consisted of four main patterns, Figure (10), and the patterns were conditioned by offshore currents and modified further by local winds and the shape of the shoreline.

The first type of circulation was found to be clockwise under the influence of south-easterly or easterly winds, occurring 50% (7/13 events) of the time. However, this circulation type also occurred during June after periods of northwesterly's. The circulation included an eddy feature near Gordon's Bay. Atkins (1970b) suggests that this circulation is a result of a remotely wind generated current flowing westward south of the Bay which is deflected northward into False Bay either as a consequence of the angle of approach or by the dominant southeasterly winds at Cape Point.

The second type of circulation was a general anti-clockwise flow after a strong northwesterly wind event, occurring less than 10% of the time (1/13 events). The last two types were tidally driven, which Atkins (1970b) found to be significant after calm, windless conditions.

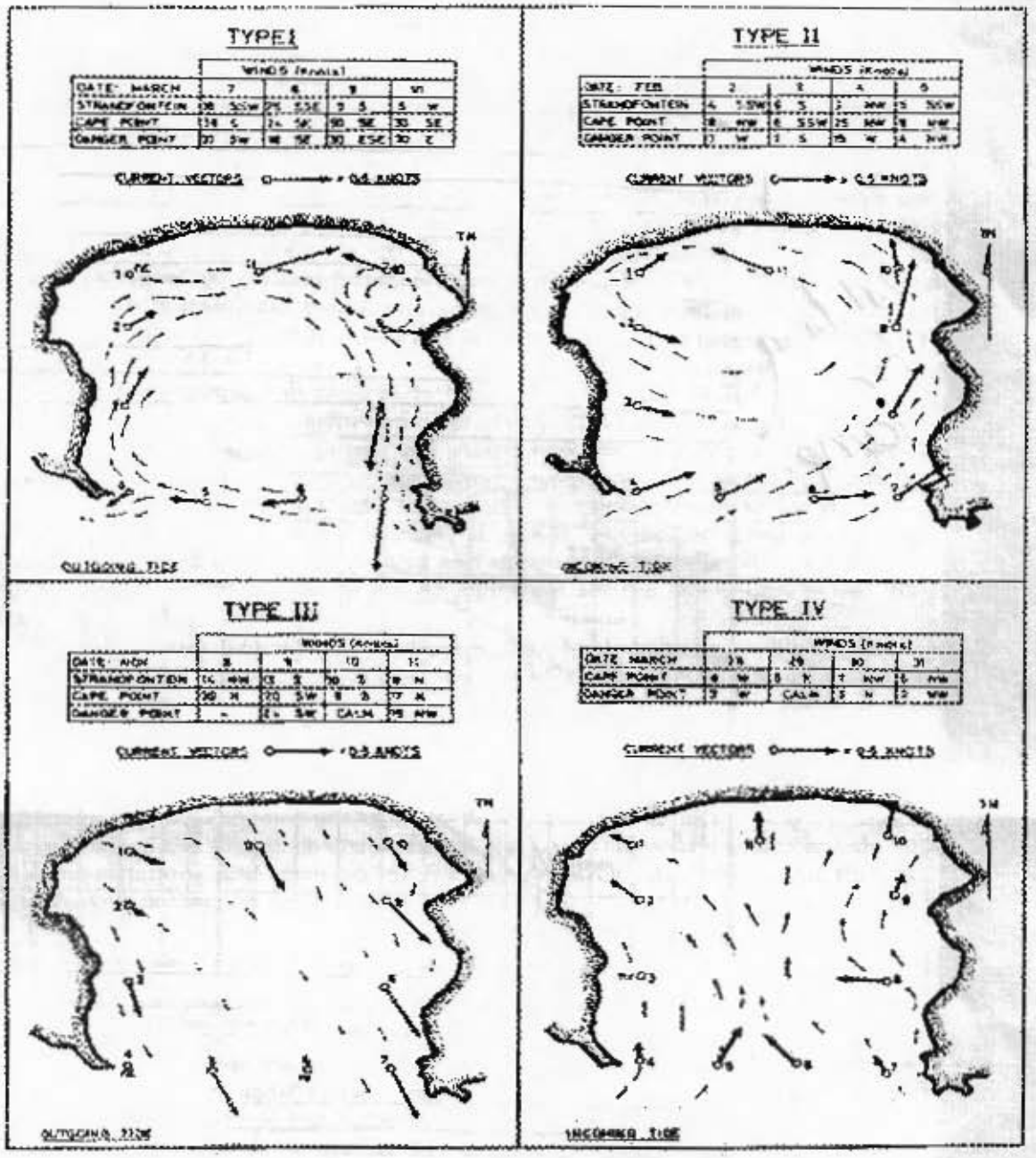

Figure 10: Nearly synoptic patterns of surface currents in False Bay as interpreted from dye-bomb tracers with corresponding weather conditions (Atkins, 1970b).

As a result of both the poor spatial resolution and the fact that the results only account for surface data, the above generalisations should be taken cautiously (Gründlingh and Largier, 1991). Although the results differed from the model output of Van Foreest and Jury (1985), they have been supported by several observational studies within the Bay (Botes, 1988; CSIR, 1991b).

In contrast to Atkins (1970b), Wainman et al. (1987) and Gründlingh et al. (1989) incorporated current moorings and had fine temporal resolutions but poor spatial resolutions. By using current moorings with continuous sampling these studies were able to obtain information on long periods (sub-tidal), whereas Atkins (1970b) could only resolve quasi-steady conditions (Gründlingh and Largier, 1991).

Wainman et al. (1987) used current meter moorings to measure the subsurface currents at four stations within the Bay located near Seal Island, Cape Point, Gordon's Bay and Cape Hangklip. The study was conducted during 23 Feb - 18 May 1985. The main findings of his study as summarised in (Gründlingh and Largier, 1991): (1) The circulation in the bay consists of a complex flow system, with a significant southerly component to the flow at all moorings. To account for this, a dipole flow pattern was suggested with water entering in the middle of Bay and leaving on either side. (2) The average flow did not agree with the numerical modelling study by Van Foreest and Jury (1985) under similar wind conditions. (3) Evidence of two-layered flow occurring at a mooring situated near Seal Island. The upper layer was in a northeasterward direction and the lower layer southeastward. (4) Temperatures rise during a northwesterly and drop during a southeasterly, a result of advection and vertical mixing. (5) Increased activity observed at a 2-3 day period in the current speed and temperature data, suggesting that coastal-trapped wave energy may leak into False Bay.

Gründlingh et al. (1989) measured the bottom currents for four moorings spread at equidistances at the entrance of the mouth of the Bay during the austral summer of 1986/1987. The results showed on average a northward flow on the western boundary, and a southward flow on the eastern boundary of the mouth, for which a general cyclonic bottom circulation could be inferred, agreeing with the results of Atkins (1970b). Gründlingh et al. (1989) found that there was a slight angle change between the measurements at 40m and 50m depths, perhaps evidence of the baroclinicity of the water column. Spectral analysis of the current data, allowed Gründlingh et al. (1989) to identify the semi-diurnal tide and inertial flow signals in the circulation

As Gründlingh and Largier (1991) concludes, as a result of the differing time and spatial scales in which the studies were undertaken, it is unsurprising that there has been lack of consistency between previous work. Atkins (1970b) measured the immediate surface currents and Wainman et al. (1987) and Gründlingh et al. (1989) meas-

ured the deeper currents while Van Foreest and Jury (1985) numerical model results were based on steady-state, fixed synoptic conditions and a barotropic water column (Gründlingh and Largier, 1991).

A schematic of the circulation summarising all of the previous observations and inferred from the existing knowledge of the physical forcing has been suggested in Taljaard et al. (2000), Figure (11). During the SE wind, both bottom and surface flows in cyclonic motion, with the exception of the small anticyclonic gyre near Gordon's Bay. Along the eastern shore the outflow was suggested to be strong and narrow. During the NW'ly wind, a weaker anticyclonic flow is believed to develop with a cyclonic gyre near Gordon's Bay. The following schematic, which was derived from the past conflicting studies, must be interpreted with caution.

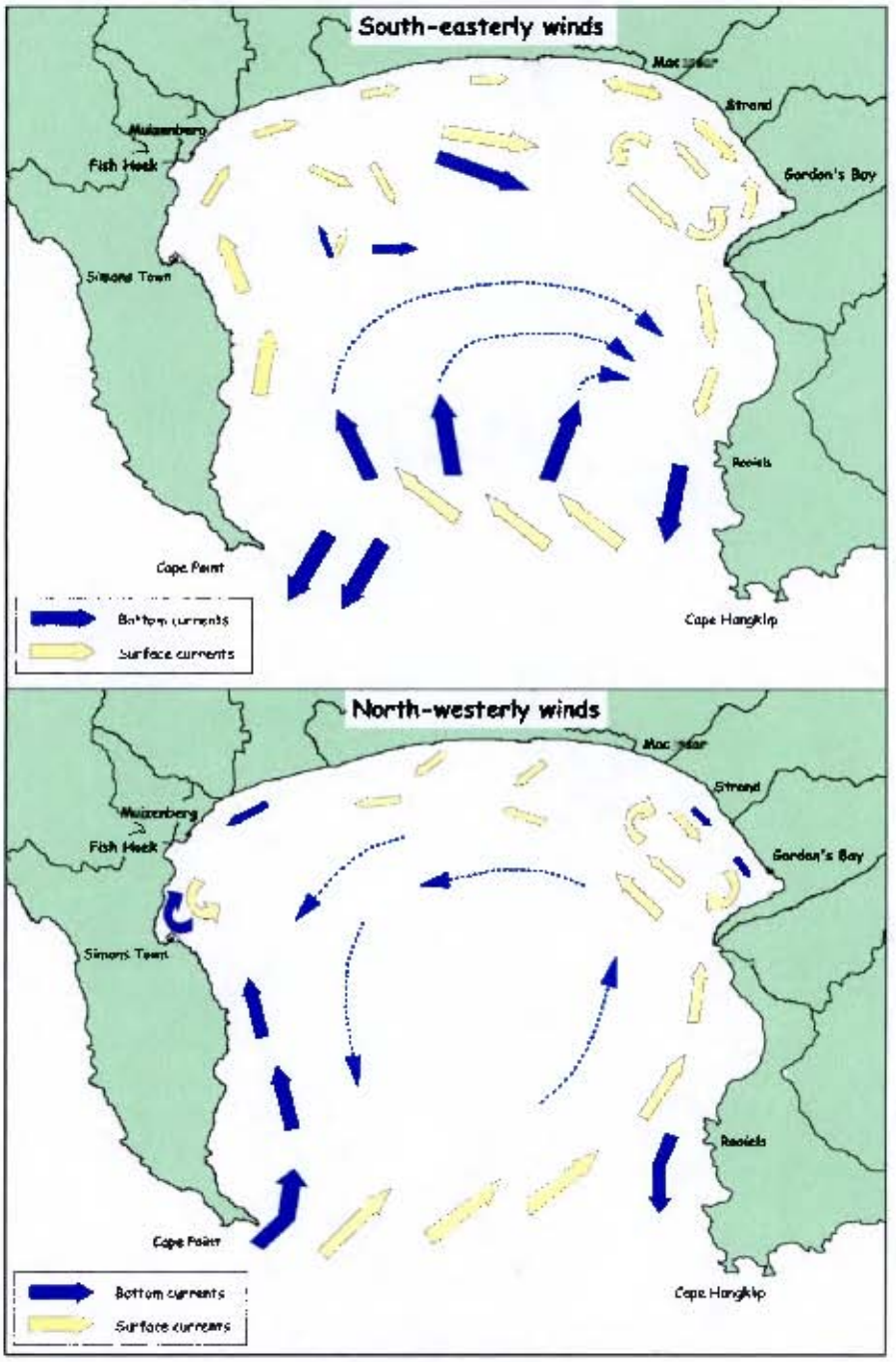

Figure 11: A schematic representing the culmination of all past knowledge and inferred, for the surface (yellow) and bottom (blue) circulation in response to the SE and NW wind (Taljaard et al., 2000).

3 Methodology

In order to attain the objectives of this thesis, two parallel strategies have been followed. The first has been to deploy and analyse ADCP current measurements in selected areas of the Bay. The second has been to setup ROMS to numerically model the circulation and thermal structure, and its seasonal evolution. For this study, the main purpose of these observations was to contribute towards a new understanding of the key driving processes. The numerical modelling experiments have been designed to systematically investigate physical processes rather than attempting to simulate reality. It is not possible to validate the model using these observations until the end stage when all processes have been understood. An ultimate aim would be to include observations by data assimilation into a suitable numerical scheme.

3.1 Observations

3.1.1 Water velocity measurements

The circulation in the Bay has been measured using three upward-looking 600khz Acoustic Doppler Current Profilers (ADCP) fixed on the seafloor. Additional current data was collected by another two ADCPs from other projects where the time period of deployment coincided. The ADCP deployment was staggered over a period of two months from the 20 August to 18 October 2010, capturing the late winter characteristics. The location of the ADCPs were restricted to the 30m depth contour for the SA diving safety regulations (Figure 12). The ADCP were positioned along a west-east transect from the western half of the Bay. They were positioned in close proximity to each other in order to increase the spatial resolution in this area of the Bay. One additional ADCP (A05) was located in Gordon's Bay, which conveniently provided the current flow on the eastern half of the Bay during part of the deployment period. A04 positioned in the middle of the Bay is the furthest offshore. A02 and A03 were deployed in an area with rocky outcrops and complex bathymetry. A01 and A05 were within close range to the coastal boundaries of the Bay. All ADCPs are at a similar depth except for A05, which was positioned in a shallow region close inshore of Gordon's bay.

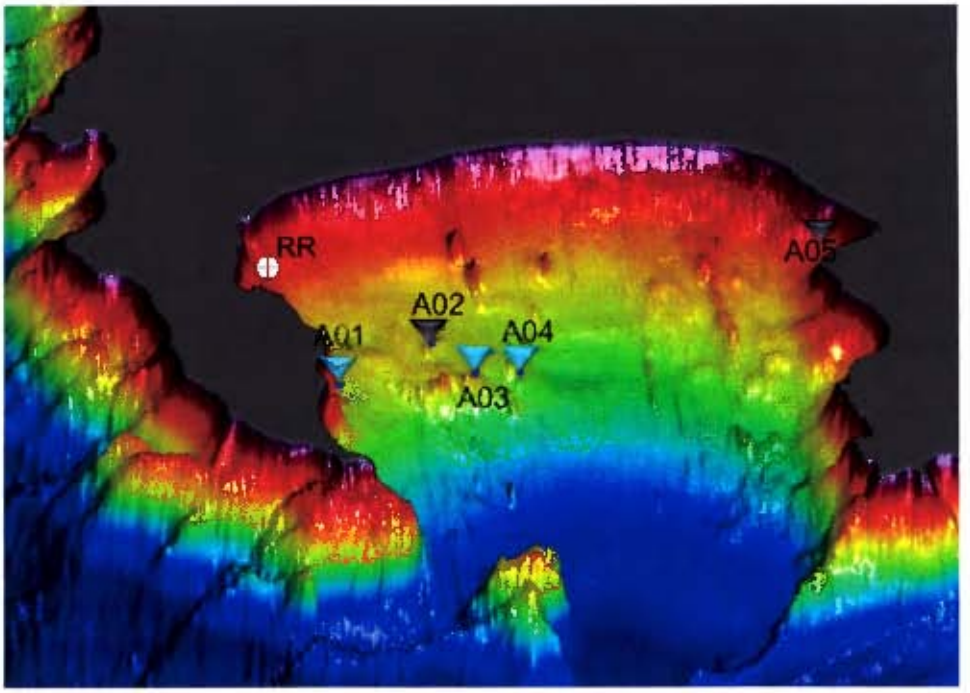

Figure 12: The bathymetry of False Bay with the location of ADCPs (A01, A02, A03, A04 and A05) and weather station at Roman Rock (RR)

The sampling time step, bin size, depth, location, offshore distance and deployment period of each ADCP is provided in Table (1) below. Unfortunately, A01 was setup to have a time step of 100 min instead of the intended 10min.

Site	Latitude,°N	Longitude°E	Depth (m)	Offshore distance (km)	Sampling time step (min)	Bin size (m)	Deployment period
A01	-34.21667	18.48333	31	1.73	100	1	27 aug-30 Sep
A02	-34.21353	18.52751	34	5.83	20	0.7	29 aug-18 Oct
A03	-34.23333	18.56667	29	8.50	10	1	27 aug-18 Oct
A04	-34.23333	18.60000	33	11.54	10	1	27 aug-18 Oct
A05	-34.15897	18.84006	12	1.38	10	0.5	20 Aug-13 Sep

Table 1: The location and sampling information for all ADCPs.

The ADCPs were set in plastic tripod frames, see Figure 13. Iron weights were used to secure each leg of the ADCP frame. The weights had been placed at the end of the legs and were approximately 1m away from the instrument to avoid any disturbance in the magnetic bearing.

Figure 13: ADCPs and plastic frame

Data analysis techniques using MATLAB software have been applied to investigate the various mechanisms influencing the circulation. The ADCP data analysis has excluded the 'shadow zone', an area of bad data near the ocean surface. As described in Gordon (1996), ADCPs typically transmit sound along narrow beams, slanted at acute angles from the vertical in four radial directions. As a consequence, ADCPs are unable to measure currents close to a 'hard reflector' such as the sea floor and sea surfaces. This is because of the reflections of leak energy, which are travelling in side-lobes of different more acute angles than the main beam. The 'shadow zone' is approximately 6% of the surface data according to Gordon (1996). In this study to be certain that the shadow zone was excluded, 10% of the surface data was removed in all the statistical analysis. In order to identify key periodicities within the data set, kinetic energy spectra were created on the unfiltered current data for the U (east-west) and V (north-south) velocity components. The kinetic energy spectra were computed using frequency-averaging, where the number of averaged frequencies increased from 2 to 10 (Mercier, 1991 cited in Andre et al., 2009). The data analysis was then split up into two frequency domains: high frequency (tidal) and low frequency (sub-tidal). To explore the high frequency tidal data, the study made use of the T-Tide toolbox, see Pawlowicz et al. (2002), which included filtering and harmonic analysis. Once all the data had been averaged into a common time step (100min), a Lanczos low-pass filter (as described in Emery and Thomson (2004) was applied to the data. The filter removed any high frequencies occurring in <25 hours thus eliminating the tidal signal from the

data. The sub-tidal data analysis included statistic analysis such as lag correlation with wind velocities at various depths, variance ellipses and principal axis, as described in Emery and Thomson (2004). For the correlations, R refers to the correlation coefficient which is an 'indication' of the strength of the relationship between two variables. R^2, which was used here, refers to coefficient of determination which is the 'measure' of the strength of the relationship.

3.1.2 Wind velocity measurements

Records of wind velocities and directions have been obtained over the period of deployment and will be collated with the data from the ADCPs to make an assessment of the Bay's circulation under various wind forcing. As a result of the shallowness of the Bay, it is anticipated there will be a strong relationship between the wind forcing and the circulation in the Bay. The wind data was collected from the Roman Rock, see figure (12), automated weather station, which is maintained by the Institute for Maritime Technology (IMT). The wind has been measured every 5 minutes at a height of approximately 17m above sea level. The weather station was chosen because of the location; Roman Rock is the closest weather station to most of the ADCPs.

3.1.3 Temperature and sea surface height (SSH) measurements

Each ADCP contained a temperature sensor, which recorded bottom temperatures. The Moderate Resolution Imaging Spectroradiometer (MODIS) Terra and Aqua satellite data sets were used to provide daily sea surface temperatures in False Bay produced by Dr. Francois Dufois, UCT. Both the Terra and Aqua satellites are polar orbiting. The Terra orbit is timed so that it passes the equator from north to south in the morning, while the Aqua satellite passes the equator in the afternoon from south to north. Combining the two products means that the satellite SST data is a culmination of both the morning and evening conditions. Monthly means have been generated from the satellite data and have been used initially for validation purposes and then as a restoring force for the model SSTs. Each ADCP had a pressure sensor which allowed for accurate measurements of depth from which the SSH was inferred. The South African Navy Hydrography Office (SANHO) provided tidal gauge data for Simons Town and

Port Nolloth. The SSH derived from the ADCPs was compared to the tidal gauge data.

3.2 Numerical modelling

3.2.1 Model background

The hydrodynamic model utilised in this study is known as the Regional Oceanic Modelling System (ROMS) (Shchepetkin and McWilliams, 2005). The origins of ROMS have been summarised in both Ezer, T. and H. Arango and F.A. Shchepetkin (2002) and Marchesiello et al. (2003). The major advances in the development of oceanic models occurred during the late 1980s when the models increased significantly in their robustness and reliability. These efforts resulted in the development of the Princeton Ocean Model (POM; Blumberg and Mellor, 1987) which incorporated essential features such as: incompressible hydrostatic primitive equations; a free surface; and terrain following vertical coordinate system (σ). Issues with the σ-coordinates occurred when trying to extend the models over the continental slope to the open ocean this resulted in the development of new algorithms for the coordinate transformation during the 1990s (Barnier et al., 1998). The improved coordinate system was incorporated into the S-coordinate Primitive Equation Model (SPEM: Haidvogel et al., 1991) and the S-coordinate Rutgers University Model (SCRUM: Song and Haidvogel, 1994). The Regional Oceanic Modelling System (ROMS; Shchepetkin and McWilliams, 2005), a successor of SCRUM, is a new generation ocean circulation model. In which the SCRUM model was rewritten and improved upon in both the numerics and the efficiency, from a single to multiple computer architectures (Marchesiello et al., 2003). The version of ROMS utilised within this project was developed by the Institut de Recherche pour le Développement (IRD).

3.2.2 Equations and discretizations

ROMS makes use of high-order numerical schemes to solve the incompressible hydrostatic primitive equations of fluid dynamics, discretized in the stretched terrain-following vertical co-ordinates and horizontal curvilinear co-ordinates (Penven et al., 2001; Marchesiello et al., 2003; Shchepetkin and McWilliams, 2005; and Penven et al.,

2006). ROMS is a split-explicit and free surface model, which includes advanced capabilities such as optimisation via shared memory parallel computer architectures (Penven and Tan, 2007; and Marchesiello et al., 2003). Other advanced features in ROMS have been summarised in both Penven et al. (2006) and Penven and Tan (2007) which include: a 2-way time averaging procedure for the barotropic mode, high ordered numeric's allowing for the generation of steep gradients and an increase in the permissible time step, and a non-local K-profile planetary (KPP) boundary layer scheme that parametrises the unresolved sub grid-scale vertical mixing processes.

$$\frac{\partial u}{\partial t} + \vec{v}.\nabla u - fv = -\frac{\partial \phi}{\partial x} + \frac{\partial}{\partial z} A_v \frac{\partial u}{\partial z} + D_u \tag{3.1}$$

$$\frac{\partial v}{\partial t} + \vec{v}.\nabla v + fu = -\frac{\partial \phi}{\partial y} + \frac{\partial}{\partial z} A_v \frac{\partial v}{\partial z} + D_v \tag{3.2}$$

$$\frac{\partial T}{\partial t} + \vec{v}.\nabla T = F_T + D_T \tag{3.3}$$

$$\frac{\partial S}{\partial t} + \vec{v}.\nabla S = D_S \tag{3.4}$$

$$\frac{\partial \phi}{\partial z} = \frac{-\rho g}{\rho_0} \tag{3.5}$$

$$\frac{\partial u}{\partial x} + \frac{\partial v}{\partial y} = -\frac{\partial w}{\partial z} \tag{3.6}$$

$$\rho = \rho(T, S, P) \tag{3.7}$$

Figure 14: The primitive equations in Cartesian coordinates (Hedstrom, 1997)

The primitive equations solved (Figure 14) are composed from important fundamentals such as: the conservation of momentum (3.1 and 3.2), the conservation of mass (equation of continuity, 3.6), heat and salt transport (3.3 and 3.4); and the equation of state (3.7) (Hedstrom, 1997). The equations have been established to describe the flow of a stratified fluid in a rotating environment. They are complex and are simplified by two important assumptions: the Boussinesq approximation (3.5) and the hydrostatic vertical momentum balance (Cushman-Roisin and Beckers, 2009). In the Boussinesq approximation density is assumed constant except for the buoyancy force in the vertical momentum equation. The hydrostatic approximation is made as a result ocean basin

dimensions, wide and shallow (H<<L), the vertical pressure gradients are assumed to balance the buoyancy force, neglecting the vertical accelerations and associated Coriolis terms. The prognostic variables solved in ROMS include surface elevation η, baroclinic horizontal velocities (u, v), barotropic horizontal velocities ($\overline{u}$, $\overline{v}$), vertical velocity w and properties such as temperature T and salinity S (Marchesiello et al., 2003).

3.2.3 Configuration and design of experiments

The ROMSTOOLS package, developed by the Institut de Recherche pour le Développement (IRD) is a collection of global data sets and MATLAB programs that have been integrated into a toolbox (Penven et al., 2007). ROMSTOOLS provided a simple means to generate the horizontal and vertical grid, surface forcing, initial conditions and open boundary conditions needed by ROMS as input data to produce the climatological simulations of False Bay (Penven et al., 2007).

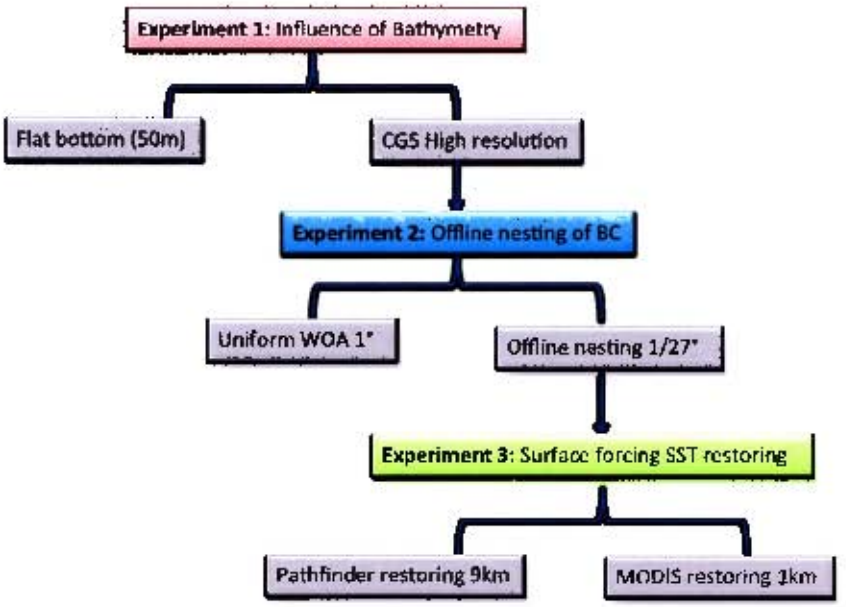

Figure 15: Framework for the hierarchy of experiments

In this study, several experiments have been designed to investigate the principal forcing mechanisms influencing the circulation and thermal structure of the Bay, Figure (15). The experiments have been set up with the same horizontal and vertical grid configurations, where they differ is in the complexity of physical forcing applied. The domain chosen encompasses the entirety of False Bay including part of the adja-

cent shelf required for the inclusion of remote forcing influences. The region covered was from 18°57'0"E to 18°59' 23.6394"E and from 33°47'59.99"S to 34°2'23.99"S. The horizontal grid resolution chosen was 1/81° (1.37km). In the vertical, the grid was composed of 20 sigma-coordinate vertical levels with surface and bottom stretching parameters of $\theta_s = 6$, and $\theta_b = 0$. The sponge defined along the boundaries of each of the configurations was 8km wide with a viscosity of $800m^2s^{-1}$. The sponge represents an active region of enhanced viscosity/diffusion (Penven and Tan, 2007), which essentially relaxes the solution of the model towards the lateral boundary conditions.

3.2.4 Experiment One: Influence of bathymetry

> *Hypothesis:* *Bathymetric features at the entrance of the Bay reduce the inflow of remotely forced circulation and furthermore act as a barrier reducing the amount of cold deep water that enters the Bay.*

False Bay has several large shallow bathymetric features, which will undeniably affect the Bay's hydrography. The most pronounced of these features is Rocky Bank, which is positioned at the entrance of the Bay. Rocky Bank is a seamount having a base with the dimensions of $\sim 7km \times 8km$, that rises rapidly from ~100m to a depth of ~22m. The feature occupies almost a quarter of the entrance of the Bay. Another noticeable feature at the Bay's mouth is the Cape Hangklip Ridge which extends outwards by ~21km in a south-west orientation, declining in depth from ~10m to ~80m . To determine the influence of the bathymetry on the Bay's circulation and thermal structure, two configurations have been designed and the results compared. The first configuration was setup with a flat bottom of a constant depth of 50m. The second configuration employed high-resolution realistic bathymetry. Both configurations make use of the same uniform climatological boundary conditions and surface forcing, to study the circulation and thermal structure.

Flat bottom and realistic bathymetry

The flat bottom was generated by adapting the ROMS get_grid.F FORTRAN function by simply setting h, the depth of the bathymetry, to be 50m for the entire domain, see Figure (16). The uniform depth was chosen at 50m because on approximation the

mean depth of False Bay is ~50m. The high-resolution coastal data, provided by the Global, Self-consistent, Hierarchical, High-resolution, Shoreline (GSHHS) data set was used in producing the coastline boundaries for both configurations.

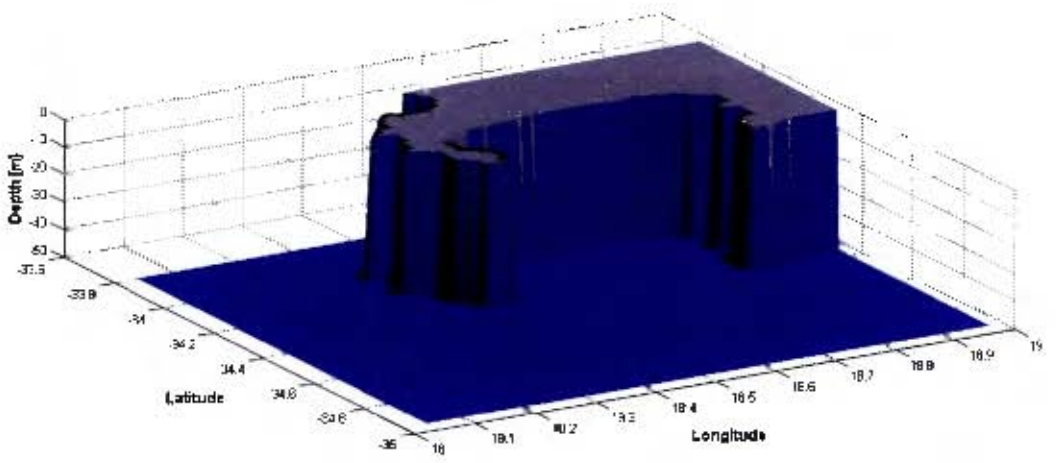

Figure 16: The flat bottom configuration with uniform depth of 50m.

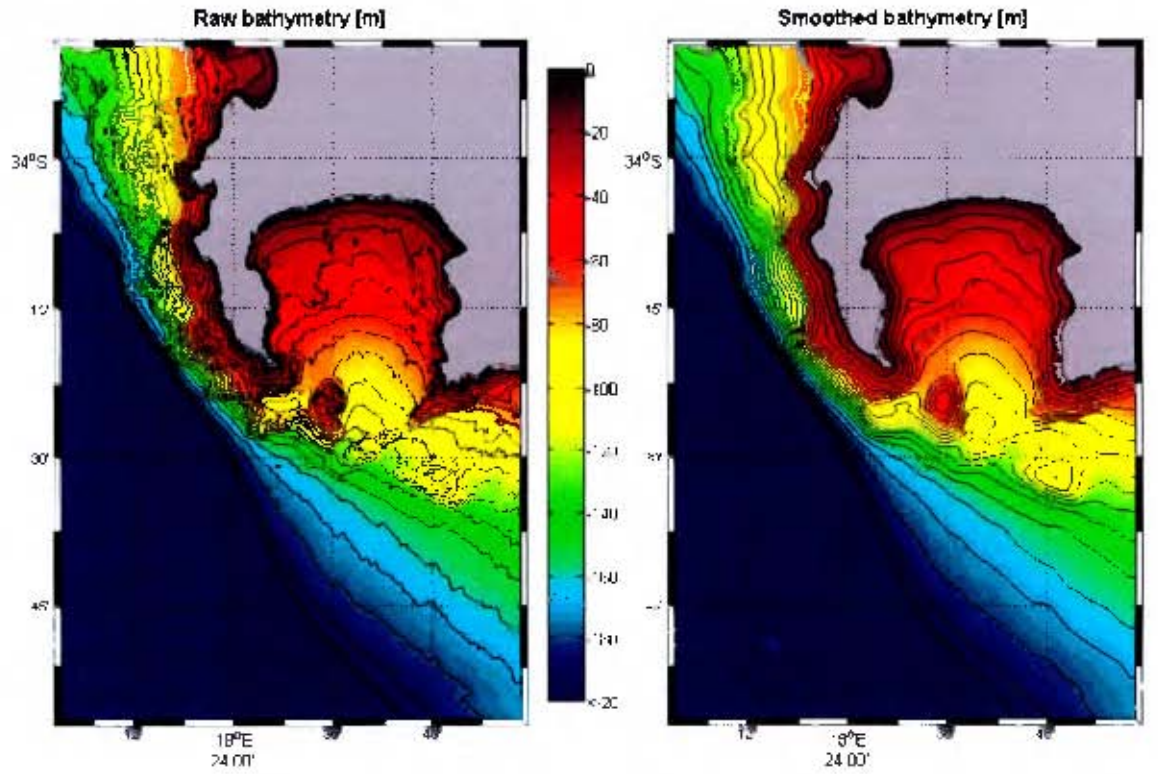

Figure 17: High-resolution raw bathymetry provided by Council for Geosciences (left) and the resulting smoothed bathymetry (left) overlaid with 10m isobaths.

The realistic bathymetry measurements were provided by the Council for Geosciences (CGS). The bathymetry data was primarily derived from fair chart so the spatial density of the data varied throughout the domain: high data density was located in the Bay and low density further offshore. The data was gridded into 100m cell sizes and nearest neighbour interpolation was employed to smooth the data. In an attempt to avoid horizontal pressure gradient errors, typical in terrain-following coordinate models, the bathymetry was smoothed further with an rtarget of 0.25. The rtarget is a variable that controls the maximum value of the slope of the sigma layers. The raw bathymetry (left) and the smoothed bathymetry (right) are displayed in Figure (17). It is evident that the smoothed data used in the simulation represents the main bathymetric features of the raw data. The effects of the smoothing can especially be seen by the change of the roughness in 10m isobaths contour lines.

Initial and lateral boundary conditions

The configurations were initiated from a state of no flow and with the January mean temperatures provided by World Ocean Atlas (WOA) 1° data set. Four open boundaries have been defined, for which the monthly climatological hydrography and geostrophic velocities from the WOA data set were employed. An example of the vertical temperatures for the January mean given at each boundary is shown by Figure (18).

Once 1° WOA data set has been interpolated onto the high-resolution grid (1/81°) it essentially represents an idealised field. Normally one would utilise the 1/3 rule to scale down from boundary conditions (Penven and Tan, 2007). For example, if a 1° lateral boundary condition data set is used then the resolution of the nested grid should be 1/3°. However, a 1/3° grid resolution is not adequate enough to resolve False Bay's circulation. Instead the approach taken here was to choose the resolution required to resolve False Bay (1/81°), thus resulting in the use of coarse lateral boundary conditions in each configuration.

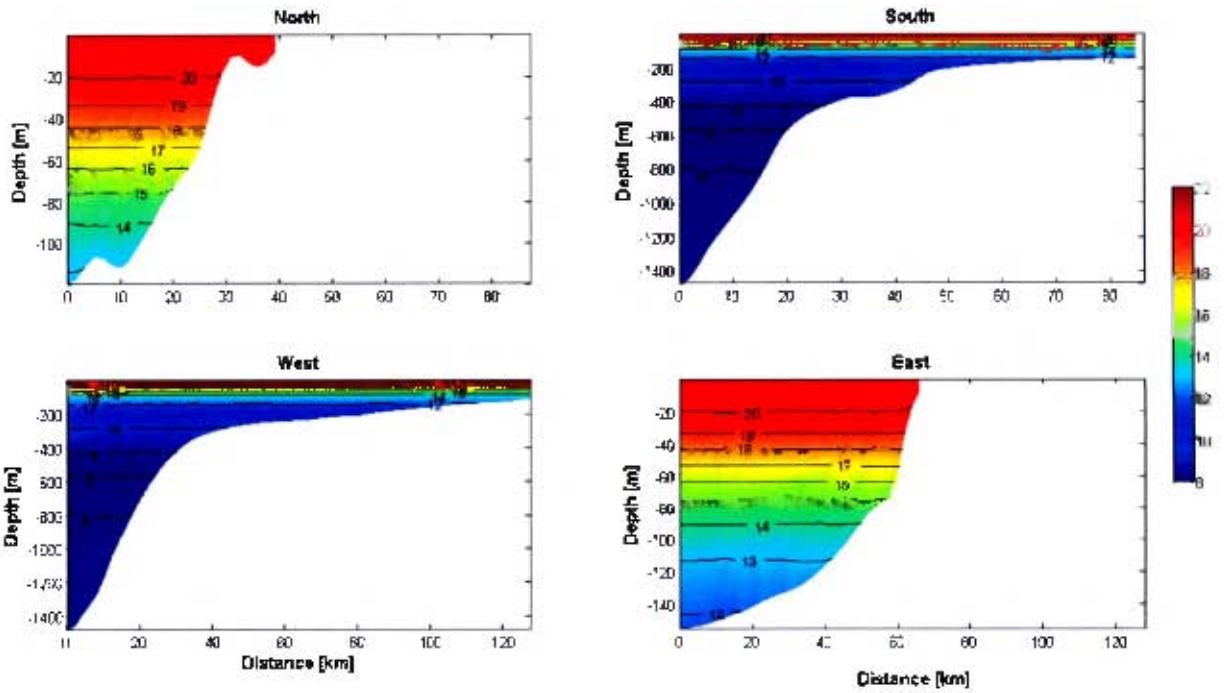

Figure 18: Lateral boundary conditions for January derived from WOA, temperature (°C) vertical sections.

Surface forcing

The surface forcing was derived from the climatological Comprehensive Ocean/Atmosphere Data Set (COADS) with resolution of 0.5° and 1°. As with the boundary conditions, once the coarse resolution surface forcing has been interpolated onto the high-resolution grid, it represents an idealised and uniform field. The SST values are calculated by the model as a response to the surface heat flux and were corrected towards the Pathfinder 9.28km climatological SSTs data set. This correction is necessary in order to compensate for the lack of ocean-atmospheric feedback, which may result in a drift in the model SST values. A similar correction is made for the surface salinities. The wind stress fields have been rotated fractionally for a more realistic wind forcing, according to the observed (Wainman et al., 1987 and Jury, 1991). The wind stress fields were rotated from a southerly to southeasterly component and a westerly to a northwesterly component during summer and winter months respectively. The resulting seasonally averaged and rotated wind stress fields are shown in Figure 19. The seasons have been averaged by JFM (January, February and March), AMJ (April, May and June), JAS

(July, August and September) and OND (October, November and December) following an example of the seasonal averages made in Atkins (1970a). The seasonal signal in the wind stress magnitudes can be seen by the fluctuation from stronger wind stress values during summer to weaker during winter. The wind stress forcing used in both configurations essentially represent steady state situations as in the Van Forcest and Jury (1985) study.

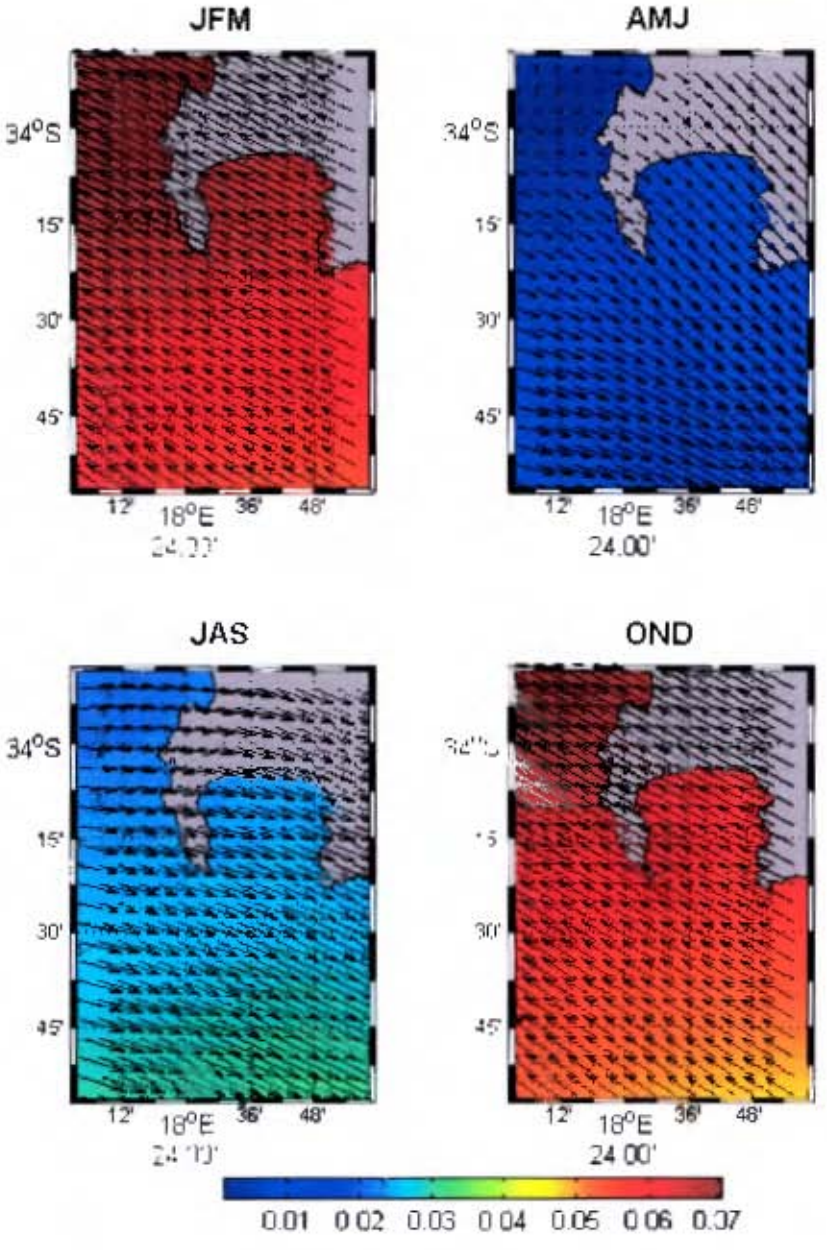

Figure 19: The seasonal mean wind stress ($N.m^{-2}$) forcing derived from COADS data set.

3.2.5 Experiment Two: One-way offline nesting of boundary conditions

Hypothesis: Finer horizontal/vertical resolution boundary condition should show an improvement of the thermal structure relative to coarse boundary conditions.

Typically in an ocean model, a set of conditions must be defined at each boundary of the models domain, which is not enclosed by land. Boundary conditions are essential for the simulation of the domains physical processes. The choice of the boundary conditions used is of critical importance as varying boundary conditions may lead to large differences in the simulation. Improper boundary conditions may result in the generation of unrealistic influences being introduced into the solution, which would have been avoided if a more appropriate set of conditions were used.

The following experiment sets out to investigate the influence of the resolution of the boundary conditions on the simulation and in doing so hopes to adopt the more appropriate boundary condition for the next experiments in the hierarchy. The experiment is carried out through two separate configurations which have adopted the high-resolution bathymetry from the previous experiment. The first configuration utilises boundary conditions from WOA (1°) data set, as described above, when interpolated onto the model grid of 1/81° it essentially represents an uniform field. The second configuration employs an offline nesting procedure to improve on the resolution of the boundary conditions used. Essentially, offline nesting is done by first computing a larger domain of the region and then extracting boundary conditions from it for the smaller domain. In this study, the larger domain, which was used to extract boundary condition from, was the child domain of the Veitch et al. (2009) study.

In the Veitch et al. (2009) study a two-way nesting procedure was utilised to simulate the dynamics of the Benguela current system. The two-way nesting approach allows the lower resolution output from the 'parent' domain to be incorporated as boundary conditions for the higher resolution nested 'child' domain, which feeds back to the parent domain (Veitch et al., 2009). The Southern African Experiment (SAfE) configuration (Penven et al., 2006) was used in the study as the 'parent' domain. The SAfE configuration domain ranges from 2.5° W-54.75°E and from 47.75°S to 4.8°S, with a horizontal grid resolution ranging between 19km in the south and 27km in the

north (Penven et al., 2006), Surface forcing is derived from COADS; and the lateral boundary conditions and initial conditions are derived from the WOA data set (Penven et al., 2006). The 'child' domain was the greater Benguela region, 3.9°E-19.8°E and 35.6°S-12.1°S, with a grid resolution ranging from 7km in the south and 9km in the north. The climatological output from Veitch et al. (2009) simulation is used as boundary conditions for the smaller domain of this study. For an example of the resulting January mean boundary conditions used, refer to Figure (20). The resolution of the offline boundary conditions used is $1/27°$ which is a significant increase from the previous 1° boundary conditions. The surface forcing applied in both configurations is described in Experiment One above.

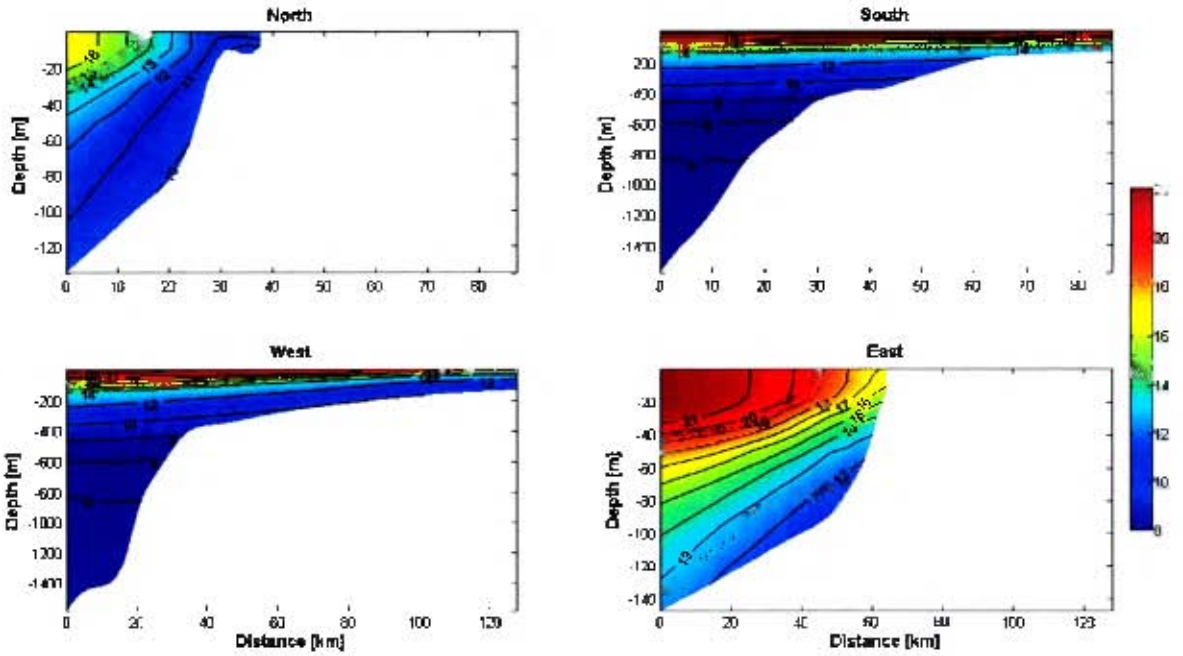

Figure 20: The lateral boundary conditions (°C) for the January mean derived from the offline nesting approach.

3.2.6 Experiment Three: Surface forcing restoring terms

Hypothesis: Incorporating a higher resolution SST climatology for the restoring term (dQdSST) will result in an improvement to the simulated SSTs.

As discussed in § 3.2.4, to prevent model SST drift, a consequence transpiring from the absence of an ocean-atmosphere feedback term, the simulated SSTs are corrected towards an observed SST climatology. The surface heat flux is given by:

$$Q_T = Q + \frac{\partial Q}{\partial T_{clim}}(T_{model} - T_{clim})$$

where, Q is the total climatological surface heat flux, $\frac{\partial Q}{\partial T_{clim}}$ is the kinematic surface net heat flux sensitivity to the SST composed of contributions from infrared, sensible heat and latent flux (Barnier et al., 1998). T_{model} is the model derived SSTs and T_{clim} is the observed climatological SSTs (Barnier et al., 1998).

In this experiment, a comparison was made between two different SSTs climatologies used for the restoring term. In the previous experiments, the model SSTs were restored to the Pathfinder SST data set of 9.28km resolution. The Pathfinder data set was derived from Advanced Very High Resolution Radiometer (AVHRR) data. To improve upon the simulated SSTs from the previous experiment, monthly means generated from the culmination of high resolution (1km) MODIS Aqua and Terra products, described in § 3.1.3, have been applied for the restoring term.

An example of the seasonally averaged SSTs for the two different data sets used for restoring is given by Figure (21). Large differences can be seen between these two SST products. This is especially evident during summer, where the Pathfinder SST was essentially uniform and unable to capture upwelling off Cape Point and the cooler waters off Cape Hangklip. These features are evident in the spatially diverse MODIS product.

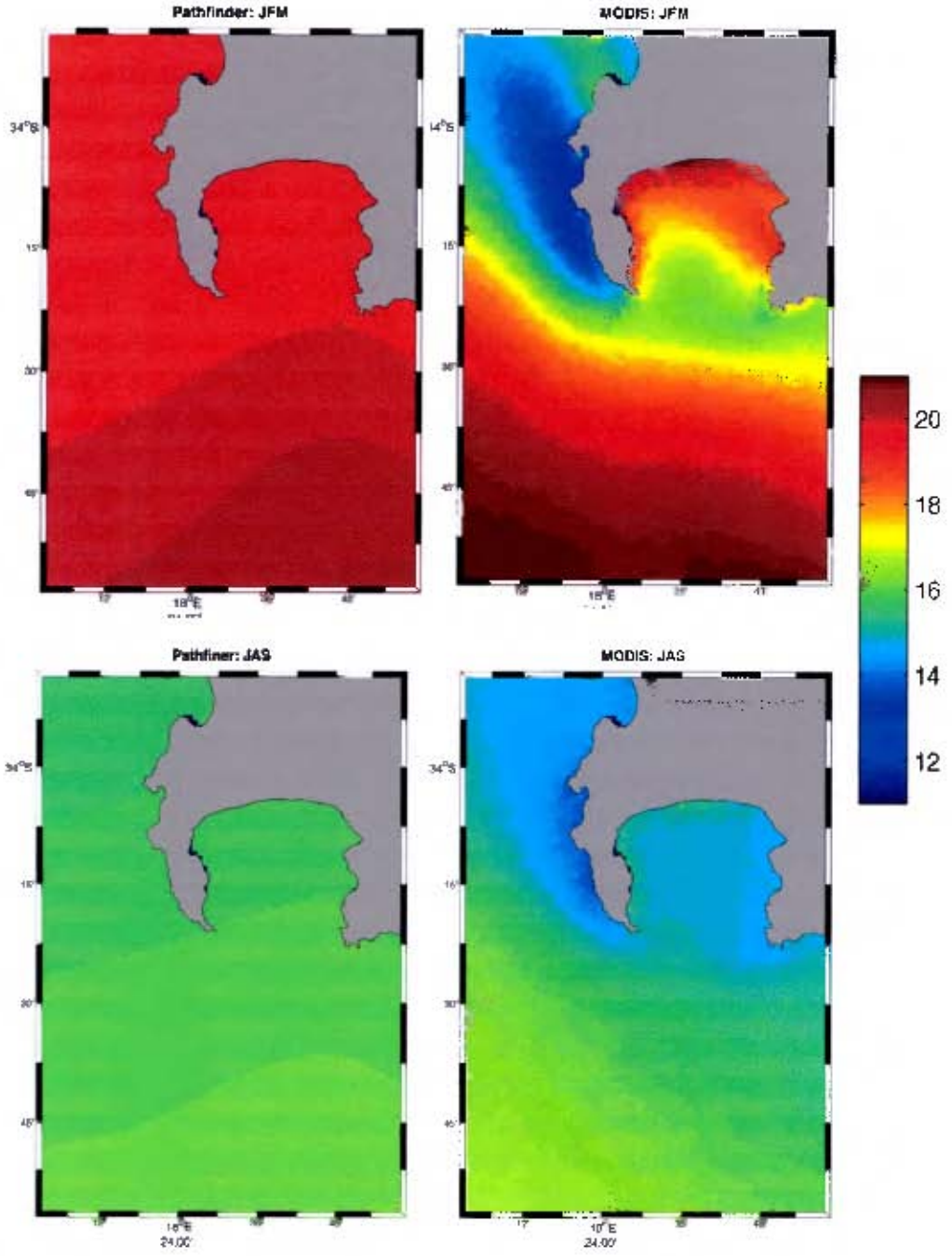

Figure 21: A comparison between the Pathfinder (9.28km) SST (°C) climatology and the MODIS (1km) monthly mean SSTs (°C). The data has been seasonally averaged for an example of summer (JFM - top) and winter (JAS - bottom) differences.

4 Results

4.1 Observations

In this section the results of the wind and ADCP data observations are presented. The results have been split into high (tidal), low (sub-tidal) and event scale (daily) timescales, in order to investigate the relative contributions of each of these scales.

4.1.1 Spectral signature

To determine the main spectral components of the flow, the ADCPs velocity record was analysed in terms of the u-component (east-west) and v-component (north-south) directions, vertically integrated with depth, Figure (22).

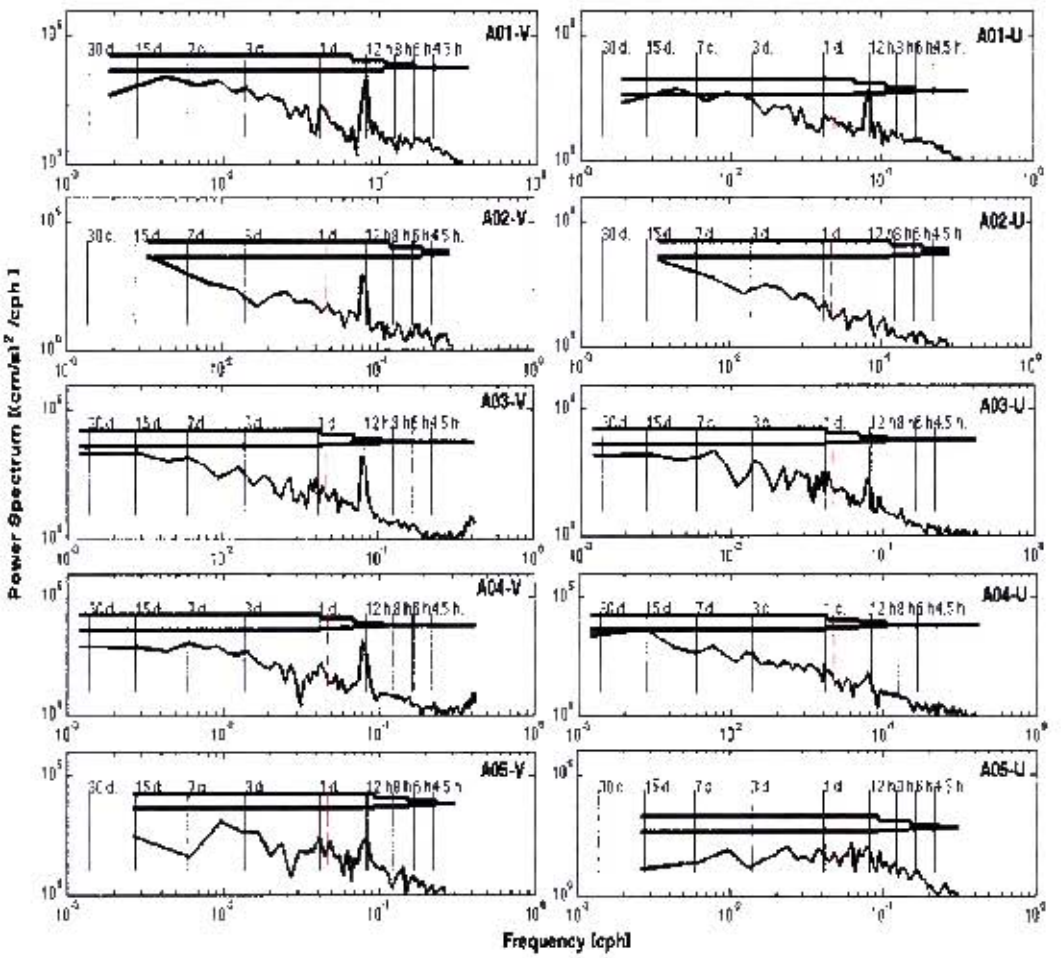

Figure 22: Kinetic energy spectra of depth integrated current data in the v (left) and u (right) velocity vector components for all ADCPs. The 95% confidence interval is marked by the bar above the graphs. The dashed line highlights the inertial period.

Insignificant differences were found between the surface and bottom depth's spectral analysis in the u and v directions, therefore depth-integrated currents were analysed in order to consolidate information. The semi-diurnal tide (~12hrs) appeared as a very significant signal in most of the spectra. The tidal signal was found to be more substantial in the v-component, with only a significant tidal peak in the u-component at A01 and A03. Interestingly, there appears to be little signal in the inertial period (~21hrs) which was found to be relevant in Gründlingh et al. (1989) who studied the bottom circulation at the Bay's entrance during the Austral summer of 1986/1987. The Schumann and Perrins (1982) study of the tidal and inertial circulations around South Africa, suggested that topographic features and density structures of the water column might cause changes in currents at different frequencies. The observations made in this study took place in late winter which has been noted to have a different vertical density structure than summer months. In the numerical modelling study by Chen and Xie (1997), the results suggested that near-inertial oscillations reach a maximum of kinetic energy near the shelf break, which decays towards the coast. This provides a basis for a potential explanation of the lack of inertial period in the observations of this study. The ADCPs were positioned in close proximity to the coast, Table 1, where the inertial energy might be damped out. Whereas, the Gründlingh et al. (1989) study, with a vertical structure characterised by summer, was at the entrance of the Bay where the influences of adjacent shelf are stronger. The results have highlighted the importance of investigating the current data on different frequencies.

4.1.2 High (tidal) frequency

Tidal flows in False Bay have previously been identified as having a significant contribution to the circulation in the Bay (Atkins, 1970b; Gründlingh et al., 1989). To investigate the tidal velocities, the T-Tide MATLAB package was used for harmonic analysis. The time series of the north-south velocities of the tidal component is presented, Figure (23). Here, the narrow fluctuation bands of inflow (red) and outflow (blue) are indicative of the tidal flows with periods of ~12 hours. The tidal signal at A01 has been smoothed, a result of the ADCP time step (100min), and is therefore not representative of the accurate tidal fluctuation. The maximum tidal velocities are on the order of $\pm 15 cm.s^{-1}$, which is a relatively significant proportion of current flow. The

maximum tidal velocities fluctuate on the period of two weeks corresponding to the fluctuations of spring tides when the tidal range was at a maximum.

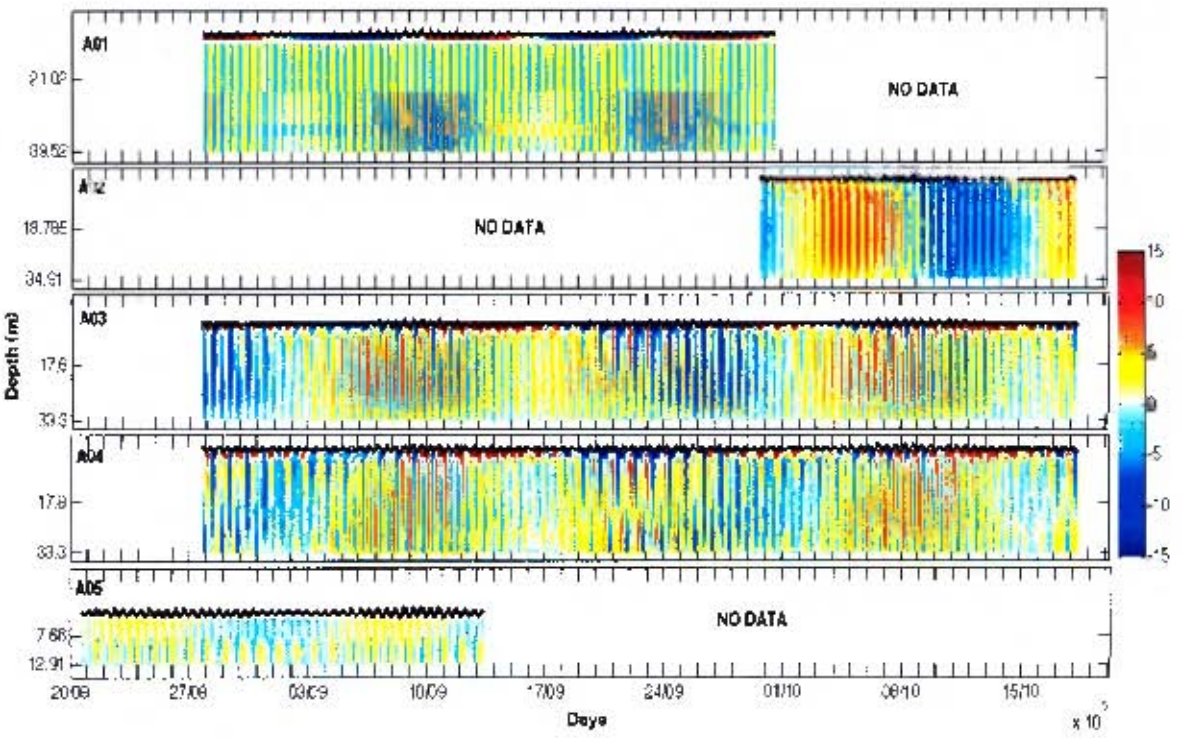

Figure 23: Time series of high frequency tidal velocities ($cm.s^{-1}$) extracted using T_Tides (Pawlowicz et al., 2002).

4.1.3 Low (sub-tidal) frequency

To investigate the sub-tidal processes, which may influence the circulation, a Lanczos low pass filter (period > 25hrs) was applied to the data. The results of the v-component of the sub-tidal data is displayed below in the form of a time series, Figure (24). Figure (24), has included the 'shadow zone', an area of bad data near the ocean surface, described in §3.1.1. As the Bay's mouth is southward facing by looking at the north-south component of the current, one can essentially infer movement in and out of the Bay. In Figure (24), northward flow is positive (red shades) and southward flow is negative (blue shades). The blue graph is the filtered v-component of wind at Roman Rock. The wind was filtered with a Lanczos low pass filter as with the currents. During the deployment period, the wind was predominantly from the S-E (45%) and from the N-W (35%), with the least occurrence from the S-W and N-E (10%), as shown in

Figure (25).

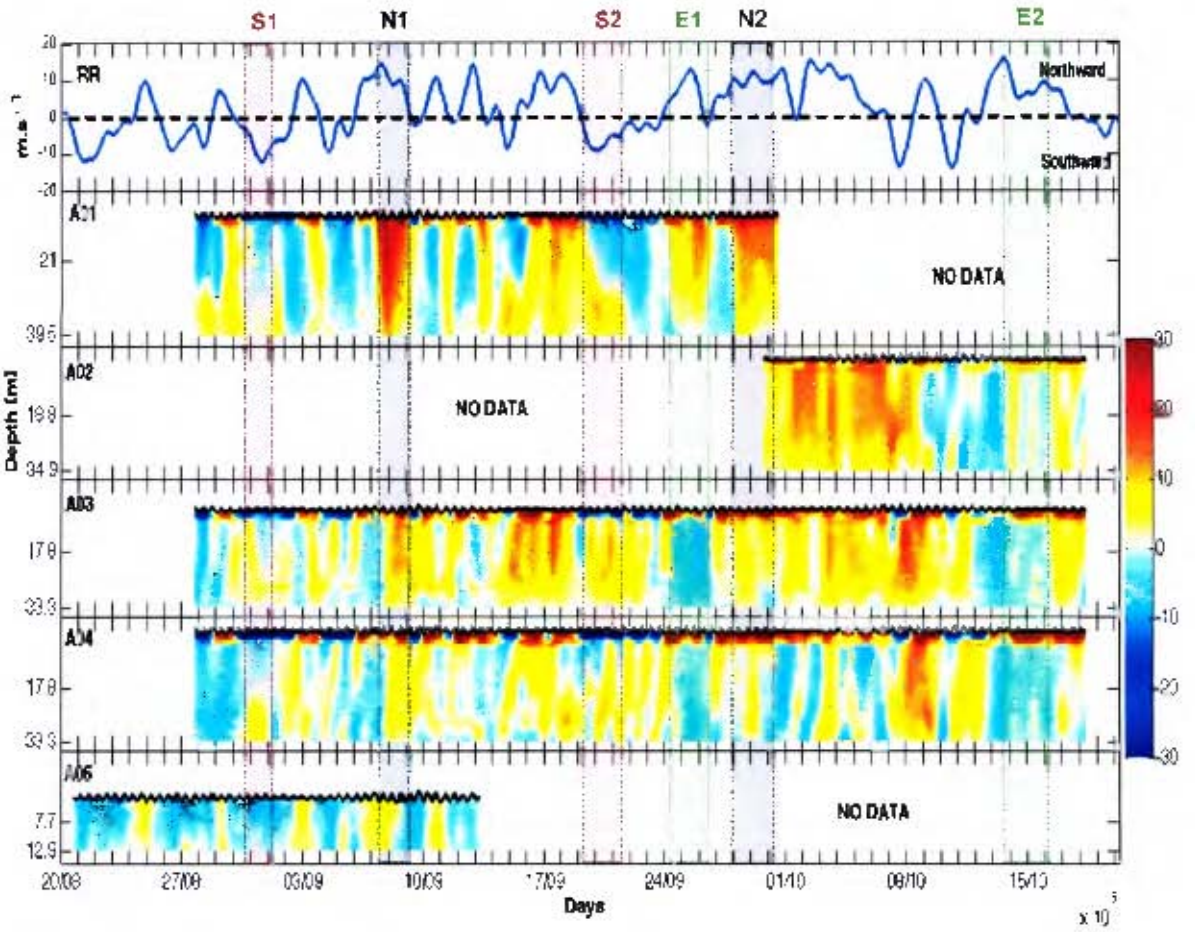

Figure 24: Time series (days) of the Lanczos low pass filtered (period >25 hrs) northward (v) current velocity ($cm.s^{-1}$) for all ADCPs and filtered v-component of wind ($m.s^{-1}$) at Roman Rock (RR). N1 and N2, highlight examples when the current and wind were both northward. S1 and S2, highlight two-layered flow at the onset of southward wind. E1 and E2, highlight exceptions when the wind and currents were in opposite directions.

The strongest wind velocities ($>15m.s^{-1}$) were from the N-W and S-E sectors. From Figure (24), the general impression found was that there were fluctuations of northward/southward flow in response to northward/southward fluctuations in wind. There was evidence of two-layered flow, on most occasions occurring after the wind reversed from northward to southward (i.e. S1/S2). One-layered flow typically occurred with northward wind (N1/N2), along with the strongest flow velocities ($\sim 30cm.s^{-1}$). Exceptions were indicated by E1/E2, where the currents at A03 and A04 were in an opposite directions to the wind.

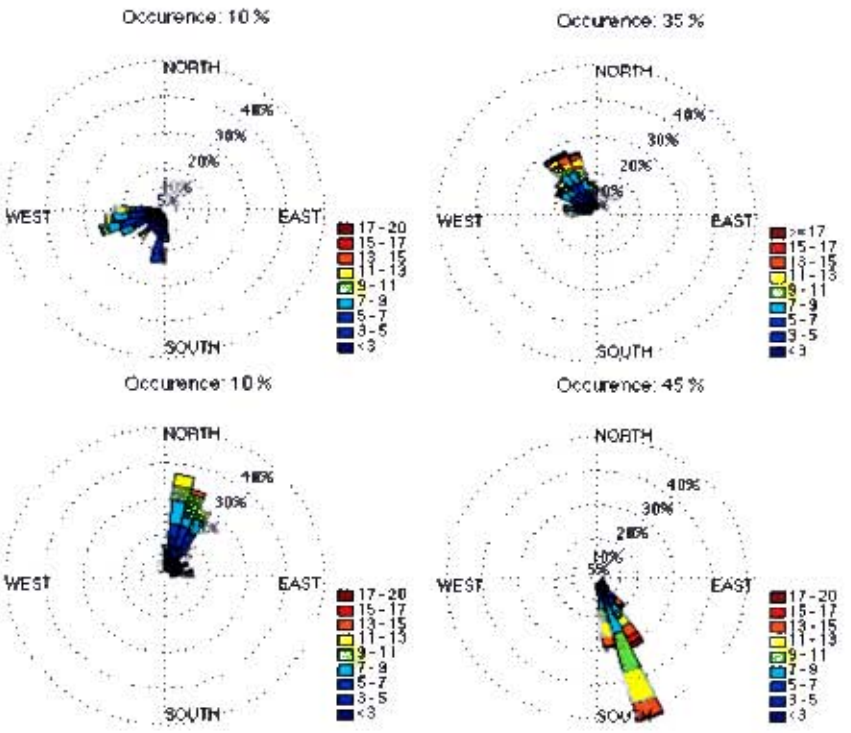

Figure 25: Wind rose's ($m.s^{-1}$) at Roman Rock, 20 Aug - 18 Oct 2010.

To investigate the relationship of the wind on the residual currents in False Bay, lag correlations have been computed. Positive and negative lag correlations (R^2) have been calculated for each ADCP with different depths, Figure (26). Here, a positive lag correlation refers to a current, which lagged behind the wind and a negative lag correlation refers to a wind, which lagged behind the current. In Figure (26.a), the highest correlation occurred at the near surface of A01 with an R^2 of 0.71 and a positive lag of 15 hrs. This means that 71% of the variability of the surface current in the v-component can be explained by the wind. At 11m from the bottom, the correlation dropped to 0.38 and the lag has increased to 17 hrs. At the very bottom there was no correlation with the wind, suggesting another mechanism was responsible for driving the circulation. The lag found was checked by comparing the SSH of A01 with tidal data and was found to be synchronous. Furthermore, the lag at A01 was confirmed by Dr. Francois Dufois from UCT, who found the same result through methods of his own. Similar lags have been found in the near-shore currents of the Southern Namaqua shelf (Fawcett et al., 2008). In the Fawcett et al. (2008) study, a 13hr lag was found to have the maximum correlation between alongshore winds and near surface currents during

winter. The second highest correlation was at the near-surface of A05 with an R^2 of 0.63 (63% explained by the wind) and no lag. At 5m from the bottom the correlation decreased to 0.4 with a lag of 1 hr. There was no significant relationship ($R^2 < 0.3$) between the wind and the current for A02, A03 and A04. The result suggests that boundaries of the Bay are strongly influenced by the wind in the v-component, and that other processes were responsible for the circulation in the middle of the Bay. For the u-component, Figure (26.b), the correlation was weak, with the highest R^2 of 0.41 (41%) at A01 and R^2 of 0.31 (31%) at A03.

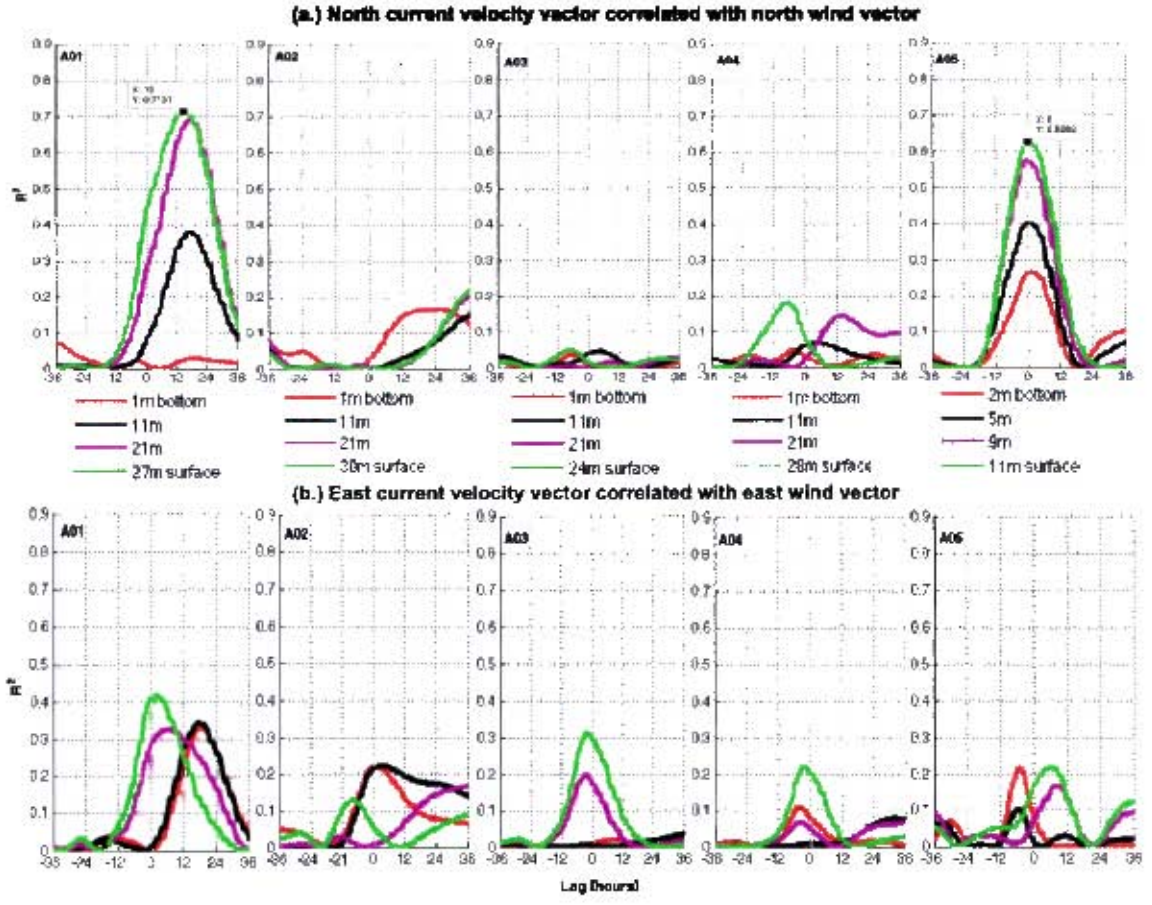

Figure 26: Positive and negative lag correlations provided by the coefficient of determination (R^2), between low pass filtered wind and currents for a.) northward velocities and b.) eastward components for all ADCPs at various distances from the bottom.

To investigate how variable the currents were at each ADCP, variance ellipses were computed for each ADCP at different depths. Variance ellipses are useful in that they can also be used to identify possible topographic steering. In Figure (27), the

variance ellipse for each ADCP at different depths are shown. The current variance ellipses have been overlaid on top of the Bay's bathymetry. The direction of the major axis of variance (principal component) is given for the surface and bottom depths, provided by the vector arrows. The major axis of variance essentially represents the main orientation of flow during the period.

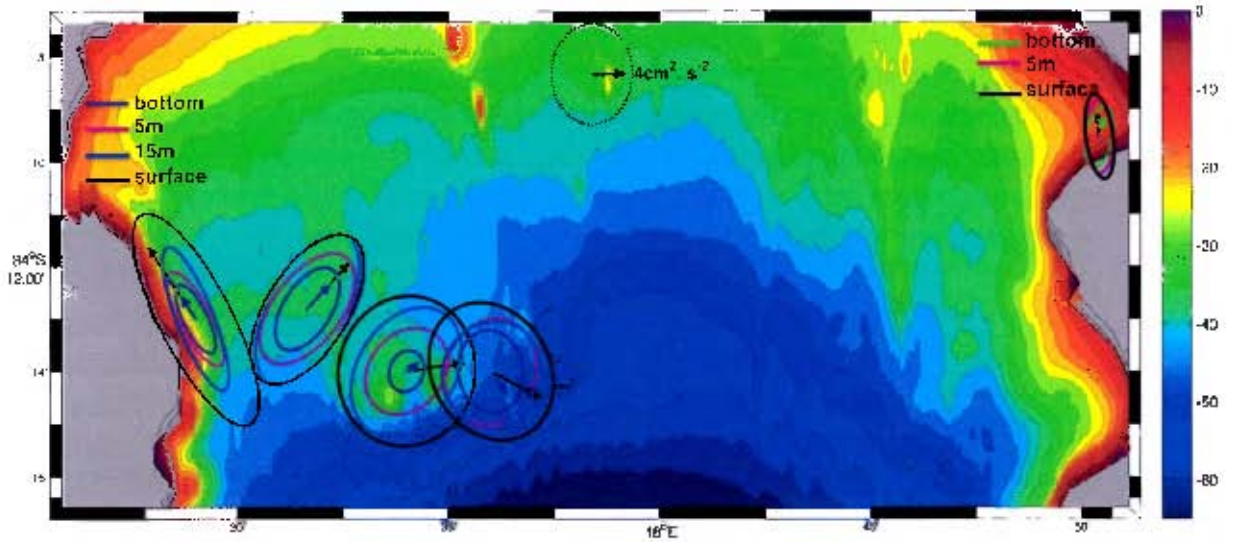

Figure 27: Bathymetry contours overlaid with variance ellipses for each ADCP at different distances from the bottom for the period of deployment. The arrows represent the direction of the major axis of variance at the surface and bottom.

The variance ellipses for A01 and A05 are elongated along the coastline and have relatively large eccentricities of ~0.66 and ~0.61 respectively. These values of eccentricities indicate that the current fluctuations were mainly rectilinear at the Bay's boundaries. In contrast, as the positions of the ADCP moved further offshore, the eccentricity of the ellipse become smaller (~0.1), the current fluctuations were multidirectional and variable in the middle of the Bay. Therefore, the flow at the Bay's boundaries was parallel to the isobaths, and the flow in the middle of the bay was complex and highly variable. The complexity of the underlying bathymetry at A02, A03 and A04 may contribute to this variable flow. The mean direction of all the ADCPs suggests a general northward movement of water. The orientation of local isobaths and the principal axis of surface and bottom currents are provided by Table (2). In addition, the principal axis of wind at RR was calculated for each individual deployment periods. For A01 and A02, there was little difference in the surface and bottom orientation of flow. At

A01, the principal axis of flow (bottom and surface) was in a similar orientation to both the principal axis of wind and the local isobaths, which may explain the similarities in bottom and surface flows. A03, A04 and A05 have different orientations of flow between the surface and bottom layers. The bottom layers appear to be more orientated towards the direction of the local isobaths, except at A04, this may suggest topographic steering of the flow at depth.

Site	Orientation local isobath °T	Principal axis bottom,°T	Principal axis surface,°T	Principal axis wind RR
A01	335	303.56	304.07	290.78
A02	56	46.79	47.45	298.78
A03	20	35.28	8.55	293.70
A04	23	306.28	332.76	293.67
A05	45	74.19	279.87	294.65

Table 2: Orientation of local isobath, principal axis of depth-integrated flow, surface flow, bottom flow and wind at Roman Rock for all ADCPs at the individual deployment period. °T refers to degrees measured in clockwise rotation with 0° at North.

In order to identify a schematic of the common circulation patterns within the Bay, the circulation was indexed and averaged according to the response from four main wind sectors (see Figure 25): south to west (S-W), west to north (W-N), north to east (N-E), and east to south (E-S), Figure (28). The surface, bottom and depth-integrated flow were averaged for each ADCP. To determine whether the mean current was representative of the response to the various wind directions or not, methods used in Dufois et al. (2008) have been applied. In Dufois et al. (2008), the significance was computed as the ratio (R) between the magnitude of the mean current vector, $||U_m||$, and the mean of the magnitude of the currents over the time, $\langle \|U(t)\| \rangle^t$, R is given by,

$$R = \frac{||U_m||}{\langle \|U(t)\| \rangle^t}$$

where $\vec{U}(t)$ is the magnitude of the current at the particular ADCP station. The ratio R essentially represents the unidirectionality of the current vector over time. If R is close to 1 (100% significance), the current direction has little variability, and the direction of the mean current vector is an accurate representative of the response to the corresponding wind sector. If R is close to 0 (0%), the current was multidirectional

and therefore the mean vector is no longer an adequate representative.

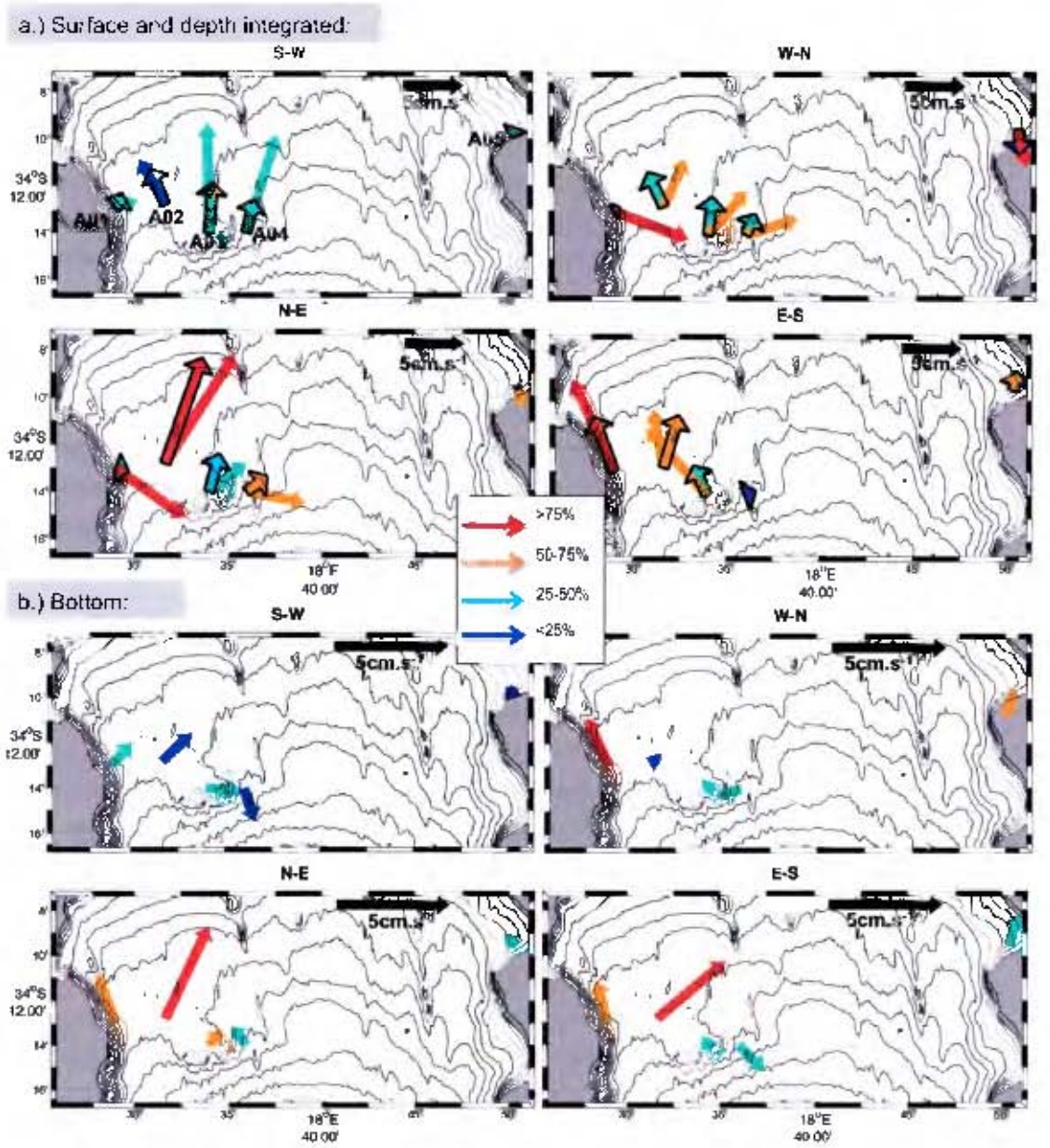

Figure 28: Schematic of the average circulation for a.) the surface and depth-integrated (bold outline) flows and for the b.) bottom flows in response to four modes of wind direction from Roman Rock: E-N, N-W, W-S, and S-E. The arrow colour represents the certainty (R) of flow direction.

In Figure 28, the colour of vector face represents its significance (i.e. red - very significant, dark blue - no significance). The surface and depth-integrated flow (bold outline) is presented separately from the bottom flow, this was due to the different scales of the flow, the bottom flow being much weaker. In the case S-W, all ADCPs stations,

apart for the A03 depth-integrated flow (50-75%), were multidirectional (<50%) and therefore the average was not representative of the circulation over the mooring period. During S-W winds, the flow in the Bay was complex. At A03, the depth-integrated flow was northwards in response to wind.

During W-N winds, mean surface currents for the period of deployment were significant at all the moorings and therefore were a good representative of the flow. The general surface flow was in an eastward and northeastward direction at all ADCPs apart from A05, which was southward. The overall surface flow appears to resemble a cyclonic pattern. The mean depth-integrated flow was not representative. In the bottom layer, moorings A01 (NW flow) and A05 (SSW flow) were significant. These bottom flows were opposite to the surface flow suggesting a mean two-layered flow at the lateral boundaries of the Bay under these wind directions. This explains why the mean depth-integrated flow was insignificant. In the case of N-E winds, the directions of flow were similar to the N-W case. Similarly, A01 had a two-layered flow. The surface flow (>75%) was in a southeastward direction and bottom flow (50-75%) in a northwestward direction. In contrast at A02, the representative mean flow was relatively uniform in direction with depth. Apart from A03 the surface flows were representative of the mean flow. The overall pattern suggests southward flow at the boundaries (A01, A05) of the Bay, and northward at the centre (A02, A03, A04). During S-E winds, the mean surface flow was significant at all ADCPs and in a southward direction. In contrast to N-W and N-E, during S-E, A01 had one-layered flow in the northwestward direction.

Filtered temperature and sea surface heights:

The thermal structure has been identified as an important physical forcing mechanism in False Bay (Gründlingh, 1993; Taljaard et al., 2000). The study was not able to investigate the seasonal fluctuations of temperature, but an investigation of bottom temperature fluctuations on an event scale is presented, Figure (29). The filtered winds and temperatures for each ADCP is given with particular events of interest marked by red and blue shading. The blue shading refers to a decrease of ADCP bottom temperatures at the onset of southward wind (i.e. NW). The red shades refer to an increase in bottom temperatures typically at the onset of a northward wind (i.e. SE).

The exception was found at A05, located in Gordon's Bay, which was opposite in its response. Here, during a northward wind there was a decrease in bottom temperatures and during a southward wind an increase. Evidence of upwelling cells have been found to occur off Gordon's Bay after a period of strong SE winds (Cram, 1970; Grindley and Taylor, 1970; Jury, 1985; Wainman et al., 1987; Taljaard et al., 2000). The bottom winter temperatures were in a similar range (11 14°C) to the results found by Gründlingh (1993).

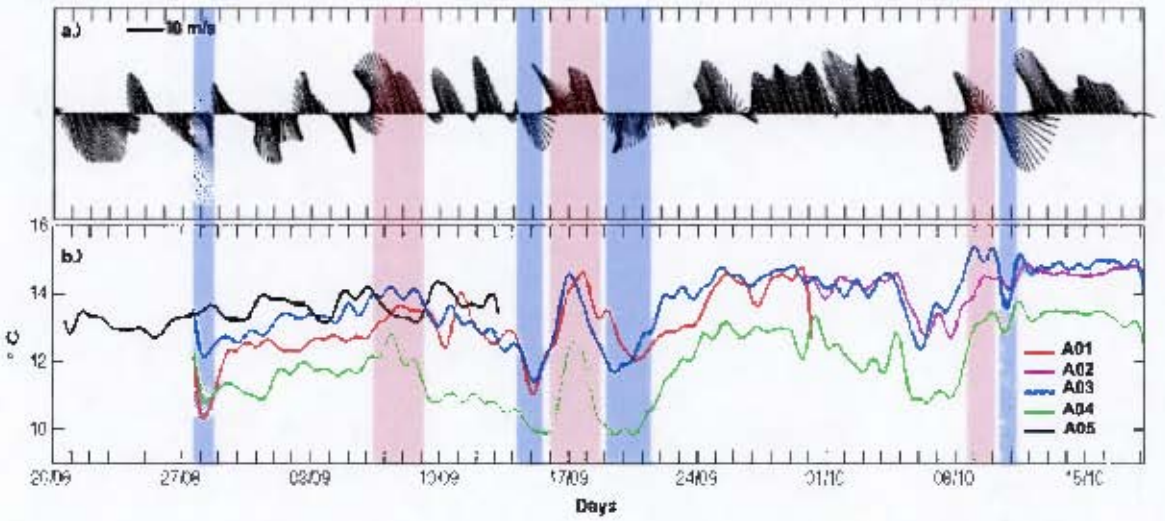

Figure 29: Filtered wind at Roman Rock (a) and ADCP bottom temperatures °C (b). The pale red and blue bars represent periods of SE (northward) and NW (southward) winds respectively.

Following an example provided by van Ballegooyen (1991) which indicated evidence of potential shelf waves influencing False Bay, an investigation was carried out on daily mean averaged sea level fluctuations at each ADCP and tidal gauges from Simon's Town and Port Nolloth, Figure (30). The results suggest fluctuations of daily mean sea levels with the period of several days to a week with maximum amplitudes of ~0.2m. The Simon's Town tidal gauge data has been provided for comparative purposes and agrees with the ADCPs. The Port Nolloth tidal gauge has been provided to investigate whether it was a remotely forced perturbation or rather due to local wind and pressure changes. Port Nolloth is situated on the west coast of South Africa, approximately 570km from Cape Town. The Port Nolloth fluctuations agreed nicely with the fluctuations found in the Bay. The ADCPs have a lag of approximately one-two days with

the Port Nolloth SSH, suggesting the perturbation might have been travelling down the coast. The fluctuations have similar properties identified by Schumann and Brink (1990). Schumann and Brink (1990) found that these perturbations travel in an anti-clockwise fashion from west coast to east coast of Southern Africa. The fluctuations might suggest shelf waves, but further investigation of winds and atmospheric pressure would be needed to elucidate this. These fluctuations of SSH may contribute to the complexity of flow in the Bay.

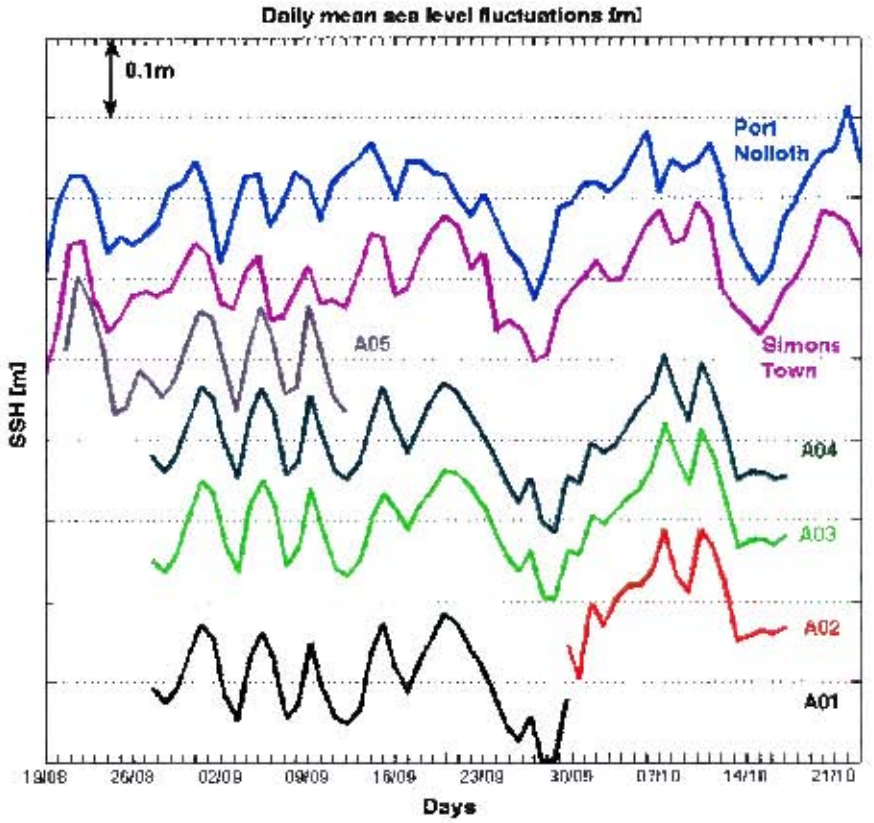

Figure 30: Daily mean sea level fluctuations (m) for all ADCPs and tidal gauges positioned at Simon's Town and Port Nolloth.

4.1.4 Event (daily) scale

To further explore the relationship between the temperature, wind and currents, a comparison was made for an individual event during the deployment period. The single event that has been presented from the rather short observational data set has been selected where concurrent current and satellite data were available. The satellite SST data is affected by clouds, which made it difficult to capture the NW wind events

typical of passing cold fronts. The MODIS Terra SSTs, bottom temperatures and winds are provided by Figure (31) for the 09-11 September 2010.

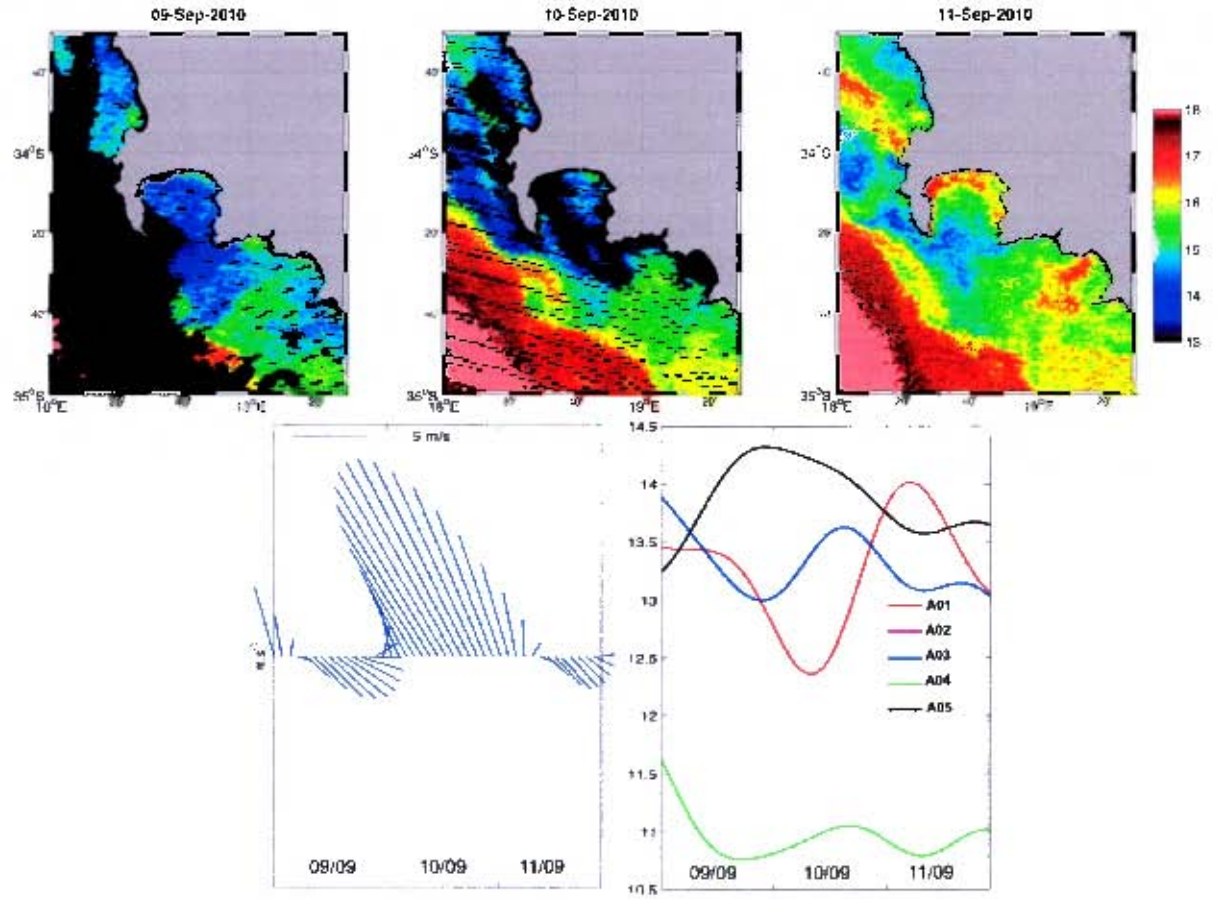

Figure 31: SST (°C) MODIS Terra morning data (top), black shades are areas with no data, wind ($m.s^{-1}$) at RR (bottom left), ADCP bottom temperatures (°C, bottom right) for 9-11September 2010.

This particular event was of interest as it included a wind reversal from NW to a SE. During the 9th of Sept, the winds were light NW. The SSTs inside the Bay were fairly uniform (14-15°C), with warmer waters in the NE corner of the Bay near Gordon's Bay. The bottom temperatures decreased at A01, A03 and A04, and increased at A05 during the NW, agreeing with the previous results. During the 10th, the wind reversed to a strong SE, which persisted throughout the day. In response, the bottom temperatures increased at A01, A03 and A04 and decreased at A05. A01, appeared to have lagged behind A03 and A04, increasing in temperature only by midday. By the morning of 11th, the warmer SST had been advected into the NW corner of the Bay, presumably in response to the strong SE from the previous day. Midday on

the 11th, the wind reversed to light NW. The bottom temperatures decreased during the transition between 10th-11th when the winds reversed to light NW. These results have demonstrated the SST and bottom temperature change under two different wind forcing. During NW wind, the SSTs were uniform and cold, with warm patch in the NE corner. The onset of the strong SE brought warmer SSTs into the NW corner of the Bay. The bottom temperatures behaved in a similar fashion, warming/cooling on the western and cooling/warming eastern side during SE/NW respectively.

The observational results have shown that the tides contribute to a significant proportion of flow. The residual flow at the boundaries of the Bay was polarised with the coastline and bathymetry. This flow was unidirectional and strongly correlated with wind. In the middle of the Bay the flow was complex, agreeing partly with the complex bathymetry beneath it, suggesting topographic steering. The variability of flow and weak correlation with wind suggests that other forcing mechanism were responsible for driving the circulation in the middle of the Bay. The fluctuations of wind at an event scale can result in a bottom temperature change of as much as 2-3°C. Fluctuations of daily mean SSH may allude to shelf waves but further investigation is required.

4.2 Numerical modelling

In this section the results of the simulations for each consecutive modelling experiment is presented. For every configuration, a three year run was carried out to allow for the appropriate spin up time needed by the model to reach statistical equilibrium. The diagnostics of each experiment is given below. The seasonal circulation and thermal structure of each configuration is presented in a comparative fashion.

4.2.1 Experiment One: Influence of bathymetry

Diagnostics: Time evolution of averaged tracers.

The model's reliability can be determined by examining the degree to which it conserves the averaged value of its tracer fields (Penven et al., 2001). As Penven et al. (2001) suggest, this can be done for example by volume averaging the temperature field for the entire domain. In Figure (32), the diagnostics for the flat bottom (left)

and the high-resolution (right) runs are presented. It is clear from this figure that both configurations exhibited stable boundary conditions as the volume, kinetic energy, heat and salt properties were conserved and hence no leakages at the surface or boundaries occurred. The surface and volume averaged kinetic energy (KE) can be used to estimate the spin-up time (Veitch et al., 2009). The flat bottom run reached statistical equilibrium almost immediately whereas the high-resolution bathymetry run took approximately one to two months of spin up time. The results of the surface averaged KE highlight the models response to varying surface forcing. In the summer months during upwelling and the strongest surface forcing, the surface averaged KE was the highest. A comparison between the volume averaged temperature, shows that both runs illustrated seasonal structure, with warmer temperatures occurring during summer months and cooler temperatures during the winter months. The flat bottom run has warmer volume averaged temperatures than the high-resolution run. The reason for this was that the flat bottom run was 50m deep through out the entire domain, whereas the high-resolution bathymetry has much deeper (>100m) water outside of the Bay. Therefore the volume averaged temperature for the high-resolution was lower because it included a larger volume of deep water into the average. This explanation was also the reason why the volume averaged salinity was higher in the flat bottom run. Additionally, the difference in depth explains why there was a large disparity in the volume anomaly when comparing the runs. The high-resolution bathymetry run was an order of magnitude larger in volume than the flat bottom run. The volume anomaly is the difference in the entire volume of the domain for each time step from the mean volume of the entire period. While the volume fluctuations were relatively small, they can be explained as a response to the seasonal changing temperatures.

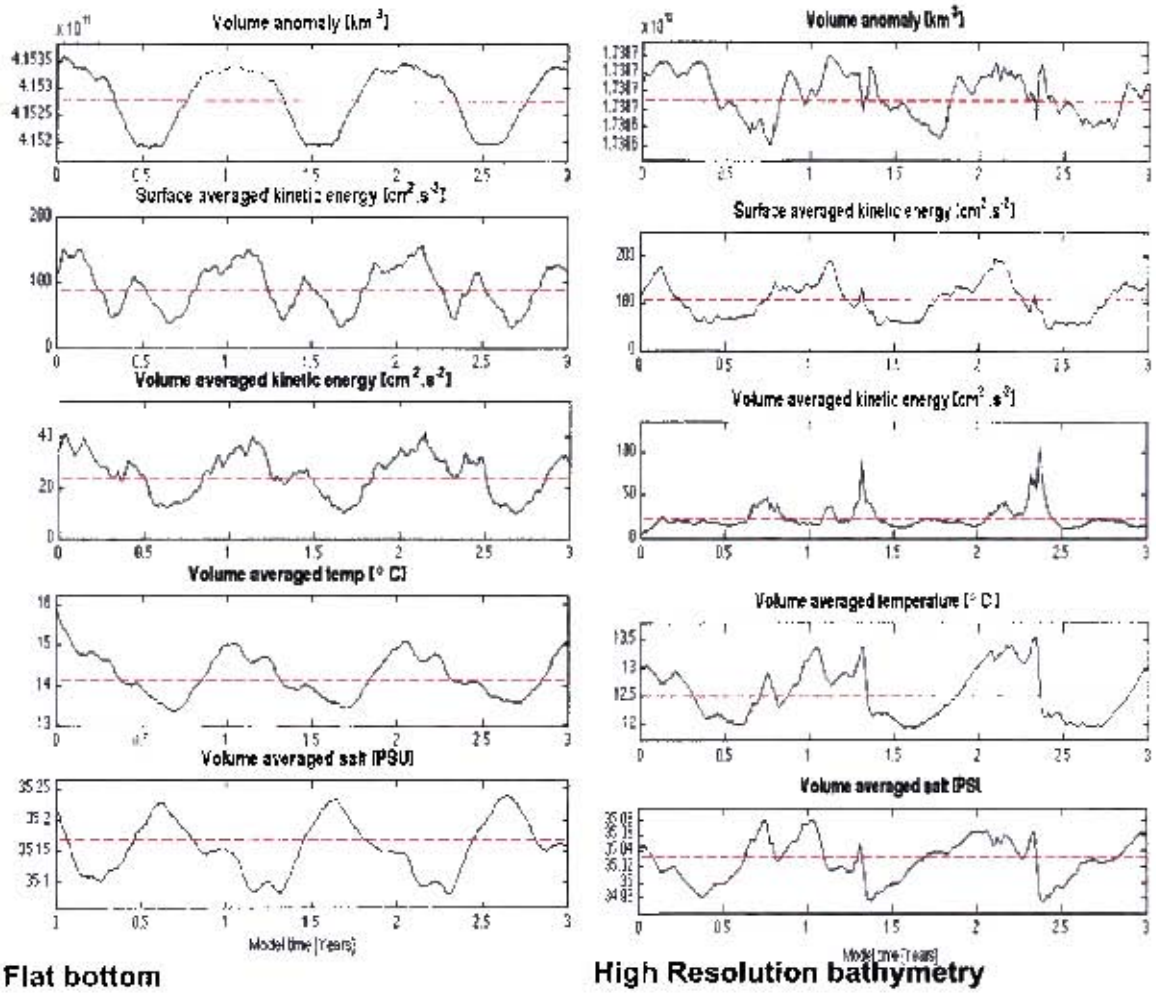

Figure 32: Diagnostics for the flat bottom (left) and high-resolution CGS bathymetry (right) configurations. The dotted red line is the mean.

The high-resolution bathymetry run had more variability associated in the volume anomaly structure with similar variability found in the other averaged tracers for this run. This variability may be attributed to an increase in the complexity of the simulation by adopting the high-resolution realistic bathymetry. The diagnostics for both runs have shown that the model configurations were reliable and stable as all averaged tracers are conserved.

Comparisons in seasonal mean circulation and thermal structure

To prove the hypothesis given by Experiment One, a comparison was drawn between the flat bottom and the high-resolution CGS bathymetry simulations. The hypothesis suggested that the bathymetric features at the mouth of the Bay restrict the inflow of

offshore circulation and in doing so reduces a proportion of the cold bottom water that enters the Bay, thus having an influence on both the Bay's circulation and thermal structure. To investigate this, Figure (33) compared vertical sections of the seasonal mean v-component (north-south) of flow for summer (JFM) and winter (JAS) at the mouth of the Bay. The northward flow is represented by positive velocities, which are in shades of red and the southward flow by negative velocities in shades of blue. Additionally, the flow has been overlaid with the isotherms in order to explore the influence of thermal structure on the flow.

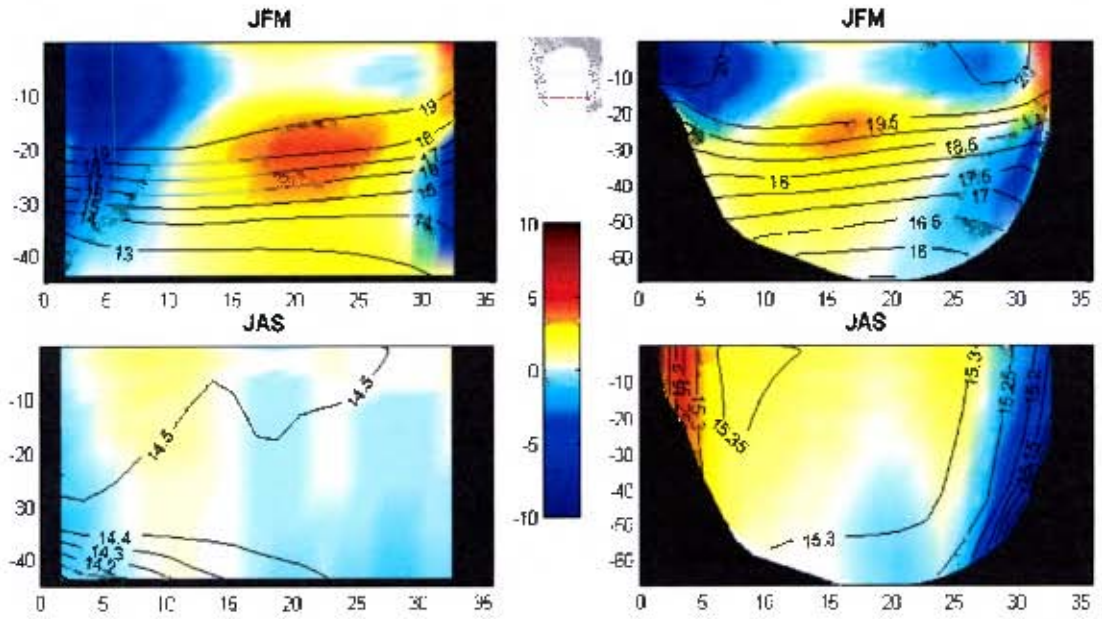

Figure 33: The N-S seasonal mean current velocities ($cm.s^{-1}$) overlaid with isotherms (°C) for summer (JFM) and winter (JAS).

In this figure, by comparing the isotherms, a clear seasonal shift in the thermal structure was evident. Both the flat bottom and the CGS bathymetry runs demonstrated seasonal change from stratification in summer to a well mixed water column during winter. This seasonal fluctuation in stratification and mixing has been documented in previous observational studies such as Atkins (1970a) and Gründlingh (1993). This study has provided the first numerical model to represent these fluctuations of thermal structure in the Bay. The first important difference to note when comparing the isotherms was that the bottom temperatures during the summer mean for the CGS bathymetry (16°C) run were warmer than the flat bottom configuration (13°C).

Similarly during winter the CGS bathymetry run was on order of 1°C warmer. In line with this disparity, it appears that the stratification for the flat bottom (13-19°C) is more intense than the CGS bathymetry (16-20°C) run. To confirm this, the Brunt-Väisälä Frequency (BVF) has been calculated for the same vertical section and plotted in Figure (34).

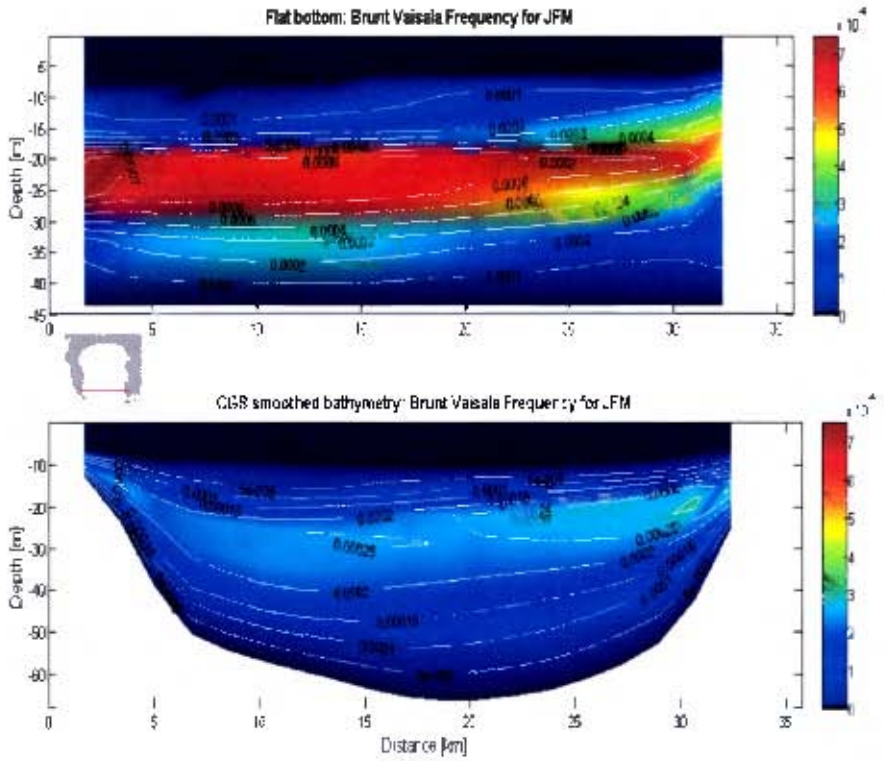

Figure 34: Vertical section of the Brunt-Väisälä Frequency for JFM seasonal mean across the mouth of the Bay.

The BVF is a measure of water column stratification (stability) and is based on principles of harmonic oscillators. The BVF frequency was higher for the flat bottom with maximum at $7 \times 10^{-4} s^{-1}$ whereas the CGS bathymetry had a maximum of $2.5 \times 10^{-4} s^{-1}$. The higher the frequency the more intense the stratification, this is based on the oscillation of a particle if displaced upwards in a stratified water column. The larger the difference between the surface and bottom water densities, the higher the frequency of oscillation. While the BVF vertical sections do not bring about any new information they do serve to further elucidate the stronger stratification found in the flat bottom run.

Similar in nature to the seasonal fluctuations of temperatures, the vertical flow structure behaved differently between the seasons. During summer, with a stratified water column, the flow had a two-layered structure with a stronger anticyclonic flow at the surface and a weaker clockwise flow in the bottom layers ($<5cm.s^{-1}$). The maximum mean summer velocities were on an order of $10cm.s^{-1}$. During winter when the water column was mixed, the flow was weaker and uniform with depth. An important difference can be seen when comparing the flow structure between the two configurations. During summer, the two-layered surface flow pattern was similar between the two runs with some discrepancies in the bottom layers, whereas in winter the difference in the flow structure was notably more significant throughout the entire column. During winter, the CGS bathymetry run has strong boundary flow associated with the location of shallow waters. The flat bottom run with constant depth has weaker current velocities with no boundary flow evident.

To further investigate these findings, Figures (35 and 36) show the bathymetry overlaid with vertically integrated flow. In order to investigate the False Bay region closely, the figures were a smaller extraction from the larger domain. In summer time the two-layered system was split up and the surface and bottom layers were vertically integrated separately, Figure (35). In this figure, the surface layers flow for the flat bottom and CGS bathymetry was very similar. A potential explanation for this similarity was that during the summer stratification, the surface layers were decoupled from the bottom layers and were primarily driven by wind, both configurations employed the same wind forcing. Therefore the bathymetry appeared to have had little influence on the simulated surface flows during summer. The bottom layers flow was very different between runs. In the flat bottom configuration, the circulation was flowing directly into the Bay and in the CGS bathymetry run the bottom flow was much more complex and was steered away from the mouth of the Bay at Rocky Bank.

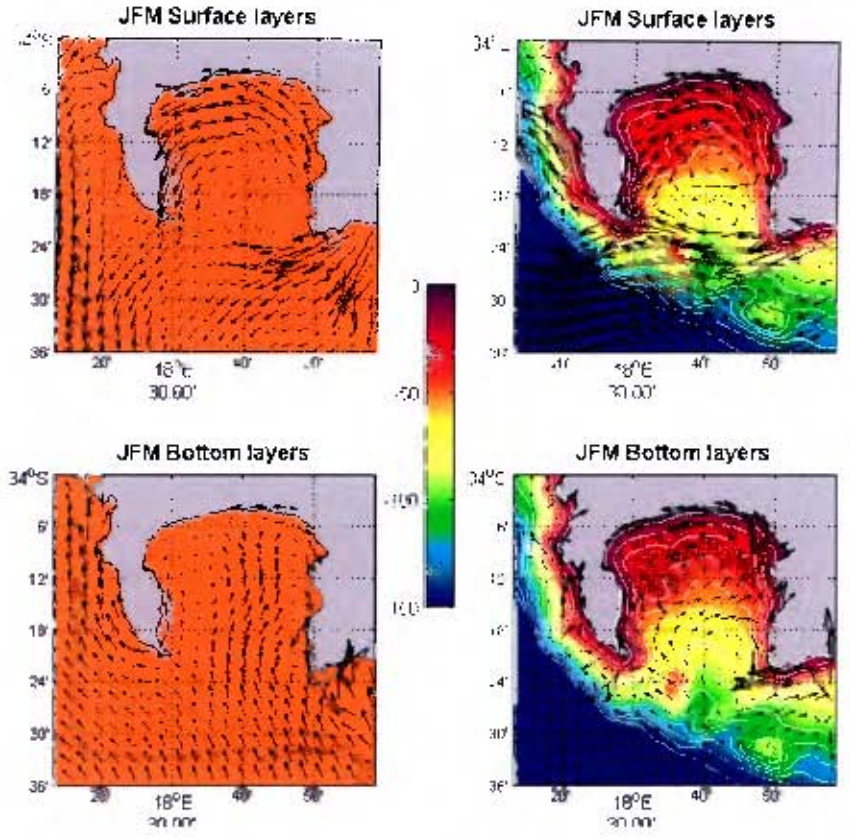

Figure 35: Bathymetry overlaid with vertically integrated surface layers flow ($cm.s^{-1}$) for JFM. Flat bottom run on the left and CGS bathymetry run on the right

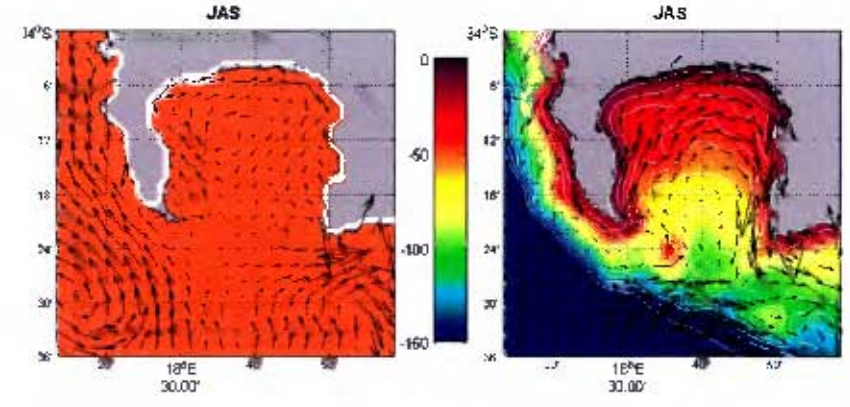

Figure 36: Bathymetry overlaid with vertically integrated bottom layers flow ($cm.s^{-1}$) for JAS. Flat bottom run on the left and CGS bathymetry run on the right

During the winter months, Figure (36), both runs illustrated a cyclonic flow with depth. However, the shallow water at the boundaries of theCGS bathymetry configuration resulted in stronger boundary flow. To illustrate the topographic steering effect of Rocky Bank, a vertical section of W-E flow is given in Figure (37).

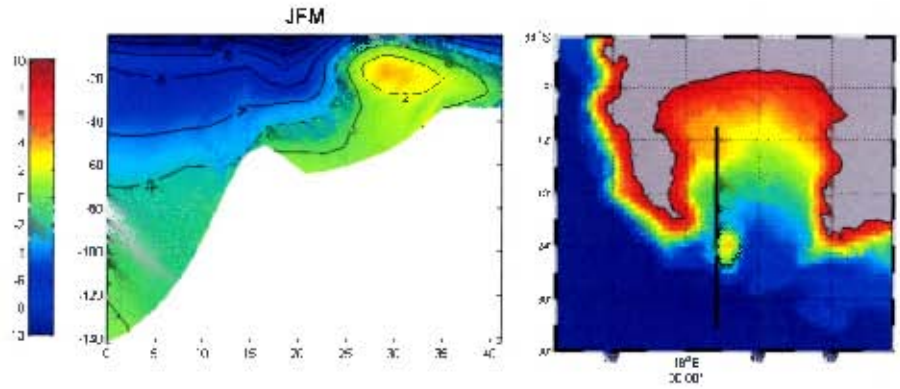

Figure 37: W-E horizontal flow ($cm.s^{-1}$) transect across Rocky Bank (left) and the position of transect on bathymetry (right). Westward represented by blue colours and eastward by red.

The results have shown that the bathymetry has important contributions to defining the circulation and thermal structure in the Bay and thus high-resolution bathymetry must be included in the further modelling experiments. While the results shown are promising, the vertical thermal structure was still too high relative to previous observational data (Atkins, 1970a and Gründlingh, 1993), by utilising higher resolution boundary conditions it is hoped to find improvements in the range of simulated temperatures.

4.2.2 Experiment Two: One-way offline nesting of boundary conditions

Adopting the high-resolution bathymetry (CGS) from Experiment One, this experiment addressed the influence of offshore conditions on False Bay. The offshore influence was investigated by employing two different boundary conditions (BCs), first by using uniform BCs from the WOA and then by adopting spatially more diverse BCs generated through an offline nesting approach.

Diagnostics: Time evolution of averaged tracers.

The diagnostics for the configurations are given in Figure (38). All averaged values of the tracer fields were conserved confirming the reliability of the models. The boundary conditions were stable as the volume, kinetic energy, heat and salt properties were conserved and no leakages at the surface or boundaries occurred. The first striking difference between diagnostics of the two runs was the increase in variability for the

higher resolution BC run. This increase in variability was due to the increase in the resolution of boundary conditions which, adds more complexity to the system. The increase in variability reflects the first steps from an idealised approach towards a more 'realistic' configuration.

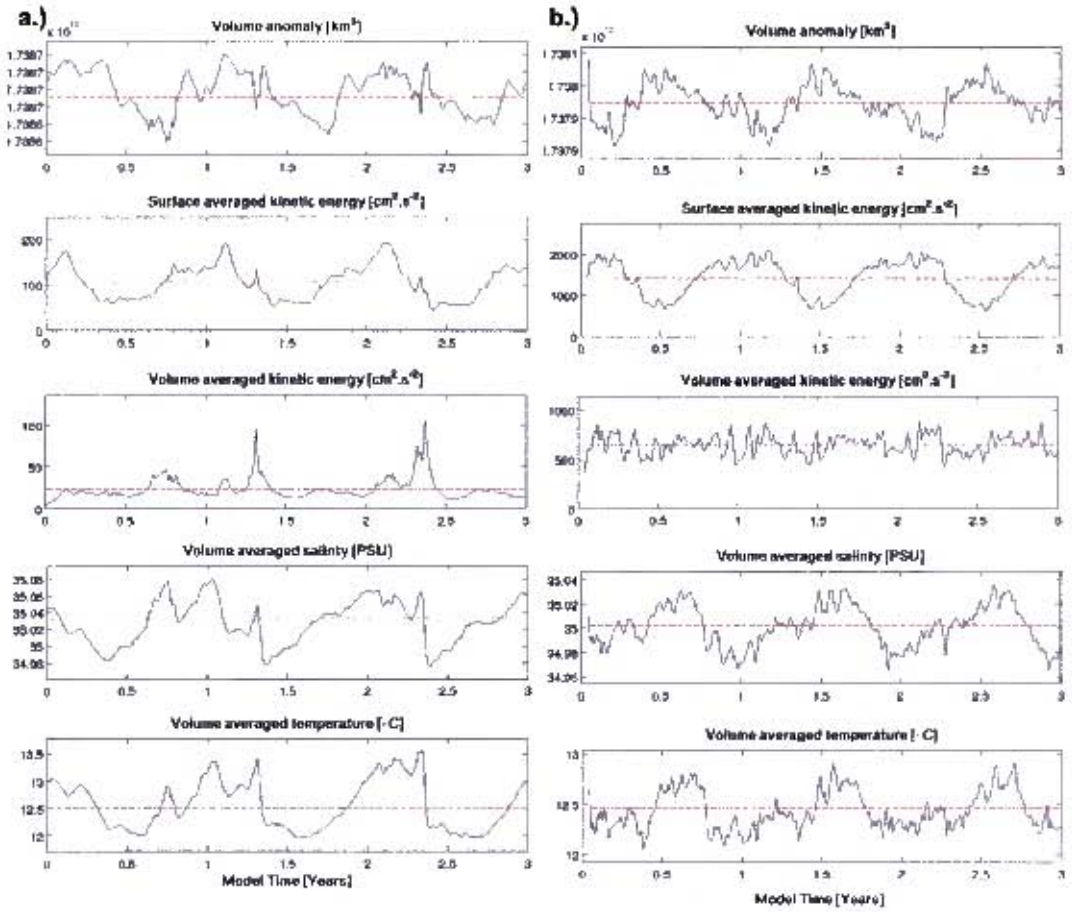

Figure 38: Diagnostics for the WOA (1°) configuration (a) and the offline nesting of boundary conditions (1/27°) configuration (b). The dotted red line is the mean.

The next interesting difference was that the lowest volume averaged temperatures occurred during summer months with the high-resolution boundary conditions run. The volume averaged temperatures dropped from October reflecting the start of the upwelling favourable winds and increased during April/May as the winter well mixed water column conditions occur in the Bay. The cold bottom waters associated with upwelling must have been cold enough to bring down the volume averaged temperature despite the increase in SST during summer time. To substantiate this, by looking at the volume averaged salt, a similar seasonal signal was seen. During the upwelling

favourable winds in the summer months cold fresher water was upwelled into the Bay. This bottom water was fresh enough to bring down the average despite the rise in salinity at the surface from evaporation in summer. Similarly the surface and volume averaged KE showed peaks during summer months in response to the stronger upwelling favourable winds.

Comparisons in seasonal circulation and thermal structure

To investigate the effects of adopting the higher resolution BC, the following results compared vertical sections and surface plots of temperature and circulation. In order to make assessments of whether the higher resolution BC has led to an improvement to the thermal structure, the results have been compared to previous observational data.

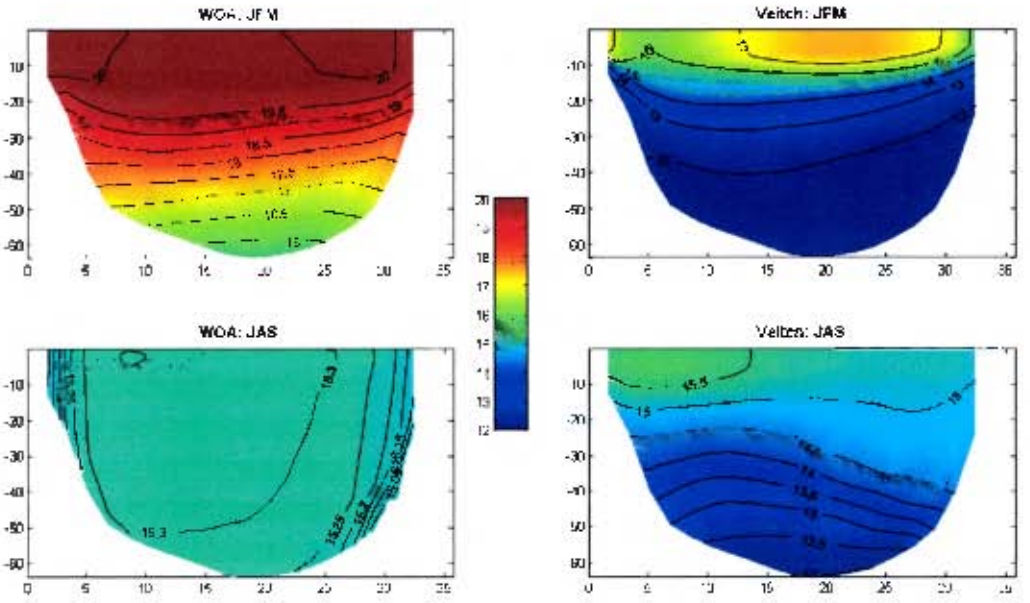

Figure 39: A comparison between the model solutions for vertical temperatures (°C) across the mouth of False Bay overlaid with isotherms, WOA BC configuration (left) and the offline nested BC (Veitch) configuration (right)

The simulated seasonally averaged vertical temperatures (°C) across the mouth of False Bay were compared for the two configurations in Figure (39), the results of the WOA 1° BC run (left) and offline nested 1/27° BC run (right) . During the summer seasons (JFM) both runs illustrated stratification however there was a significant difference in the temperatures between the simulations. In relation to the WOA configuration, the offline BC has resulted in a significant decrease in both surface and

bottom temperatures for JFM and JAS. During JFM, the temperature difference was as much as ~3-4°C. The thermal structure of the offline nested BC simulation agreed nicely with the results of (Atkins, 1970a), who found temperature ranges of 10-18°C for JFM and 13-15°C for JAS, Figure (6).

The surface structure of temperatures from the offline nested BC configuration have also shown some improvement relative to satellite observations, Figure (40).

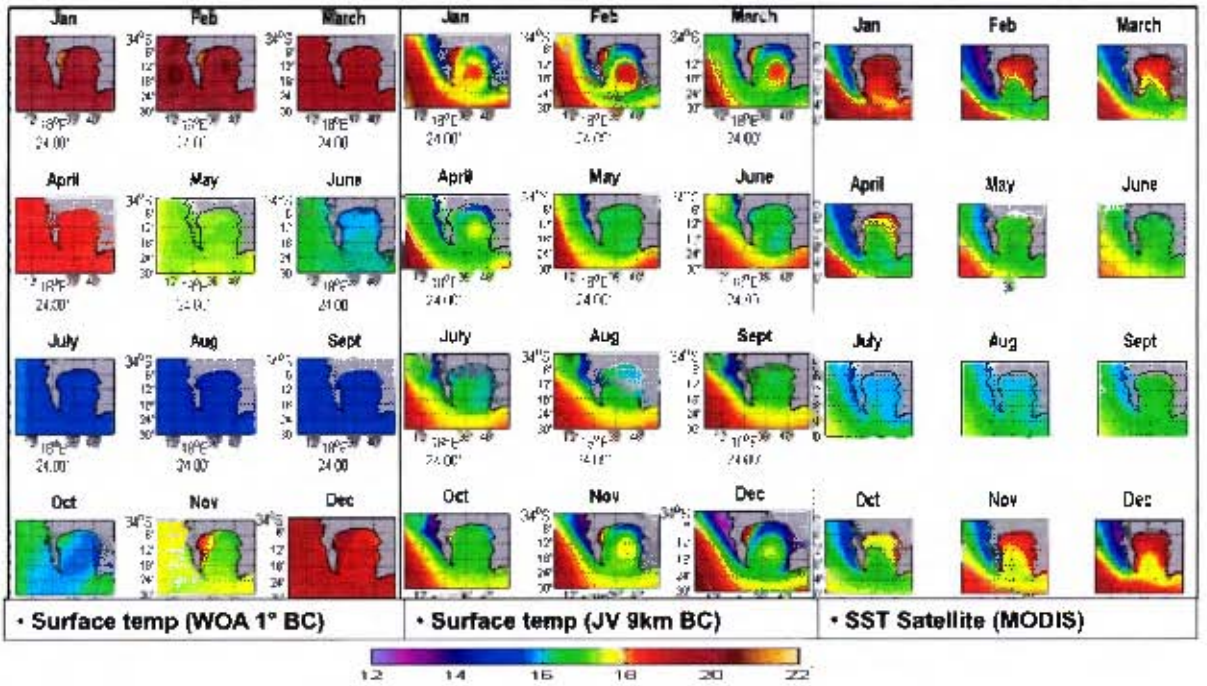

Figure 40: A comparison in simulated monthly mean SSTs (°C) of the WOA configuration (left) and the offline nesting configuration (middle) with the observed MODIS 1km resolution satellite data (right)

Here, it can be seen that the offline nested BC configuration (middle) produced spatially diverse SSTs, whereas the WOA BC (left) produced uniform SSTs. This higher spatial diversity agrees with the satellite observations (right), which were in similar temperature ranges. However there were some discrepancies, for example, the large upwelling cell occurring at Gordon's Bay, warmer SSTs plume in the centre of the Bay during summer and the warmer offshore water during July, August and September was not present in satellite data. The large upwelling cell found at Gordon's Bay during summer months in the offline nesting BC, might be exaggerated due to the lack of wind shadow which has been found to occur in this region of the Bay (Jury, 1991). Although, this feature was not present in the monthly mean satellite data, upwelling

cells off Gordon's Bay have been observed in past studies (Cram, 1970; Grindley and Taylor, 1970; Jury, 1985; Wainman et al., 1987; Taljaard et al., 2000).

A comparison of the seasonally averaged vertical v-component of the simulated velocity shows that there has been an intensification of current velocities for the offline BC. The intensification was most apparent in the surface layers of the JFM seasonal average. The surface flow was considerably stronger than the bottom flow during JFM, this agreed with observations from Gründlingh (1992) who found the bottom waters move slower during summer months. During JAS the northward flow has intensified on the western boundary while the southward flow on the eastern boundary has decreased in velocity. Due to the lack of current velocity observations, it was not possible to asses whether or not adopting the new BC have led to an improvement to the seasonally averaged circulation.

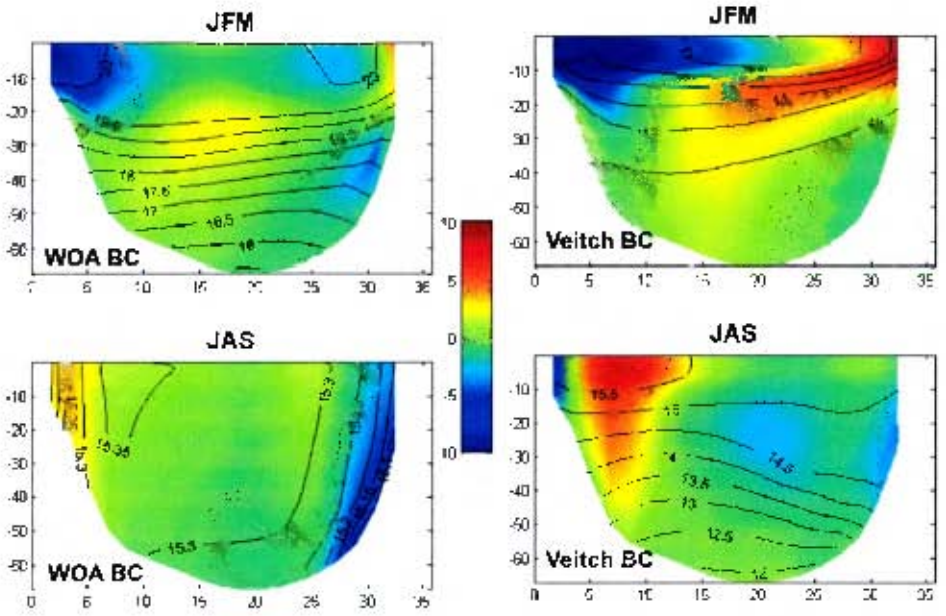

Figure 41: Seasonally averaged vertical sections of the simulated v-component of velocity ($cm.s^{-1}$) across the mouth of the Bay overlaid with isotherms (°C) for WOA BC (left) and offline nesting BC (right) configurations.

4.2.3 Experiment Three: Surface forcing restoring terms

The purpose of this experiment was to improve upon simulated SST structure of Experiment Two, Figure (40). In the results for the previous experiment, it was noted that during summer the simulated SSTs showed large upwelling cell off Gordon's Bay, which

was not evident in the satellite images. Another summer difference was the simulated warm water in the middle of the Bay, a result of the anticyclonic flow. In order to address the discrepancies in the SST structure, the MODIS monthly mean 1km data was utilised as the SST restoring term. In previous experiments, the model configurations have incorporated the Pathfinder SST climatology of 9.28km as a restoring term. The problem with this approach was that the MODIS SST satellite data could no longer be used as validation, resulting in a loss of data independence.

Diagnostics: Time evolution of averaged tracers.

The diagnostics for the MODIS configuration were compared with the Pathfinder restoring configuration from the previous experiment, Figure (42).

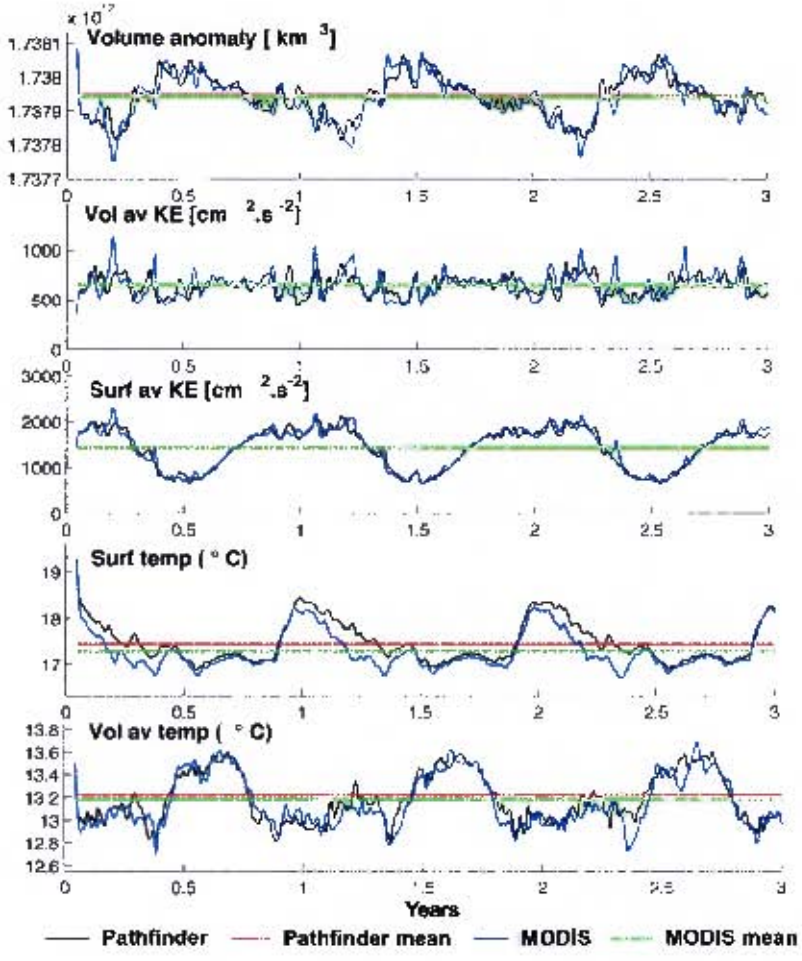

Figure 42: A comparison of diagnostics for Pathfinder SST restoring term (black) with the MODIS SST (blue). Time axis is years. Dotted lines are Pathfinder (red) and MODIS (green) means.

The temperature tracers were conserved, confirming the reliability of the model. The boundary conditions were stable as the volume, kinetic energy and heat properties were conserved and no leakages at the surface or boundaries occurred. The diagnostics for the two configurations do not vary significantly, with only subtle changes in the finer structure. The largest difference was seen in the surface temperatures between the January and May. During these months, the averaged surface temperature for the domain decreased as a result of the MODIS restoring term. During the winter months, there was very little change in the surface averaged temperatures.

Comparisons in monthly surface thermal structure:

To investigate the impact of adopting the higher resolution MODIS data set for the SST restoring term, a comparison has been made between the simulated monthly mean SSTs of the two configurations, which utilised different restoring terms (MODIS-pathfinder), Figure (43). It is evident that the MODIS restoring term has impacted the simulated SSTs. The most prominent differences occurred during the summer months, where the two restoring products utilised had the largest differences, Figure (21). During these summer months, as a result of the MODIS SST restoring, there was a decrease of temperature in the centre of the Bay. The decrease of temperature helped to reduce the warm pool of simulated SSTs found in the Experiment Two. A decrease of temperature off Cape Point region has resulted in an enhancement of the upwelling cell located there. During winter months, the SSTs generally decreased in the middle of the Bay.

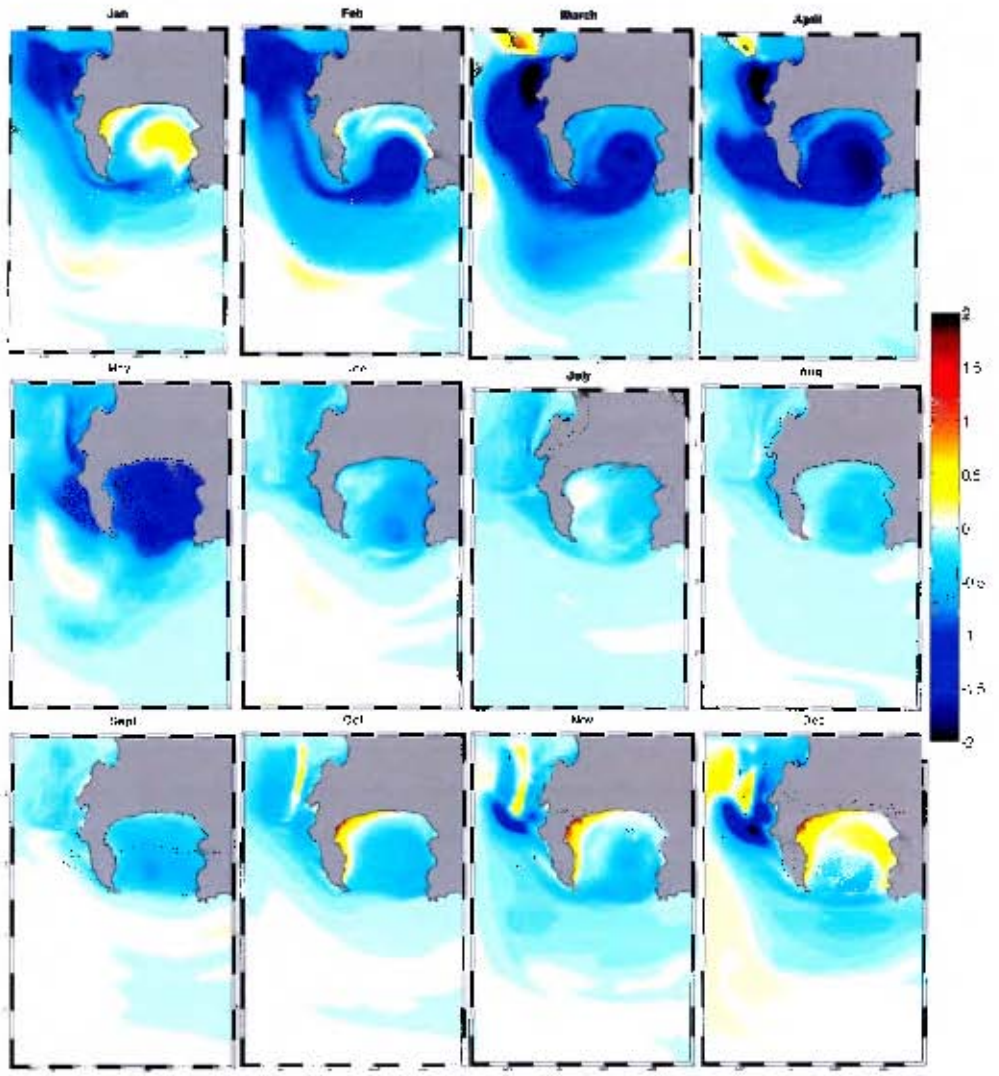

Figure 43: The simulated SST (°C) difference between the MODIS and the Pathfinder restoring term configurations.

While, the MODIS restoring term has resulted in a decrease in the warm pool of water in the centre of the Bay, it was not able to remove the large upwelling cell off Gordon's Bay. Higher resolution wind structure, which includes features such as deep/shallow SE and wind shadows, is the next step towards improving the SST structure.

5 Discussion and conclusion

In this Chapter, results of the observations and idealised process modelling experiments have been synthesised and compared with previous studies. The main goal of this dissertation was to investigate the physical forcing influencing the circulation of False Bay. With this in mind, the discussion has been split into the main forcing mechanisms identified previously as being key in understanding the circulation (see § 2.3). In each section the modelling and observational results are discussed. The discussion has excluded the effects of wave forcing as this was not addressed in this study. The results of this study and previous studies have been briefly discussed in a global context.

Thermal structure

The thermal structure is believed to have important influences on the circulation of False Bay. In the review by Taljaard et al. (2000), it was anticipated that the stratification of the water column might result in a decoupling of the surface and bottom flows. As a consequence of this two-layered system, Taljaard et al. (2000) postulated that the surface flow might be more directly influenced by wind forcing, whereas the bottom flow is weaker, tending to flow in a different direction.

The seasonal evolution of the thermal structure was investigated through numerical modelling. The results showed significant seasonal differences; both vertically and horizontally. In the vertical, the simulated seasonal structure fluctuated from being highly stratified (11°C on the bottom, 18°C at the surface) in summer to weakly stratified (12.5°C on the bottom, 15.5°C at the surface) during winter. The results agreed with previous studies, see Figure (6), which observed seasonal fluctuations from a stratified water column during summer (10-18°C) to a well mixed column during winter (13-14.9°C) (Atkins, 1970a; Gründlingh, 1993; and Wainman et al., 1987). The model simulated bottom temperatures were 1-2.5°C colder during summer. This corresponds closely to the difference of 1-3°C found by Atkins (1970a). As discussed in Taljaard et al. (2000), the results reflect the increased upwelling under typical summer SE winds, along with the inflow of bottom water from the adjacent shelf, which has been observed to be colder in summer (Swart and Largier, 1987). The same reasoning can be applied in understanding the simulated model results.

The seasonal changes in thermal structure were mirrored by the seasonal fluctuations in the v-component of flow. During the summer months, the simulated flow was two-layered in response to the stratification. The surface layers were lighter and had larger mean velocities (>10cm.s^{-1}) in an anti-clockwise direction. The bottom layers were denser and the flow was weaker (<5cm.s^{-1}) in a clockwise direction. The result agrees with the study by Gründlingh (1992), who found the bottom waters to move slower during the summer months. During the winter months, the flow was uniform with depth, responding to a well mixed water column. The model results confirm the postulation given above by Taljaard et al. (2000).

Like the vertical structure, the horizontal thermal structure undergoes a seasonal change within the Bay. The model results demonstrated seasonal differences in SST structure. During summer months the simulated SSTs were spatially more diverse (12-21.5°C), whereas in winter months the SSTs distribution was more spatially uniform (13-16.5°C). This result agrees with both the MODIS satellite SSTs (JFM: 12.9-21.8°C, JAS: 13.7-15.9 °C) and the observations made by Atkins (1970a). There were some discrepancies in the distribution of the simulated SSTs in relation to the satellite observations. In the simulated SSTs, a large upwelling cell off Gordon's Bay was a persistent feature during the summer mean which was not evident in the satellite summer monthly mean composites. While there have been past observations noting the occurrence of a small upwelling cell at Gordon's Bay (Cram, 1970; Grindley and Taylor, 1970; Jury, 1985; Wainman et al., 1987; Taljaard et al., 2000), this did not appear to be a realistic feature.

An attempt was made to reduce the model simulated upwelling cell. This was done by restoring the model SSTs to the more finely detailed MODIS satellite monthly mean SSTs. The results had little impact on reducing the size of the upwelling cell. However, this approach decreased the warm temperatures in the centre of the Bay. These warmer temperatures were due to the anticyclonic circulation of the Bay. The large upwelling cell simulated by the model was likely a result of the uniform SE wind forcing which did not have the spatial variability typically observed in summer months. These winds excluded important features such as the deep and shallow SE winds. The occurrence of a wind shadow on the eastern side of the Bay has been found to occur during shallow SE (Wainman et al., 1987). In reality, this wind shadow may reduce the upwelling on

the eastern half of the Bay. As upwelling is strongly driven by wind shear (Jury, 1985), a high spatial resolution wind field that captures these features is needed to accurately simulate near coastal upwelling in the Bay.

Temperature measurements made by the ADCPs and daily satellite SST data allowed for an investigation of the observed daily variations during the winter months. This provided some insight to the daily variations of bottom temperatures under varying wind speeds and directions. The model, which was forced by uniform climatological winds from only the NW direction during winter, was not able to reveal this fine scale detail. The results showed that typically with the onset of a northerly wind, the bottom temperatures decreased for all ADCPs except at A05 (Gordon's Bay), which increased. In contrast during southerly winds, bottom temperatures increased at all ADCPs apart for A05, which decreased. Therefore, the bottom temperatures on the western and eastern half of the Bay reacted differently to different wind conditions.

One hypothetical scenario explaining the bottom temperature structure under a SE wind, could be that warm surface water within the Bay was advected towards the northwestern boundary and then downwelled, thus warming the bottom layers of the western half of the Bay. This movement of warmer surface waters in False Bay was observed in the sequence of satellite SST images. The results of the observed mean circulation under a SE wind showed northwestward surface currents at A01, A02, A03 and A04, which could bring warm waters to the NW corner of the Bay. The bottom circulation at A03 and A04 indicated a flow in the opposite direction towards the Bay mouth. The eastern half of the Bay is known to be prone to upwelling under a SE wind, which might explain why A05 decreased in temperature.

The opposite could potentially be true under NW forcing; surface waters on the northwestern side of the Bay are blown offshore with cold bottom waters advected in from the mouth of the Bay to replace the surface water. This was seen in the mean circulation under NW, especially at A01, where surface flow was southeastwards and bottom flow was northwestward. The eastern side of the Bay could trap warmer surface waters resulting in downwelling at regions like Gordon's Bay, hence the increase in bottom temperatures.

The changes in the thermal structure have important implications on both the physical and biological functioning of the Bay. From modelling the physical forcing

and response, it has been shown that the circulation in the Bay can fluctuate between one-layered to two-layered flow in response to the transition from a well mixed to a stratified water column. The flow velocities were also affected: during stratified conditions bottom velocities were weaker than the surface flow, which was driven by the wind.

There are important biological implications transpiring from structural changes in the water column. Biologically, False Bay is an important region as it is recognised as an area with elevated phytoplankton biomass (Pitcher et al., 2010). Harmful algae blooms have been known to occur in False Bay during late summer months (Grindley and Taylor, 1970; Horstman et al., 1991; Pitcher et al., 2008, 2010). It is believed that the Bay acts as a site of accumulation for the widespread blooms forming on the Western Agulhas Bank that enter the Bay during upwelling favourable winds (Pitcher et al., 2010). The combination of a cycle of upwelling of nutrient rich waters followed by strongly stratified conditions in the Bay further enhances algal bloom development (Taljaard et al., 2000; Pitcher et al., 2010). Vertical mixing and oxygenation of the bottom waters may be suppressed by strong stratification in the Bay leading to anoxic conditions (Taljaard et al., 2000). The occurrence of harmful algae blooms has been well documented in False Bay and has been found to cause a large number of marine mortalities. During 1962, an estimated 100 tons of fish and invertebrates washed up on the beaches from Strand to Gordon's Bay (Grindley and Taylor, 1970; Pitcher et al., 2008). During 1980, a bloom was responsible for extensive marine mortalities including 40 tons of abalone. More recently, in 2007, a bloom persisted for three and a half months, which resulted in three fish-kill events and two shellfish-kill events.

Bathymetric forcing

According to Gille et al. (2004), bathymetry is said to have two main influences on ocean circulation: firstly by steering the flow, and secondly by preventing the mixing of cold bottom waters. Furthermore, Gille et al. (2004) goes on to suggest that the extent to which the ocean flow is steered by the bathymetry is strongly controlled by the stratification of the water column. For example, in a weakly stratified ocean the flow is virtually uniform with depth, the bottom and surface currents are essentially

aligned in the same direction and as a result the effects of topographic steering is more important. This information was useful for explaining some of the results. Topographic steering was identified in both the numerical modelling and the observational results as an important influence of flow, particularly in the bottom layers.

In the numerical modelling, the influence of bathymetry was addressed by comparing the simulated thermal structure and flow for a model with a flat bottom (50m) and one with high-resolution bathymetry (CGS). The results showed that the CGS run simulated warmer bottom temperatures inside the Bay for both JFM (~3°C warmer) and JAS (~1°C warmer). Comparisons were made between the simulated v-component of flow across the mouth of the Bay for the flat bottom and the CGS model runs. During summer months (two-layered), there was little difference between the flow structures of the two runs. However, in winter the difference in the structure of the v-component of flow was notably more substantial.

This difference can be attributed to the thermal structure of the water column, which as described previously was well mixed during the winter season. During the winter months the flow was essentially uniform with depth, flowing barotropically, and the entire water column was influenced by the bathymetry underneath it. Therefore, the effects of bathymetric forcing were more influential on the circulation during winter. Whereas in the summer months, the stratification results in a two-layered decoupled flow. The lighter surface waters move faster and are forced directly by the wind and the denser bottom layers move slower and are topographically steered.

This finding was further elucidated by vertically integrating the bottom and surface flows separately for summer. The surface integrated flows were the same in both simulations. The reason for this is that the surface layers are influenced by the wind, which were being forced identically in both configurations. The bottom layers were very different. The flat bottom configuration simulated bottom circulation to flow directly into the bay whereas the CGS simulated bottom flow was more complex and was steered away from the mouth of the Bay at Rocky Bank. Rocky Bank and the other features at the mouth of the Bay, such as the extension of Cape Hangklip ridge, deviate this bottom flow reducing the inflow of colder, denser water. These features strongly affect the thermal structure of the Bay, resulting in higher simulated bottom temperatures than were found in the flat bottom run.

Evidence of topographic steering was also found in the observations. The principal axis of bottom flow closely agreed with the orientation of the local isobaths. The flow nearer the Bay's boundaries was polarised and flowed parallel to the isobaths. Towards the middle of the Bay, the flow was more complex which may reflect the complexity of the bathymetry beneath it. The boundary flow was found to occur in the simulated flow for winter.

The results shown agree with the main points summarised from the Gille et al. (2004) study on seafloor topography and ocean circulation. The results have shown that the bathymetry, as a physical process, makes important contributions to defining the circulation and thermal structure in the Bay.

Remote forcing

At present, there is limited understanding of the interaction between the currents of the western Agulhas Bank and those within the Bay. However, it has been acknowledged that the functioning and structure of the Bay are strongly influence by external mesoscale processes (Pitcher et al., 2010). False Bay is considered to be an 'open bay' (Pitcher et al., 2010), having a wide mouth of 30km, allowing access to the adjacent flow. While it was shown in Experiment One, that bathymetric features at the mouth of the Bay affect this inflow, there was still a significant proportion of water that entered the Bay. The study revealed the influence of this remotely forced flow on the Bay.

Through varying the models boundary conditions in Experiment Two, the approach was able to test whether or not the properties inside the Bay change under different external conditions. The employment of two different BCs - the coarse resolution (1°) World Ocean Atlas (WOA) and the high-resolution (1/27°) BC obtained from the offline nesting of the Veitch et al. (2009) domain - led to significant differences in thermal structure in False Bay. By adopting the offline nested BC with a higher resolution, the simulated vertical thermal structure in the Bay revealed a closer agreement to previous observations (Atkins, 1970a; Gründlingh, 1993). This was especially evident in a decrease of bottom temperatures in the Bay during summer months. The WOA BC was too coarse to capture upwelling and the advection of cold bottom waters into the Bay resulting in warmer than observed bottom temperatures. These key

features were included in the offline nested BC, Figure (20). The higher resolution, offline nested BC increased the heterogeneity of the thermal structure inside the Bay, both horizontally and vertically. Thus, adding variability to the external conditions resulted in an increase in complexity inside the Bay. The results have shown that varying the conditions outside of the Bay significantly affect the conditions inside the Bay, especially the thermal structure thus demonstrating the strong link between the outside conditions and the Bay processes. Due to conflicting historical observations, it was not possible to validate whether the offline nesting resulted in an improvement to the flow structure in the Bay.

In the present set of limited observations, it was difficult to investigate the influence of remote forcing. It is anticipated that remote forcing would be the most pronounced at deeper regions and the centre of the Bay (Taljaard et al., 2000). Unlike the flow at the boundaries, there was a weak correlation with wind in the centre of the Bay. This suggests that other forcing mechanisms were mainly dominant; it is likely that the circulation from the adjacent shelf was one of them. However, a more in-depth observational program is necessary to confirm such a hypothesis, with additional current moorings across the mouth of the Bay and the adjacent deeper continental shelf region.

Following an example given in the van Ballegooyen (1991) study, the daily mean sea level fluctuations at each ADCP and tidal gauges from Simon's Town and Port Nolloth were studied. The results showed sub-tidal fluctuations with the period of several days to a week and with amplitudes of up to 0.2m. The Port Nolloth tidal gauge was included to investigate whether these fluctuations were a remotely forced perturbation travelling southwards along the west coast of South Africa, or rather due to local wind and pressure changes. Port Nolloth is located approximately 570km up the west coast. The Port Nolloth fluctuations mirrored those inside the Bay with a 1-2 day lag (rough speeds of 285-570km.day^{-1}). The fluctuations agreed with the properties of shelf waves identified by Schumann and Brink (1990). Moreover, the range of speeds agrees with Schumann and Brink (1990) who reported speeds to be on the order of 360-580km.day^{-1}. While these fluctuations hinted at coastal-trapped shelf waves, to confirm this, a more in-depth investigation of winds and atmospheric pressure is needed.

There are implications of remote forcing on both the physical and biological prop-

erties of the Bay. The inflow of remote circulation introduces offshore water properties into False Bay. In the bottom layers, colder water that has been advected into the Bay from the western Agulhas Bank result in an increase in the Bay's stratification during summer. As mentioned previously stratification has important physical and biological ramifications. In the surface layers, wind driven circulation has been noted to transport algae blooms, which have formed on the adjacent shelf into False Bay (Pitcher et al., 2010). Together with the thermal structure and topographic steering, the remote forcing may add complexity to the circulation and thermal structure in False Bay.

Wind forcing

As previously discussed, the circulation and thermal properties in the Bay are dominated by the bi-directional seasonal wind regime consisting predominantly of SE and NW winds, occurring in summer and winter respectively. In the numerical modelling, the circulation and thermal structure was forced by uniform idealised climatological winds, lacking the spatial variability needed to accurately represent the wind fields over False Bay. In reality, the interaction of synoptic scale anticyclonic wind with the local mountain topography results in far more mesoscale variability in the structure of the wind fields over False Bay. It was not viable to compare the simulated seasonal mean flow with any of the observations as they lack the temporal and spatial resolution required to generate seasonal means for circulation over the entire Bay. Additionally, the numerical modelling was based on idealised winds, once the model is forced by the appropriate wind forcing, one which includes the fine scale structure, then it would make sense to attempt to compare and validate the simulated circulation. For now, the numerical modelling was compared with the Van Foreest and Jury (1985) who similarly used uniform winds to force the model.

In response to the seasonal bi-directional wind forcing, the simulated seasonal currents were counter-rotational in direction. Under a uniform SE (~6.5m.s^{-1}) wind forcing during summer, the simulated surface circulation was found to flow in an anticyclonic direction in the Bay. A similar result was found by the Van Foreest and Jury (1985), who found anticyclonic flow under a constant SE (9m.s^{-1}). Cyclonic circulation was apparent in the bottom layers on the southern half of the Bay. Unfortunately, this bottom

flow could not be compared with the results of the Van Foreest and Jury (1985) study, which was conducted with a vertically integrated hydrodynamic model and therefore unable to provide detail of the vertical flow structure. In contrast, during winter when forced with the constant NW (~4m.s^{-1}) wind the simulated circulation was cyclonic, entering the Bay at Cape Point and exiting the Bay at Cape Hangklip. This only partly agreed with Van Foreest and Jury (1985) who found the flow to exit the Bay at the boundaries and enter in the centre.

It was possible to compare the results of the present measurements with previous observational findings. The circulation along the steep boundaries of the Bay was expected to be mainly wind driven (Taljaard et al., 2000). This postulation was confirmed in correlations between residual circulation and wind, which indicated a strong relationship at the boundaries of the Bay (A01-71% and A05-63%) and a weak relationship at the ADCPs in the centre of the Bay. This was further shown by the close comparison between principal axis of surface flow at the Bay's boundaries and the wind.

It was possible to postulate schematics of flow in response to the wind from four principal directions. The SE and NW schematics in part agreed with that given by the Taljaard et al. (2000), Figure (11). A comparison between the schematics produced in this study and that of Taljaard et al. (2000) is provided here, Figure(44). During SE wind, both schemes suggested northward surface flow on the western boundary of the Bay, as well as at Gordon's Bay. The bottom flows appeared to agree with each other as both schematics show tendency towards a cyclonic bottom circulation. Under NW wind forcing, the bottom flow on the western side was northwards for both studies. The southward surface and bottom flows at Gordon's Bay were a feature in both schematics. There was some disparity between the circulation in the centre of the Bay for the two schematics, which was complex in the observations of this study. The schematic of this study illustrated a tendency towards a more two-layered flow during a NW and a more one-layered flow under SE winds during winter. This was not clearly evident in the Taljaard et al. (2000) study.

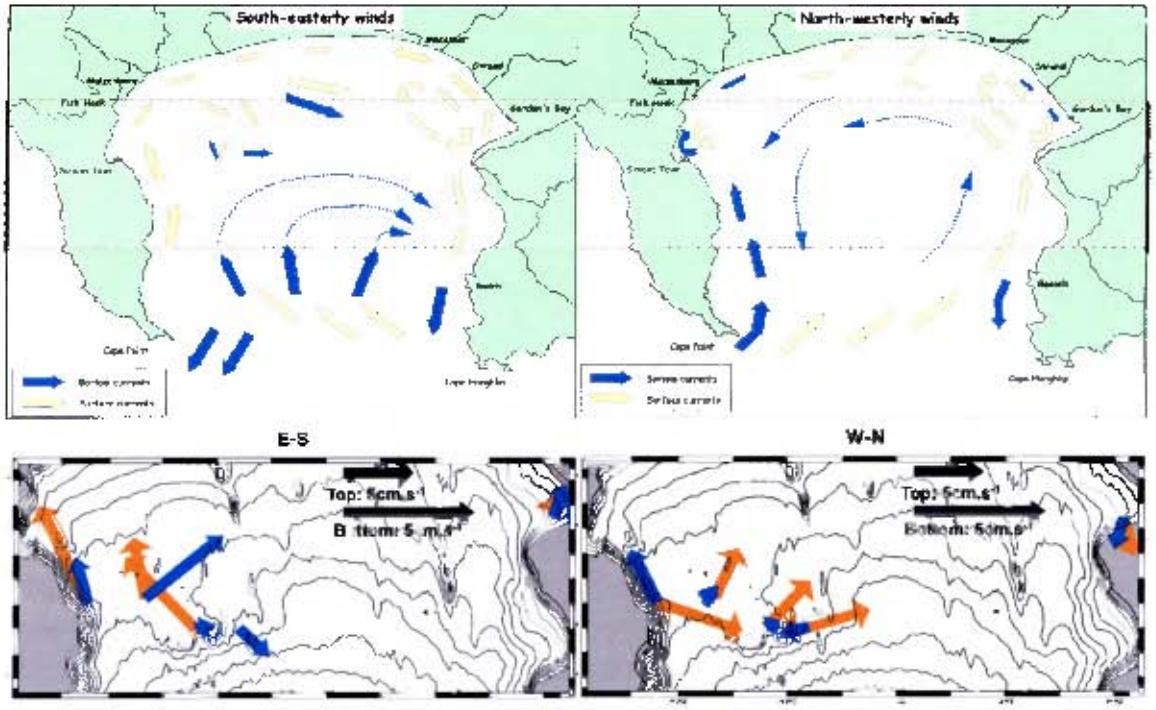

Figure 44: A comparison between the circulation modes under SE and NW wind forcing. Top: Taljaard et al. (2000) summary based on past studies. Bottom: mode identification from the five ADCPs of this study. Blue arrows represent bottom flow and yellow/orange represent the surface flow.

The study has shown that under different wind forcing the circulation and thermal structure differed considerably. This was particularly noticeable at the Bay's boundaries. The numerical modelling has shown mean seasonal differences in the circulation in response to the seasonal change in winds. The observations have shown that the circulation fluctuates on synoptic timescales corresponding to the passing of low and high-pressure systems. In order to accurately simulate the circulation, wind fields with the spatial and temporal resolution and variability required to accurately portray the wind fields over False Bay would be necessary.

False Bay in a global context

While the oceanographic conditions surrounding False Bay are unique as described in § 2.2, there is merit in comparing it to other studied upwelling bays which function in relatively similar environments. Such knowledge may help to place False Bay within a global context. As mentioned previously, § 2.2, False Bay is located within an eastern

boundary current system. There are four eastern boundary current systems in the world: the Canary Current System, the California Current System, the Humboldt Current System and the Benguela Current System. The dynamics of these systems are controlled by common large-scale ocean and atmospheric forcing's. It is anticipated that bays existing within these systems would operate in a similar manner.

A good example of an upwelling bay is Bodega Bay in California. Bodega Bay is a small embayment found in the Californian Current System. In an extensive study carried out byRoughan et al. (2005), the bay's circulation and thermal structure was investigated. Similarly to False Bay, Bodega Bay is influenced by seasonal bidirectional winds and is disposed to upwelling events during the summer months when the equatorward winds prevail. Two important findings found during summer months are relevant to the findings of False Bay both in past studies and this study. These are namely, the stratification of the Bay and the presence of a two-layered flow structure in part of the Bay during upwelling favourable winds. It was found that under strong upwelling favourable conditions, the surface currents were wind driven equatorward throughout the entire bay including the offshore domain. Where as the eastern side of the bay had colder bottom waters flowing polewards counter directional to the wind. Furthermore, the study found that under downwelling and relaxation conditions the circulation was poleward throughout the water column flowing on the eastern boundary of the bay. False Bay has been found to operate similarly. Atkins (1970a) found seasonal fluctuation of stratification. Gründlingh (1993)and Taljaard et al. (2000) postulated two-layered flow during summer months. These results have been further substantiated in this study. Other upwelling bays demonstrating similar nature include Monterey Bay in California and Coquimbo Bay in Chile.

Research questions

What is the role of bottom topography on the Bay's circulation and thermal structure?

Bottom topography has been shown to play a key role in defining the Bay's circulation and thermal structure. This was clear in both the numerical modelling and the observations. Large topographic features at the Bay's mouth were found to reduce the

amount of cold bottom flow entering the Bay by deflecting a portion of inflow. This had effects on both the circulation and the thermal structure. The bathymetry was shown to add complexity to the bottom flow in both the observation and the modelling. This was especially apparent during winter months when the flow was more barotropic. Topographic steering was evident at the steep boundaries, where strong boundary flow was shown to flow parallel to the isobaths. In the centre of the bay the flow was complex. Evidence in the observations suggested topographic steering of the bottom flow around the irregular bathymetry found there might have contributed to the complex flow.

Is remote forcing an important physical forcing factor to include in investigations on the Bay, and if so, how does it influence the circulation and thermal structure?

Remote forcing was found to influence both the circulation and thermal structure, and must certainly be taken into account as an important physical forcing mechanism. In the numerical modelling, by changing the external boundary conditions, significant changes were found inside of the Bay. During summer months, surface waters and colder bottom waters from the adjacent shelf are advected into the Bay by the SE wind. The advection of colder bottom waters would affect the thermal structure by increasing the stratification, which in turn affects the circulation. Stratification of the water column was found to result in two-layered flow, with colder bottom waters moving slower and in opposite directions to the warmer, faster surface waters driven by wind. It is expected that remote forcing will be pronounced in the middle and deeper regions of the Bay. In the observations, the weak correlation of wind in the centre of the Bay suggested that other mechanisms were responsible for the circulation there; remote forcing could be one of them. There was potential evidence of shelf waves affecting the circulation, however further more detailed investigation is needed.

Is wind forcing a dominant forcing factor in the Bay?

The wind was shown to be a key driving force determining the direction of the circulation in the Bay. The effects of the wind forcing were found to be more prominent

at the Bay's boundaries, with~70% of variance in flow explained by the wind. The seasonal evolution of circulation was shown to vary considerably between winter and summer responding to the bi-directional seasonal winds. During summer months, the warm surface flow was lighter than the denser bottom waters, and the effects of wind forcing were enhanced in these top layers. The lack of spatial sampling of past circulation studies have made it difficult to compare the simulated circulation of the entire Bay with historical observations. There was some agreement between the observations made in this study and the historical measurements. The wind forcing has also been demonstrated to affect the thermal structure in the Bay. The SST and bottom temperature fluctuations were synchronised to the changes in wind direction. The numerical modelling simulated three upwelling cells during summer in response to the SE winds. These were seen at Cape Point, Cape Hangklip and Gordon's Bay. This agreed with satellite observations and previous studies. There were however disparities in the simulated SSTs when compared to satellite SSTs. The next step in the numerical modelling hierarchy would be to incorporate high-resolution, spatially and temporally varying winds, which include the mesoscale variability observed in the wind field over False Bay. The incorporation of high-resolution winds has been described in further detail in the recommendations.

How important is tidal forcing?

Spectral analysis of the u and v-component of the unfiltered circulation illustrated the semi-diurnal tide (~12hrs) as a very significant signal in most of the spectra. The tidal signal was found to be more substantial in the v-component. The tidally forced circulation was as much as 15cm.s^{-1}, which is a significant portion of the flow (residual ~30cm.s^{-1}). The tidal circulation was in the form of oscillatory in and out flows. The numerical modelling excluded the effects of tides in this study, but it is recommended that they be incorporated into future numerical modelling studies of False Bay.

The numerical modelling in this study was specifically kept as a processes-oriented approach. The first domain, run with uniform boundary conditions, idealised forcing and with a flat bottom provided the platform on which further numerical modelling could be advanced in a step-by-step fashion. This allowed for a more controlled approach as

opposed to adding all the relevant processes in one simulation resulting in a complex solution difficult to decipher. The main objective of this thesis was not to attempt to simulate actual conditions, but rather to further develop the current understanding of the physical processes driving the circulation. Each modelling experiment was based on distinct processes that could be investigated. The hypothesis set by each modelling experiment has been tested and proven. The study provides a stimulus for future numerical modelling studies in the Bay. Suggestions for future modelling work have been provided in Chapter 6. While, the observations provided some additional insight, they were difficult to interpret, and lacked the spatial and temporal resolution that numerical modelling is now capable of producing.

6 Recommendations for future work

The recommendations for future numerical modelling studies conducted in False Bay are presented in this section. Figure (45) below, is an example of a framework which could be used in planning future modelling of False Bay circulation. Experiments 1, 2 and 3 have been completed in this Masters dissertation, and suggestions for the improvements of these experiments along with the plausible steps for experiments 4, 5 and 6 are discussed below.

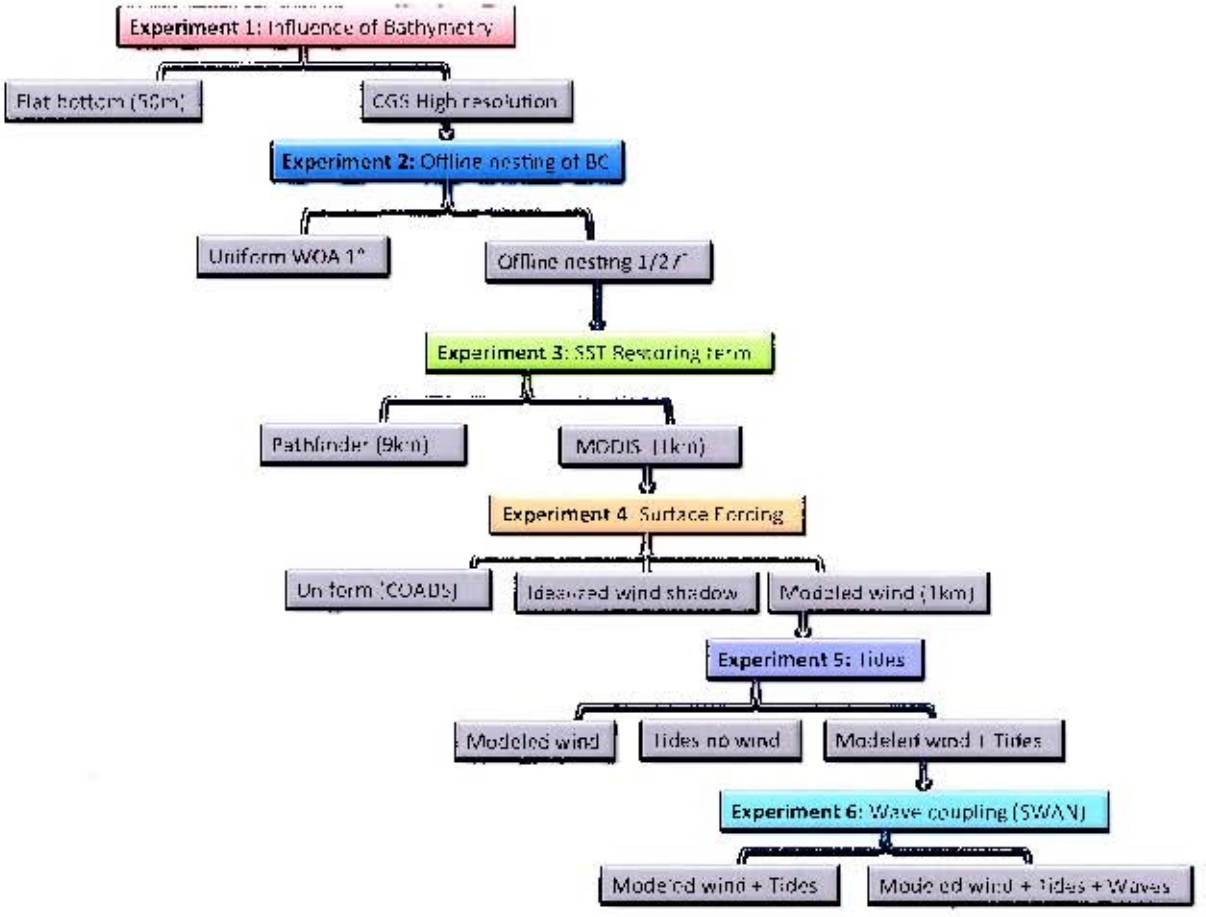

Figure 45: Hierarchy of experiments for future numerical modelling

6.1 Two-way nesting

An offline nesting approach was chosen in this study, however, a two-way nesting could be used. The two-way nesting approach allows the lower resolution output from the 'parent' domain to be incorporated as boundary conditions for the higher resolution nested 'child' domain, which then feeds back to the parent domain. The benefits of

taking two-way nesting approach is that it allows for boundary conditions that are more reliable than observed data sets which have often been collaborated from scarce temporal and spatial measurements (Veitch et al., 2009). Additionally, the method is less computationally expensive than running the parent domain at a higher resolution (Veitch et al., 2009).

According to Penven and Tan (2007), in order to maintain the CFL (Courant - Friedrichs – Lewy) criteria, a factor of 3 should be used to downscale from parent to child in ROMS simulations. Based on this rule one can adopt a two-way nesting approach for future modelling of False Bay. The SAfE configuration (Penven et al., 2006) could be used as the parent domain (19-27km), embedded within this the child domain with a 7-9km resolution. This could be embedded further by a second child domain with a resolution of 3km and embedded within that child domain, a third child domain with the resolution of 1km as required for False Bay, Figure (46).

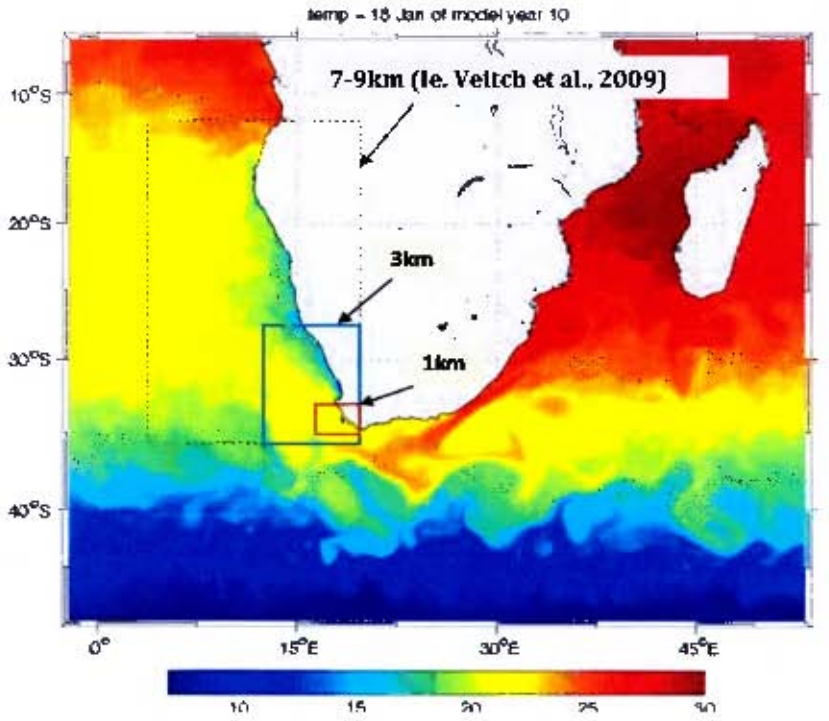

Figure 46: The hypothetical Nesting arrangement for Modelling False Bay using the SAfE configuration as the parent domain (adapted from Penven et al., 2006)

6.2 Surface forcing

As discussed in Van Foreest and Jury (1985), and found in the observational results of this study, the circulation in the Bay is sensitive to the spatial variability and detail of the wind fields. The wind data needed to accurately model the circulation would have to be capable of representing several different wind regimes under various synoptic forcing. These would include the northwesterly storms, deep southeasters, shallow southeasters and southwesterly wind conditions (Van Foreest and Jury, 1985; Taljaard et al., 2000). The idealised surface forcing chosen for this study lacks the spatial and temporal variability required in accurately modelling the circulation of False Bay. MSc. research conducted by Roux (2009) under supervision of Francois Engelbrecht from CSIR, provides as an example of plausible high-resolution wind fields which could be used in this study, Figure (47). To obtain high-resolution data (1km) over the southwestern Cape, that study made use of a variable-resolution global model, the conformal-cubic atmospheric model (CCAM), applied with a multiple nudging strategy. In order to obtained synoptic-scale circulation, the model was first applied at a resolution of 60km over southern Africa. From this, the higher resolution 8km (nudged from 60km) and 1km (nudged from 8km) simulations were obtained consecutively. An example of the 1km simulated results for February is presented in Figure (47).

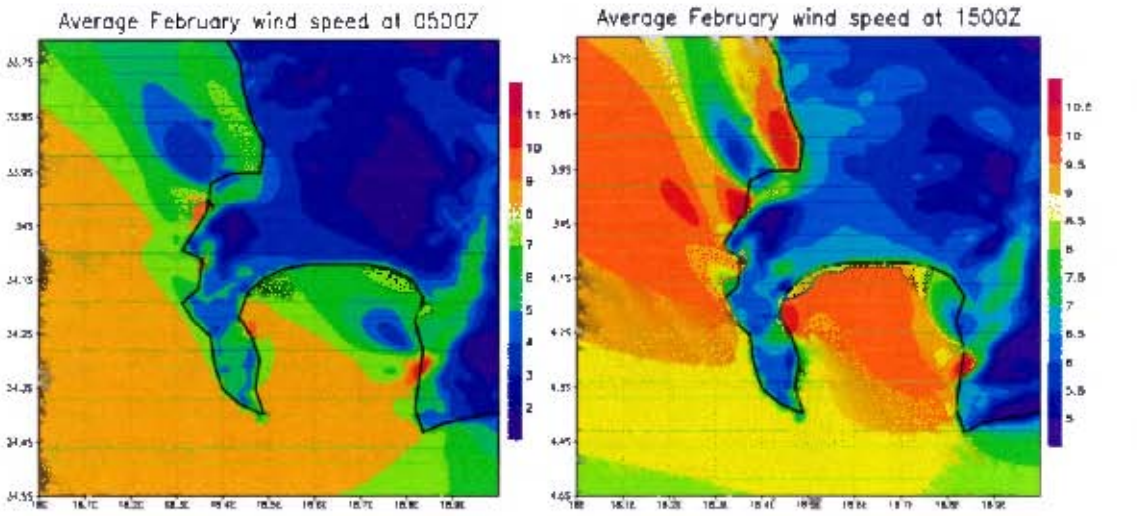

Figure 47: Screen-height wind speed ($m.s^{-1}$) over the south-western Cape for February at 0500Z and 1500Z as simulated by CCAM for 1976 at a resolution of 1km (Roux, 2009).

The simulations appear to demonstrate the wind shadows observed off the Gordon's Bay region and the complexity of the wind field. There are other options available for atmospheric modelling to obtain high-resolution winds, for example the WRF (Weather Research Forecasting) model. The main issue with using the high-resolution modelled wind data is the lack of spatially distributed observational data needed for validation.

Following the idealised wind forcing experiment by Van Foreest and Jury (1985), who applied a wind shadow to investigate the circulation under a shallow SE, an idealised experiment of similar nature could be applied to this study. Their wind stress shadow was sinusoidally decreased to zero and was located in the lee of Kogelberg Mountain, refer to Van Foreest and Jury (1985).

6.3 Wave and tidal Coupling

The model configurations that were setup in this study have excluded both the effects of waves and tides on the circulation. As discussed previously, both wave and tidal influences are relatively important contributors to the circulation, the next step in the process would be the inclusion of such forcing. ROMS can be configured to include tidal forcing effects in the configuration. The different tidal constituents, typically derived from the TPXO7, are propagated from the lateral boundaries (Penven and Tan, 2007). TPXO7 is a global model (0.25 ° resolution) of the ocean tides, which assimilates satellite altimetry data (Penven et al., 2007). For this to work the model boundary conditions must be defined according to the Flather (1976) open boundary radiation scheme (Penven and Tan, 2007). For the inclusion of the wave forcing, ROMS could be coupled with a wave model such as SWAN (Simulating WAves Nearshore).

7 Acknowledgements

I would like to start by thanking the supervisors of this MSc dissertation, Prof Frank Shillington, Dr Howard Waldron and Dr Jennifer Veitch, for their assistance and willingness throughout the on goings of this project. A huge thank you to, Dr Francois Dufois for his invaluable assistance with data analysis of ADCPs. Additionally, I would like to thank Prof. John Largier for his time and input at the Bodega Marine Labor-

atory. I am extremely grateful for their continued support and knowledge they have shared with me which has made this project a success.

Thank you to everyone involved from IMT who helped with the ADCP deployment/retrieval and for the use of two of their ADCPs. Thank you to the Research Diving Unit (RDU) for providing the divers needed in the deployment and retrieval of ADCPs.

Additional thanks to the following for their willingness to share data crucial to the project: Michael Machutchon from Council of Geophysical Science for the high-resolution bathymetry data used. Marius Rossouw from CSIR for the ADCP data. Francois Dufois for the MODIS terra and aqua satellite SST data. Additional thanks to IMT for providing wind data from Roman Rock and to the SAWS for providing wind data from Cape Point.

Thanks to Dr. Penven and the IRD for the development of ROMSTOOLS package consisting of the relevant data needed for this project. The ROMSTOOLS package has made the processes considerably easier.

Thanks to the following for their interests and input during the workings of the project: Prof. Geoff Brundrit, Prof. Chris Edwards, Dr. Marjolaine Rouault, Dr. Pierrick Penven, Gabriel Reygondeau, Dr. Juliet Hermes and Dr. Natalie Burls.

I am grateful for the support from my office members who have courageously put up with continued cries of frustration coming from my desk.

Finally, I would like to give a big thank you to MA-RE BASICS for funding the project and funding the research visit to the Bodega Marine Laboratory in California. Thank you to UCT for the Merit Scholarship.

References

Andre, G., Garreau P. and Fraunie P. (2009), 'Mesoscale slope current variability in the Gulf of Lions. Interpretation of in-situ measurements using a three-dimensional model.', *Continental Shelf Research* **29**, 407–423.

Atkins, G.R. (1970a), 'Thermal structure and salinity of False Bay.', *Trans. Roy. Soc. S. Afr.* **39**(2), 117–128.

Atkins, G.R. (1970b), 'Wind and current patterns in False Bay.', *Trans. Roy. Soc. S. Afr.* **39**(2), 139–148.

Barnier, B., P. Marchesiello, A. Pimenta de Miranda, J. M. Molines and M. Coulibaly (1998), 'A sigma-coordinate primitive equation model for studying the South Atlantic. Part I: model configuration with error estimates.', *Deep-Sea Res.* **45**, 543–572.

Blumberg, A.F. and G.L. Mellor (1987), 'A description of a three-dimensional coastal ocean circulation model.', *Three-Dimensional Coastal Ocean Models Coastal Estuarine Studies* **4**, 1–16.

Botes, W.A.M. (1988), 'Shallow water current meters comparative study: False Bay.', *CSIR Report TSEA 8803* p. 14.

Chen, C. and L. Xie (1997), 'A numerical study of the wind-induced, near-inertial oscillations over the Texas-Louisiana shelf.', *Geophysical Research* **102**(C7), 15583–15593.

Cram, D.L. (1970), 'A suggested origin for the cold surface water in central False Bay.', *Trans.Roy. Soc. S. Afr.* **39**(2), 129–137.

CSIR (1990), Pollution assessment in north eastern False Bay (POLLNEF): Dissolved nutrient distribution patterns.

CSIR (1991b), 'Ocean outfall studies in False Bay. Report no. 2: Offshore data interpretation and an initial assessment of possible offshore pipeline discharges into False Bay', *CSIR Report EMAC 9117*.

Cushman-Roisin, B. and J.M. Beckers (2009), *Introduction to Geophysical Fluid Dynamics Physical and Numerical Aspects.*, Vol. 98.

Dufois, F., P. Garreau, P. Le Hir and P. Forget (2008), 'Wave and current induced bottom shear stress distribution in the Gulf of Lions.', *Continental Shelf Research* **28**(15), 1920–1934.

Emery, W. J. and R. E. Thomson (2004), *Data Analysis Methods in Physical Oceanography*, Elsevier.

Ezer, T. and H. Arango and F.A. Shchepetkin (2002), 'Developments in terrain-following ocean models: intercomparisons of numerical aspects.', *Ocean Modelling* **4**, 249–267.

Fawcett, A.L., G.C. Pitcher and F.A. Shillington (2008), 'Nearshore currents on the southern namaqua shelf of the benguela upwelling system', *Continental Shelf Research* **28**(8), 1026 – 1039.
URL: *http://www.sciencedirect.com/science/article/pii/S0278434308000447*

Flather, R.A. (1976), 'A tidal model of the northwest European continental shelf', *Memoires de la Societe Royale des Sciences de Liege* **10**, 141–164.

Gill, A.E. and E.H. Schumann (1974), 'The Generation of Long Shelf Waves by the Wind', *Journal of Physical Oceanography* **4**(1), 83–90.

Gille, S.T., J.E Metzger and R. Tokmakian (2004), 'Seafloor Topography and Ocean Circulation', *Oceanography* **17**(1), 47–54.

Gordon, R.L (1996), 'Acoustic Doppler current profiler principals of operation: a practical primer', *Second edition for Broadband ADCPs, RD Instruments, San Diego, California* .

Grindley, J.R. and F.J.R. Taylor (1970), 'Factors affecting plankton blooms in False Bay', *Trans. Roy. Soc. S. Afr.* **39**(2), 201–210.

Gründlingh, M.L (1992), 'Quasi-synoptic survey of the thermohaline properties of False Bay', *S. Afr. J.Sci.* **88**, 325–334.

Gründlingh, M.L (1993), 'Unique Thermal Records in False Bay', *South African Journal of Science* **89**, 510–512.

Gründlingh, M.L., I.T. Hunter and E. Potgieter (1989), 'Bottom currents at the entrance to False Bay, South Africa', *Cont. Shelf Res.* **9**(12), 1029–1048.

Gründlingh, M.L. and J.L Largier (1991), 'Physical oceanography of False Bay: A Review', *Trans.Roy. Soc. S. Afr.* **47**, 387–400.

Haidvogel, D. B., A. Beckmann and K. S. Hedstrom (1991), 'Dynamical simulations of filament formation and evolution in the coastal transition zone', *J. Geophys. Res.* **96**, 15017–15040.

Hedstrom, K. S. (1997), 'User's Manual for an S-Coordinate Primitive Equation Ocean Circulation Model (SCRUM) Version 3.0', *Institute of Marine and Coastal Sciences, Rutgers University.* (116 pp).

Horstman, D.A., S. McGibbon, G.C. Pitcher, D. Calder, L. Hutchings and P. Williams (1991), 'Red Tides in False Bay, 1959 to 1989, with Particular Reference to Recent Blooms of Gymnodinium sp.', *Trans Roy. Soc. S. Afr.* **47**(4 and 5).

Jury, M.R. (1985), 'Case Studies of Alongshore variations in wind-driven upwelling in the Southern Benguela Region. South African Ocean Colour and Upwelling Experiment. Shannon L.V(Ed). ', *Sea Fisheries Research Institure* pp. 29–46.

Jury, M.R. (1991), 'The Weather of False Bay.', *Trans.Roy. Soc. S. Afr.* **47**, 401–418.

Marchesiello, P., J.C. McWilliams and A.F Shchepetkin (2003), 'Equilibrium structure and dynamics of the California Current System', *J. Phys. Oceanogr.* **33**, 753–783.

Nelson, G. and A. Polito (1987), 'Information of currents in the Cape Peninsula area, South Africa', *S.Afr. J. mar. Sci.* **5**, 287–304.

Nelson, G. and L. Hutchings (1983), 'The Benguela upwelling area', *Progress in Oceanography* **12**, 333–356.

Pawlowicz, R., B. Beardsley and S. Lentz (2002), 'Classical tidal harmonic analysis including error estimates in MATLAB using TTIDE', *Computers and Geosciences* **28**, 929–937.

Penven, P., C.Roy, G.B Brundrit, A. Colin de Verdiere, P. Freon, A.S. Johnson, J.R.E Lutjeharms and F.A Shillington (2001), 'A regional hydrodynamic model of upwelling in the Southern Benguela', *South African Journal of Science* **97**, 472–475.

Penven, P., J.R.E. Lutjeharms and P.Florenchie (2006), 'Madagascar: A pacemaker for the Agulhas Current System?', *Geophysical Research Letters* **33**.

Penven, P., P. Marchesiello, L. Debreu and J. Lefevre (2007), 'Software tools for pre- and post processing of regional simulations', *Environ. Model. Softw.* .

Penven, P. and T. Tan (2007), 'ROMSTOOLS user guide.', *Institut de Recherche pour le Development (IRD)* .
URL: *http://roms.mpl.ird.fr/*

Pitcher, G.C, B. Stewart and J. Ntuli (2008), 'Contrasting Bays and Red tides in the Southern Benguela Upwelling Region', *Journal of The Oceanography Society* **21**(3).

Pitcher, G.C., F.G. Figueiras, B.M. Hickey and M.T. Moita (2010), 'The physical oceanography of upwelling systems and the development of harmful algal blooms', *Progress In Oceanography* **85**(1-2), 5 – 32. Special Issue on Harmful Algal Blooms in Upwelling Systems.
URL: *http://www.sciencedirect.com/science/articleB6V7B-4YCFYX5-2/2/31c30166c72d97af0040dda7ddd8d9e6*

Rasmussen, L. L., B. D. Cornuelle, L. A. Levin, J. L. Largier and E. Di Lorenzo (2009), 'Effects of small-scale features and local wind forcing on tracer dispersion and estimates of population connectivity in a regional scale circulation model', *J. Geophys. Res.* **114**(C01012).

Roberts, M. J. (2005), 'Chokka squid (Loligo vulgaris reynaudii) abundance linked to changes in South Africas Agulhas Bank ecosystem during spawning and the early life cycle', *Journal of Marine Science* **62**, 33–55.

Roughan, M., A. J. Mace, J. L. Largier, S. G. Morgan, J. L. Fisher and M. L. Carter (2005), 'Subsurface recirculation and larval retention in the lee of a small headland: A variation on the upwelling shadow theme', *J. Geophys. Res.* **110**.

Roux, B. (2009), Ultra high-resolution climate simulations over the Stellenbosch wine producing region using a variable-resolution model. MSc. dissertation. University of Pretoria.

Schumann, E. H. and K.H. Brink (1990), 'Coastal-Trapped Waves off the Coast of South Africa: Generation, Propagation and Current Structures', *American Meteorological Society* **20**, 1206–1218.

Schumann, E.H. and L.A. Perrins (1982), 'Tidal and Inertial Currents Around South Africa', *Coastal Engineering* pp. 2562–2580.

Shchepetkin, A. F. and J. C. McWilliams (2005), 'The Regional Ocean Modeling System: A split explicit, free-surface, topography following coordinates ocean model', *Ocean Modelling* **9**, 347–404.

Song, Y.T and D.B Haidvogel (1994), 'A semi-implicit ocean circulation model using a generalized topography following coordinate system', *J. Comput. Phys.* **115**, 228–248.

Spargo, P.E. (1991), 'False Bay, South Africa- An Historic and Scientific Overview', *Trans Roy Soc. S. Afr.* **47**(4-5).

Swart, V.P. and J.L. Largier (1987), 'Thermal structure of the Agulhas Bank water', *South African Journal of Marine Science* **5**, 243–254.

Taljaard, S., R.C. Van Ballegooyen and P.D. Morant (2000), 'False Bay Water Quality Review, Volume 2: Specialist Assessments and Inventories of Available Literature and Data, Report to the False Bay Water Quality Advisory Committee', *CSIR Report ENV-S-C 2000-086/2* **2**.

van Ballegooyen, R (1991), 'The Dynamics Relevant to the Modelling of Synoptic Scale Circulations within False Bay', *Trans Roy Soc. S. Afr.* **47**, 419–430.

Van Foreest, D. and M.R. Jury (1985), 'A numerical model of the wind-driven circulation in False Bay', *South African Journal of Science.* **81**.

Van Niekerk, M (1983), 'False Bay outfall studies: Measurement techniques and analysis of field data collected during two exercises in 1983', *CSIR Report C SEA 8620.Stellenbosch.* p. 14.

Veitch, J., P. Penven and F.A. Shillington (2009), 'The Benguela: A laboratory for comparative modelling studies', *Prog. Oceanogr.* .

Wainman, C.K, A. Polito and G. Nelson (1987), 'Winds and Subsurface Currents in the False Bay Region, South Africa. The Benguela and Comparable Ecosystems', *S. Afr. J. Mar. Sci.* **5**, 337–346.

Waldron, H. N and C.K Wainman and M.E Waldron and C.Whittle and G.B Brundrit (2008), 'A prominent colour front in false bay, south africa: Cross-frontal structure, composition and origin', *Estuarine, Coastal and Shelf Science* **77**(4), 614–622.